# Quantifying demand response under uncertainty in power systems

Pan Li

A dissertation
submitted in partial fulfillment of the
requirements for the degree of

Doctor of Philosophy

University of Washington

2018

Reading Committee:

Baosen Zhang, Chair

Daniel Kirschen

Sreeram Kannan

Program Authorized to Offer Degree:
Electrical Engineering

University of Washington

**Abstract**

Quantifying demand response under uncertainty in power systems

Pan Li

Chair of the Supervisory Committee:
Assistant Professor Baosen Zhang
Department of Electrical Engineering

The new perspective of looking at power system operation is to utilize the flexibility from electricity consumers and distributed energy resources. Demand response, by promoting the interaction and responsiveness of the consumers, offers a broad range of potential benefits on system operation and expansion and on market efficiency. It is therefore crucial to accurately estimate the effect of certain demand response signals, especially given that consumers' behavior is uncertain and noisy. Depending on how the system operator curates consumer data, we develop different ways to estimate this effect using either offline or online data. We first consider that demand response signals are binary and model the consumption behavior by a linear model. We compare several different linear estimators of demand response effect and propose an optimal demand response signal assignment strategy that improves the performance of the linear estimator in terms of optimal reduction in estimation variance. In a more realistic setting where demand response signals from the operator are continuous, i.e., price signals, we assume that the operator does not know the cost function of consumers and cannot have multiple rounds of information exchange with consumers. We formulate an optimization problem for the operator to minimize its operational cost considering time-varying demand response targets and responses of consumers. We develop a joint online learning and pricing algorithm and show that our online algorithm achieves logarithmic regret with respect to the operating horizon.

Besides, as a future of urban power system development, the generation of electricity from renewables constitutes a large portion of the total generation in the power grid. The inherent uncertainty of renewables and their wide distribution in the network bring new challenges in planning and operation. We design a decentralized market to engage the participation of small scaled distributed renewable energy resources. It is known that most deterministic capacity games tend to result in very inefficient equilibria, even when there are a large number of similar players. In contrast, we show that due to the inherent uncertainty of renewable resources, the equilibria in our capacity game becomes efficient as the number of players grows and coincides with the centralized decision from the social planner's problem. In addition, we use reactive power compensation as demand response to alleviate the problem of fluctuated voltage resulted from introduction of renewables. We adopt a chance constrained approach that accounts for arbitrary correlations between renewable resources at each of the buses in the system. We show that the problem can be solved efficiently using historical samples via our proposed descent algorithm. We also show that this optimization problem is convex for a wide variety of probabilistic distributions. We use both synthetic generated and real-world energy data to validate the claims and the proposed algorithms.

# TABLE OF CONTENTS

# LIST OF FIGURES

# LIST OF TABLES

# GLOSSARY

DR: Demand response.

SLR: Simple linear regression.

LS: Least squares.

MLR: Multiple linear regression.

MCM: Modified covariate method.

ATE: Average treatment effect.

SDP: Semi-definite programming.

DER: Distributed energy resources.

PV: Photovoltaic.

MIP: Mixed integer programming.

SQG: Stochastic quasi-gradient.

# ACKNOWLEDGMENTS

It has been the very fruitful four years since I started working towards my doctoral degree at University of Washington. First and foremost, I cannot express more of my gratitude to my advisor, Professor Baosen Zhang, for his support, patience, and immense knowledge. Professor Zhang's guidance helped me in all the time of research and most importantly, he serves as an exemplary role model for my career. I could not have imagined having a better advisor and mentor for my PhD study.

I then would like to express my appreciation for Professor Daniel Kirschen, for giving me a chance to start my study at University of Washington, and for being more than supportive of my research and career goals. My appreciation also goes to the rest of my thesis committee, Professor Sreeram Kannan, whom I took several classes with and which I really enjoyed, and Professor Shuai Huang, who generously serves as GSR for my final exam. I thank all of them for their great advices which incented me to widen my research from various perspectives.

I thank my fellow lab-mates for the simulating discussions and collaborations, consisting of Hao Wang, Shreyas Sekar, Yishen Wang, Ahlmahz Negash, Zeyu Wang, Yury Dvorkin, Mushfiqur R. Sarker, Ting Qiu, Ricardo Fernandez-Blanco, Yushi Tan, Bolun Xu, Yuanyuan Shi, Yize Chen, Chase Dowling, Atinuke Ademola-Idowu, Abeer Almaimouni, Ryan Elliott, Jesus Elmer Contreras Ocana, Daniel Olsen, Yao Long, Yi Wang, Yao Chang, Jingkun Liu. Thanks for all the fun we have had in the past four years. I am also grateful to my friends outside the lab at University of Washington, and the colleagues at Pinterest, for their advices and support.

I would also like to acknowledge the generous funding support I have received from the following sources: NSF grant CNS-1544160, Clean Energy Institute at University of

Washington, and Keith and Nancy Rattie Endowed Fellowship.

Thanks to all the UWEE faculties and staffs who have helped me in the past few years.

Last but not least, my most sincere gratitude goes to my beloved family, especially my parents, my cousin and my cousin-in-law, and Dai, who unconditionally support my PhD study and research. Their encouragement and love is crucial for me to make it so far today. This dissertation is dedicated to all of you.

# DEDICATION

to my family, to Xiaoxia

# Chapter 1

# INTRODUCTION

## *1.1 Changes and emerging problems in power system*

Power system is undergoing a new era of revolution. Traditionally, the operation of power system comprises two stages: planning and scheduling for large scale transmission level generators. This approach is usually top-down, which dispatches available generation (for example from hydro units and coal units) to satisfy demand from end consumers. With the recent advanced technology in communication, the system operator is able to access more easily the local devices of these consumers, stimulating and changing their consumption profile to achieve better energy efficiency. The new aspect of power system operation thus focuses more on demand themselves and is more bottom-up. Such operation is known as *Demand Response (DR)* and is introduced in Section 1.1.1. Since demand from end consumers is considered flexible, it is crucial to come up with new ways to estimate consumers' responsiveness to the operator, especially in the presence of uncertainty where operator does not know the exact response in advance. A detailed discussion is provided through Section 2 to Section 4 for different scenarios.

Besides improving energy efficiency from consumers, emerging technologies in distributed photo-voltaic (PV) generation and small-scale distributed wind farm also provide fruitful local information and suggest new means to enhance the overall operation of the power system. An appropriate management of those new resources is vital to maintain a healthy and sustainable power system. However, their planning vastly differs from that of large-scale generators due to two reasons. First, renewable energy resources are highly uncertain and intermittent. Second, they are dispersed widely in the system, making a central management applied to large-scale generators hard to implement in practice. More backgrounds are

introduced in 1.1.2 and a viable solution is provided in Section 5.

In addition, end consumers and distributed resources co-exist in the power system and it is essential that those new flexibilities support a secured operation of the power system. Voltage is one of the criteria to evaluate if a power system operation is tolerable within physical constraints. However, uncertainties from renewable generation causes voltage fluctuations. Either too high or too low a voltage will damage electric equipments that requires a steady voltage source and even lead to blackouts in the system. How to deal with the uncertainty using reactive power as a mean of DR is introduced in Section 1.1.3 and will be discussed in Section 6 using data-driven methods.

### *1.1.1 DR in power system operation*

In a typical implementation of DR programs, customers receive a DR signal to elicit a change in their consumptions. This signal can be a modification of electricity prices or simply a message requesting a change in consumption [1]. An effective DR program improves the efficiency and sustainability of power systems and is a central pillar of the envisioned smartgrid [2–5].

One main challenge for the effective implementation of a DR program is the learning and prediction of consumers behavior towards DR signals. Response can depend on many consumer specific parameters like availability, temperature sensitivity, fatigue due to repeated scheduling and other stochastic factors like weather. Consumer specific parameters are typically private information. However, learning such parameters are essential for efficient scheduling of consumers in order to achieve a reliable load reduction via DR programs. We therefore aim to solve two problems:

- We start with a vanilla example by assuming the DR signal is binary. The goal of the operator is to purely estimate the average impact of this DR signal. Estimating its impact is nontrivial because operators can often times only send a limited number of signals. In addition, customer behavior also depends on a large number of exogenous

covariates. These two features lead to a high dimensional inference problem with limited number of observations. It is therefore a question as to assigning DR signals strategically in order to learn its impact. We treat this assignment as an experimental design problem and propose an optimal strategy that accurately estimate the DR impact.

- In reality, the operator is more likely to send out different DR signals (i.e., different prices) to elicit different amount of reduction in consumption. The operator faces two key challenges. [1] The first is uncertainty, where operators often do not know the exact response of the customers to the signals. Secondly, operators often have specific DR targets at a particular time. For example, if the operator wishes to reduce the demand of a residential area by 100 KW, it is suboptimal to receive either 50 KW or 200 KW from a DR call. Thus DR programs are faced with the fundamental problem of optimizing the responses under uncertainty about its customers. We address this problem by designing optimal algorithms that can optimize and learn simultaneously.

### *1.1.2 Renewable energy participation in electricity market*

As a future of urban power system development, the generation of electricity from renewables constitutes a large portion of the total generation in the power grid. It is clean, efficient, and can operate nearly free. Wind and solar energy are the two examples to provide such flexibility. In particular, solar energy, as one of the emerging resources in renewable resources, plays an important role in generating clean and sustainable energy. The installment of PV panels has grown exponentially during the past few years [7] and has provided promising support for the power generation in the new era.

One intrinsic difference between renewable energies such as solar and traditional generators is their inherent randomness. The generation from renewable resources depends on climate and are not controllable. What is more, those resources are distributed across the

[1] We do not consider direct load control for DR in this dissertation (e.g., see [6]).

network, providing much more flexibility than the traditional generators. In addition, it is more realistic to consider a competitive environment when solar energy generation is distributed in the power system, for example, the rooftop PV panels. Those PV panels might be privately owned and are not controlled by a single operator. It is very likely that each of the PV panel owners competes with each other to enter the electricity market. In this setting, each PV owner makes their own optimal investment and price bidding strategies based on the information they have, as opposed to a centralized decision made by a single operator.

### *1.1.3 Voltage control*

Power system is a large networked physical system where the power consumption (and generation) and the voltage level at each bus are closely related according to physical laws. Therefore, when a system operator calls upon available DR services, one major concern is to dispatch and acquire available DR as efficiently as possible, while maintaining a healthy operation of the system.

Voltage control is crucial to a secured operation of power distribution systems, where it is used to maintain acceptable voltages at all buses under different operating conditions [8]. To control voltage, reactive power is traditionally regulated through tap-changing transformers and switched capacitors [9]. With recent advances in cyber-infrastructure for communication and control, it is also possible to utilize distributed energy resources (DERs, i.e., electric vehicles [4], PV panels [10,11]) to provide voltage control. There exists an extensive literature in controlling voltage in a distribution network, some of them focus on centralized control [12, 13], while the others address distributed algorithm [8, 9, 14, 15]. In this dissertation, we focus on centralized control frameworks to regulate voltage through DERs, when uncertainty is present in the system.

## *1.2 Contribution of this dissertation*

The contributions of this dissertation can be summarized in following categories:

- First, we model consumption behavior as a linear model and the DR signal is assumed to be binary. We provide a thorough analysis on several linear estimators to quantify the effect of DR signals. More specifically, we show that a tailored DR assignment strategy enables a better estimator as compared to the "golden standard" – random assignment, when the number of features in the model is large. Our algorithm is tractable, and it achieves optimal reduction in estimation variance independent of the number of features in the model.

- Second, we extend the analysis into a more realistic setting, where the operator sends out continuous DR signals sequentially to elicit change in electricity consumers' consumption behavior. Specifically, the operator does not know the cost function of consumers and cannot have multiple rounds of information exchange with consumers. We formulate an optimization problem for the utility to minimize its operational cost considering time-varying DR targets and responses of consumers. Our proposed joint online learning and pricing algorithm achieves sub-linear regret with respect to the operating horizon. In addition, our algorithm employs linear regression to estimate the aggregate response of consumers, making it easy to implement in practice.

- Then, we take into consideration the rapid development of distributed renewable resources and study their investment strategies. Because of the unique properties of those resources, we propose a decentralized market instead of a centralized market, which is a better fit. More specifically, we consider a two level capacity-pricing game among multiple uncertain renewable energy producers. We show that contrary to commonly held belief, randomness improves the quality of the Nash equilibria. In addition, we explicitly characterize the Nash equilibria and show that the social cost and efficiency improve as the number of producers grows.

- Last, we use reactive power compensation to control voltage in the presence of uncertainty due to DER installation. We adopt a chance constrained optimization problem

and propose an efficient and tractable descent algorithm by finding a valid descent direction at each iteration using historical samples. Our algorithm avoids integer programming formulation which is widely adopted in literature and does not compute cumbersome integrals. In addition, we show that if the uncertainty in the DERs comes from a log-concave distribution, the optimization problem is actually convex and our algorithm is guaranteed to be global optimal given enough samples.

### *1.3 Organization*

The rest of this dissertation is organized as follows.

- Chapter 2 discusses the fundamental practice in deploying and estimating DR, i.e., random trial. We focus on three different linear models and compare the model performance by the variance of the estimators.

- Chapter 3 builds upon Chapter 2 and proposes an optimal assignment strategy in a high dimensional setting where random trial fails to efficiently estimate the effect of DR.

- Chapter 4 considers an optimization problem for the operator to minimize its operational cost considering time-varying DR targets and responses of consumers. We design a joint online learning and pricing algorithm and measure the performance of our algorithm using regret analysis.

- Chapter 5 proposes an optimal investment strategy of distributed renewable energy resource in an electricity market. We consider a more realistic setting where resources compete with each other in a decentralized market to maximize profits. We compare the proposed framework with a centralized market and analyze the efficiency of such competition.

- Chapter 6 considers a DR program that deals with randomness from distributed energy resources to control voltage fluctuation. In this DR program, the regulative power is the available reactive power from energy resources. The goal is to maintain a acceptable voltage level for the system considering uncertainty and communication latency. More specifically, we propose a robust data-driven approach that uses available reactive power to control voltage without knowing the explicit distribution of the uncertainty.

- Finally, Chapter 7 concludes the whole dissertation work and suggests some future research directions.

# Chapter 2

# LEARNING DEMAND RESPONSE

## *2.1 Literature review*

An accurate estimate of the change in consumption due to a certain DR signal is central to the operation of DR programs. Most of existing work in this area of demand response have approached the problem from a market optimization point of view. For example, authors in [5, 16] considered how to optimize the social welfare; and authors in [17] have considered how to create an efficient market for demand response. In all these settings, customers' responses are captured by well-defined utility functions. These functions are assumed to be known to the operators, or at least to the users themselves.

In practice, these market based approaches can be difficult to implement because customers often do not have a clear model of their own utilities. *In practice, accurately estimating how customers respond to signals is a crucial step to the design and evaluation of DR programs.* As a motivating example used throughout this chapter, consider a building that participates in a demand response program. The building manager may receive a signal and take a set of actions, but the consumption of building depends on a multitude of (exogenous) variables, including external temperature, occupancy, etc. Therefore estimating the change in consumption because of a DR signal is not a trivial problem. Alternatively, consider a household with a smart energy management system (e.g., a NEST thermostat). This household will respond to a DR signal, but the response can be a complicated function of the current conditions in the household–e.g., temperature, appliances that are on, number of people at home and so on– and the user may not be consciously aware of the households' utility function. Therefore the operator needs to *learn customers' responses* from past history. Furthermore, because of the advancement of household sensors, this response need to

be learned under a possibly *high dimensional setting*.

By performing enough experiments with enough customers, that is, sending enough DR signals, the operator will eventually learn the users' response with accuracy. Repeated experimentation with large group of customers, however, is impractical for two reasons. The first is that operators only sends out DR signals if the demand need to be modified appreciably, and this event does not occur all that often in the power system. The second is that because of use fatigue [18], most utilities have agreements with their customers that a single household will only receive a limited number of DR requests [19]. Under these *limited data* regimes, accurately learning the response of users is nontrivial.

We first consider estimating the impact of DR from the perspective of experimental design. Formally, we define the treatment effect of DR signals using the standard Neyman-Rudin model [20]. In this model, the outcome $y_i$ (in our case is the energy consumption) takes on one of the two values: $y_i(0)$ or $y_i(1)$, depending on whether a DR signal is sent or not. Note that an observation can represent a user when the samples are extracted from a pool of different users , or it can represent a time slot when the samples are from the same user but during different time periods. Throughout this chapter, we refer to sample $i$ as the particular observation with index $i$, where the context of the observation should always be clear from the problem setting. In total, there are $N$ observations.

## *2.2 Motivation*

The fact that adding more data does not always improve estimation of the average treatment effect is not new. This can be seen as the difference between prediction and inference [21]. Adding more data will almost always improve prediction. But in our context, we are trying to estimate *the effect of a single variable, the DR signal, on the output*. Naively using more knowledge about customers may actually "drown out" the relationship between the DR signal and customer consumption. A message from this chapter is that the interactions between covariates and the treatment variable need to be carefully modeled to correctly leverage additional information contained in the covariates.

The need to provide inference also limits us in our choice of algorithms. Popular machine learning tools such as neural networks and regression trees often improve prediction, but they are not easy to interpret and use in estimation (see [22] and the references within). Hence we study three types of linear models in this chapter: simple linear regression (SLR), multiple linear regression (MLR), and modified covariate method (MCM). SLR has only one regressor which is the indicator of whether a DR signal is received, MLR has multiple regressors including the DR signal and the covariates that may affect consumption level. MCM is a multiple linear regression model with modified covariates discussed in detail in Section 2.4.

As a motivating example, we consider a large multifamily residential building with heating and cooling devices that participates in a demand response program. There are 8 apartments with central corridor on each floor, and office on first floor. An illustration of the building is shown in Fig. 2.1. Here we consider time as discrete intervals (on the scale of hours), and during any interval the building may receive a DR signal. This model of the building is constructed in the EnergyPlus software [23] based on a Seattle residence. We then use EnergyPlus to generate ground truth consumption data about the operation of the building. We add a linear term that represents the effect of demand response to create consumption data under a DR signal. The covariates of the building includes temperature, details of the fabrics of the roof, HVAC information, etc... These sample points are collected from many different time slots during various days.

Here we run both SLR and MLR to compare their performances. The magnitude of the demand response provided by the building is approximately 20% of its total consumption. When the building receives a DR signal fairly often, for example about 50% of the time periods, MLR outperforms SLR. But in the more likely scenario when the building rarely receives DR signal, SLR tends to out perform MLR. For example, when the building only receives DR signals 15% of the time, the estimation error (of the average impact of the DR signal) is around 7.6% from SLR, but 24.5% from MLR. This also motivates us to introduce the MCM estimator in Section 2.4, which under many settings is more robust than MLR but

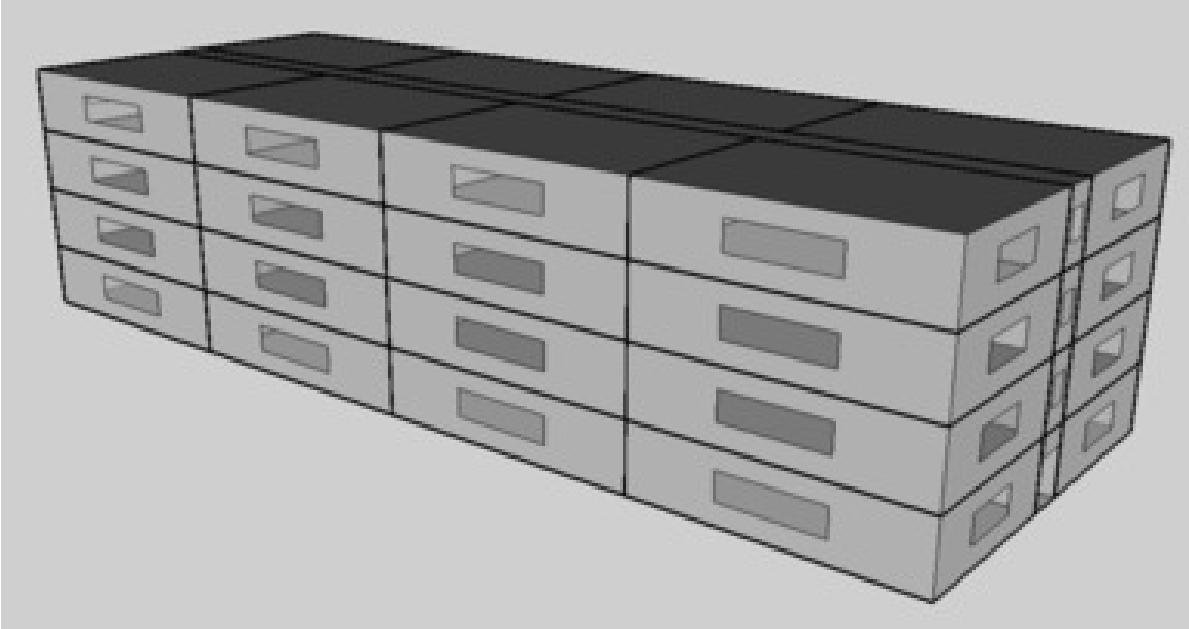

Figure 2.1: An illustration of the building used in this chapter. There are four floors in this multi-family residential building, with total floor area 3135 $m^2$.

more data efficient than SLR.

### *2.3 Problem setup*

Formally, we define the treatment effect of DR signals using the standard Neyman-Rudin model [20]. In this model, the outcome $y_i$ (in our case is the energy consumption) takes on one of the two values: $y_i(0)$ or $y_i(1)$, depending on whether a DR signal is sent or not. Note that an observation can represent a user when the samples are extracted from a pool of different users , or it can represent a time slot when the samples are from the same user but during different time periods. Throughout this chapter, we refer to sample $i$ as the particular observation with index $i$. In total, there are $N$ observations.

Let $x_i$ be the binary indicator variable of the DR signal. Then the two values of $y_i$, $y_i(0)$ and $y_i(1)$, are the potential outcomes either under the DR signal (when $x_i = 1$) or with no

DR signal (when $x_i = 0$). Using the experimental design terms, we sometime refer to all of the observations that have $x_i = 1$ as the treatment group and the observations with $x_i = 0$ as the control group.

In most settings, the consumption $y_i$ also depend on the covariates $\mathbf{z}_i$, and we can explicitly write $y_i$ as a function of $x_i$ and $\mathbf{z}_i$ as:

$$y_i = x_i y_i(1) + (1 - x_i) y_i(0) \tag{2.1a}$$

$$= f(\mathbf{z}_i) + g(\mathbf{z}_i) x_i, \tag{2.1b}$$

where $f(\mathbf{z}_i) = y_i(0)$, $g(\mathbf{z}_i) = y_i(1) - y_i(0)$. For the given $\mathbf{z}_i$, $g(\mathbf{z}_i)$ is the *treatment effect* of the DR signal: it is the difference in consumption for an observation with and without the signal. Most of the time, we are after the *averaged treatment effect (ATE)*, which is the empirical mean of $g(\mathbf{z}_i)$:

$$\bar{g} = \frac{1}{N} \sum_{i=1}^{N} g_i(\mathbf{z}_i). \tag{2.2}$$

In addition, we call $f_i(\mathbf{z}_i)$ the main effect for $i$. In the following sections, we write $f(\mathbf{z}_i)$ as $f_i$ and $g(\mathbf{z}_i)$ as $g_i$ for notational simplicity.

### *2.3.1 Assumptions*

We assume a randomized trial scenario, where the treatment assignment for each sample is independent Bernoulli ($p$) random variables, so they are independent of the covariates of the samples. This means that the treatment $x_i$ is a Bernoulli random variable which takes value 1 with probability $p$ and 0 with probability $1 - p$, independent to everything else [20].

Note that this assumption might seem strict, but it is not beyond unreasonable. First, if a utility or operator do not know the treatment effect of DR, it is natural to model the process as a random trial. For example, utilities typically ask buildings for demand response based on the condition of the entire system and there is no direct relationship between the requests and the state of the building, so the requests can be thought as randomized treatments. Second, if one observation group is significantly preferred for demand response over another

(e.g. commercial vs. residential users), the groups can be studied separately and modeled as receiving independent signals.

### *2.4 Linear regression*

In this section, we describe three different linear methods (shown in Table 2.1) to estimate the ATE ($\bar{g}$): SLR on treatment variable, MLR on both the treatment variable and the covariates, and a regression using MCM introduced in [24].

Table 2.1: Input for the least square estimation.

| **Model** | **Input** |
|---|---|
| SLR | $x_i$ and intercept |
| MLR | $x_i$, $\mathbf{z}_i$ and intercept |
| MCM | modified covariate $(x_i - p)\mathbf{z}_i$ and intercept |

$x_i$: binary indicator of DR signal, $p$: probability of receiving signal, and $\mathbf{z}$: covariates containing side information.

In all of these methods, we use least square (LS) to compute the estimator in the linear regression. Algorithm 1 depicts the estimation procedure for the following canonical linear regression model:

$$y_i = \tilde{\boldsymbol{z}}_{\boldsymbol{i}}^{\top} \boldsymbol{\beta}^{\dagger} + \epsilon_i, \tag{2.3}$$

where $\tilde{\boldsymbol{z}}_{\boldsymbol{i}} = [x_i \ \boldsymbol{z}_i \ 1]$, $\boldsymbol{\beta}^{\dagger} = [\beta; \boldsymbol{\gamma} \ ; \gamma^{(0)}]$, $y_i$ is observed power consumption, $\epsilon_i$ is the noise, and we call $\tilde{\boldsymbol{z}}_{\boldsymbol{i}}$ the regressor variable. The regressors $\tilde{\boldsymbol{z}}_{\boldsymbol{i}}$ include a binary variable $x_i$ that indicates the treatment assignment, a possible set of covariates $\mathbf{z}_i$ such as temperature and building device information, and an intercept. Note that since an intercept is included, LS estimator on ATE, i.e., on $\beta$, is the same if we use $x_i - p$ as the regressor instead of $x_i$, where

$p = \frac{1}{N}\sum_i x_i$. In addition, parameter $\boldsymbol{\beta}^\dagger$ is the weight associated with the regressor variable $\tilde{\boldsymbol{z}}_{\boldsymbol{i}}$ where $\beta$ turns out to be the ATE.

**Algorithm 1** Linear regression estimation

1: **Input**: $N$ observations $(y_i, \tilde{\boldsymbol{z}}_{\boldsymbol{i}})$ for $i = 1, \ldots, N$. Stacking into output vector $\mathbf{Y} = [y_1, \ldots, y_n]$, and regressor (input) matrix $\tilde{\boldsymbol{Z}}$ with rows $\tilde{\boldsymbol{z}}_{\boldsymbol{1}}^\top, \tilde{\boldsymbol{z}}_{\boldsymbol{2}}^\top, \ldots, \tilde{\boldsymbol{z}}_{\boldsymbol{N}}^\top$ as observations of regressors. The weights are denoted by $\boldsymbol{\beta}^\dagger \in \mathcal{R}^d$.

2: The least square estimation for $\boldsymbol{\beta}^\dagger$ is:

$$\hat{\boldsymbol{\beta}}^\dagger = (\tilde{\boldsymbol{Z}}^\top \tilde{\boldsymbol{Z}})^{-1} \tilde{\boldsymbol{Z}}^\top \boldsymbol{Y}. \tag{2.4}$$

3: **Ouput**: The estimator $\hat{\beta}$, the first element of $\hat{\boldsymbol{\beta}}^\dagger$, which will be the estimate of the ATE.

For the three regressions in Table 2.1, their differences are in how the regressor ($\tilde{\boldsymbol{z}}$) and noise ($\epsilon$) are defined. The rest of this section show how they can be written in the canonical form in (2.3) and how to find the ATE.

For all three regressions the LS estimator in Algorithm 1 turns out to be consistent, i.e., as the number of samples grows, it will eventually converge to the correct value [25]. Therefore, to compare their performances, we look at the *variances* of the estimators, in particular in how fast the variances decrease as the number of samples increases.

### *2.4.1 SLR on Treatment*

Define $p = \frac{1}{N}\sum_i x_i$, which means that $pN$ samples are getting treatments (the DR signal). It can also be interpreted as the probability that each sample gets treated. The two interpretation are equivalent for estimation [21]. We then rewrite (2.1b) into the following form by centering the variables:

$$\begin{aligned} y_i &= (x_i - p)\bar{g} + \bar{g} + \bar{f} + x_i(g_i - \bar{g}) + (f_i - \bar{f}) \\ &= \begin{bmatrix} x_i - p \\ 1 \end{bmatrix}^\top \begin{bmatrix} \bar{g} \\ \bar{g} + \bar{f} \end{bmatrix} + \epsilon_i, \end{aligned} \tag{2.5}$$

where the noise $\epsilon_i = x_i(g_i - \bar{g}) + (f_i - \bar{f})$, with $\bar{g} = \frac{\sum_i g_i}{N}$ and $\bar{f} = \frac{\sum_i f_i}{N}$. In canonical form of (2.3), $\tilde{\boldsymbol{z}}_{\boldsymbol{i}} = \begin{bmatrix} x_i - p & 1 \end{bmatrix}^T$ and $\boldsymbol{\beta}^\dagger = \begin{bmatrix} \bar{g} & \bar{g} + \bar{f} \end{bmatrix}^T$, where $\beta = \bar{g}$. Let $\bar{x}_i = x_i - p$ and using the fact that $\sum_i \bar{x}_i = 0$, the LS estimator for the average treatment effect $\bar{g}$ is:

$$\hat{\bar{g}}_{SLR} = \frac{\sum_i x_i(g_i + f_i)}{\sum_i T_i} - \frac{\sum_i (1 - x_i) f_i}{\sum_i (1 - T_i)}. \tag{2.6}$$

The result in (2.6) shows that the estimator from SLR is the same as the difference-in-mean estimator [26]. It simply takes the difference between the average outcome between the treatment group and the control group to estimate the impact of the DR signal. However, this estimator is data inefficient, since it ignores any side information about the covariates that may be available.

### *2.4.2 MLR on Treatment and Covariates*

Now suppose that we know some covariates of each customer $i$ and they are denoted by $\mathbf{z}_i$. A multiple linear regression model is carried out when both the treatment variable $x_i$ and $\mathbf{z}_i$ are included as regressors in (2.3) and the estimate of ATE is again the first parameter of the estimate of $\boldsymbol{\beta}^\dagger$: $\hat{\bar{g}}_{MLR} = \hat{\beta}$. However, the noise term maybe significant if the underlying true model is not linear.

The simulation results of the MLR estimator is presented in Section 5.6. If we compare SLR and MLR by the reduction in the variance of the estimators, the latter does not always improve the estimation performance compared with the former. This phenomena is mainly due to the fact that if the underlying true relationship is nonlinear, modeling covariates has having a linear relationship with consumption introduces large noises, especially if $p$ is small. More detailed theoretical discussions are presented in Section 2.5.

### *2.4.3 Modified Covariate Method*

Even if including covariates directly into the linear model does not necessarily improve performance, it is still desirable to somehow use the covariate information. One possible improvement is to *only assume linearity in the treatment effect for each customer $i$*. That is,

only $g_i$ is linear in the covariates, and no assumption is made about how the main effect $f_i$ depends on the covariates.

We thus use a new method called *Modified covariate method* (MCM), proposed in [24]. This method assumes that the treatment effect is linear in the covariate, i.e., $g_i = \mathbf{z}_i^\top \gamma$, but we do not impose any conditions on $f_i$. In this case, the average treatment effect is:

$$\bar{g}_{MCM} = \frac{1}{N} \sum_i \mathbf{z}_i^\top \boldsymbol{\gamma}. \tag{2.7}$$

We then have the following linear regression model: $Y_i = f_i + T_i \mathbf{x}_i^\top \boldsymbol{\gamma}$. Again, rewrite it in a canonical form:

$$\begin{aligned} y_i &= (x_i - p)\mathbf{x}_i^\top \boldsymbol{\gamma} + \bar{f} + p\bar{\mathbf{z}}^\top \boldsymbol{\gamma} + (f_i - \bar{f}) + p(\mathbf{z}_i - \bar{\mathbf{x}})^\top \boldsymbol{\gamma} \\ &= \begin{bmatrix} (x_i - p)\mathbf{z}_i \\ 1 \end{bmatrix}^\top \begin{bmatrix} \boldsymbol{\gamma} \\ \gamma^{(0)} \end{bmatrix} + \epsilon_i, \end{aligned} \tag{2.8}$$

where the noise $\epsilon_i = (f_i - \bar{f}) + p(\mathbf{z}_i - \bar{\mathbf{z}})^\top \boldsymbol{\gamma}$. We refer to $(x_i - p)\mathbf{z}_i$ as the *modified covariate*. The LS estimator is still consistent [24] and we can estimate the treatment effect of the DR signal as $\hat{\bar{g}}_{MCM} = \frac{1}{N} \sum_i \mathbf{z}_i^\top \hat{\boldsymbol{\gamma}}$.

There are two reasons that MCM is potentially useful in estimating the ATE. First, MCM trades off between how much covariate information to use and model simplicity. The covariate information is only used with respect to the treatment effect, which is a weaker assumption than MLR. On the other hand, MCM captures more information by still using the covariates, which makes it more data efficient than SLR. Secondly, its formulation fits an interesting regime in the context of demand response. For example, the DR capability of a building could very well proportional to the covariates (e.g., proportional to the occupancy of the building).

## 2.5 Variance analysis

### 2.5.1 Comparison between SLR and MLR

In this section, we compare the linear models assuming that $\mathbf{z}_i$ is one dimensional, $z_i$. The multidimensional case is discussed in Section 2.6. The main result is presented in Theorem 1, where we adopt the notation that $\text{Cov}(\cdot,\cdot)$ stands for the empirical covariance between two vectors, i.e., $\text{Cov}(\mathbf{f},\mathbf{z}) = \frac{\sum_i (f_i-\bar{f})(z_i-\bar{z})}{N}$, and $\text{Cov}(\mathbf{g},\mathbf{z}) = \frac{\sum_i (g_i-\bar{g})(z_i-\bar{z})}{N}$.

**Theorem 1.** *If $Cov(\mathbf{g},\mathbf{z}) = 0$ or $p = 0.5$, then MLR always yields a better performance than SLR. Otherwise, the performance of the two estimators depends on the value of $p$ and $\Upsilon = \frac{Cov(\mathbf{f},\mathbf{z})}{Cov(\mathbf{g},\mathbf{z})}$. Assuming WLOG that the covariate $z_i$ has unit variance, then:*

$$Var(\hat{\bar{g}}_{SLR} - \bar{g}) - Var(\hat{\bar{g}}_{MLR} - \bar{g}) = \frac{\Delta}{p(1-p)N}, \tag{2.9}$$

*where:*

$$\begin{aligned}\Delta &= (Cov(\mathbf{f},\mathbf{z}))^2 + 2(1-p)\, Cov(\mathbf{g},\mathbf{z})\, Cov(\mathbf{f},\mathbf{z}) \\ &+ (2p-3p^2)(Cov(\mathbf{g},\mathbf{z}))^2.\end{aligned} \tag{2.10}$$

Detailed proof is left in [27] for interested readers. Note that $\Upsilon$ represents the intensity that how $f$ and $g$ are correlated: a negative $\Upsilon$ implies negative correlation whereas a positive $\Upsilon$ implies positive correlation. The important conclusion from Theorem 1 is that $\Delta$ can be both negative and positive. The sign of $\Delta$ includes many factors such as the choice of $p$ and the correlation between the responses and the chosen covariate. The simplest case is when $g_i$ is a constant. In this case, $\Delta \geq 0$, which means that MLR is at least as good as SLR, given any arbitrary assignment probability $p$. When $p \neq 0.5$ and $g_i$ is not a constant across all samples, the sign of $\Delta$ depends both on $\mathbf{g}$ and $\mathbf{f}$. Figure 2.2 depicts the $(p,\Upsilon)$ region that results in a negative $\Delta$, which means that MLR is worse than SLR.

From Fig.2.2, we observe that the shaded region is asymmetric with respect to ratio $\Upsilon$. This is mainly due to the fact that the signal-to-noise ratio in the MLR model is not symmetric with respect to $\Upsilon$. In addition, from Fig.2.2, we further observe that if $\mathbf{g}$ and $\mathbf{f}$ is positively correlated, i.e., $\Upsilon > 0$, then SLR performs better when a lot of samples get

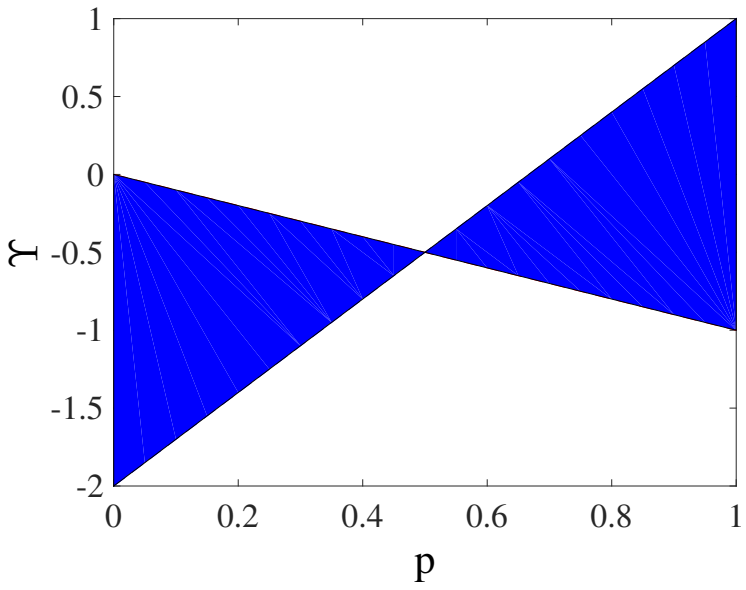


Figure 2.2: $(p, \Upsilon)$ region (in blue) that results in a negative $\Delta$, where $p$ is the treatment assignment probability and $\Upsilon = \frac{\text{Cov}(\mathbf{f},\mathbf{z})}{\text{Cov}(\mathbf{g},\mathbf{z})}$. The blue region also represent the pair of $(p, \Upsilon)$ when SLR is better than MLR.

treatment ($p$ is large, and $\Delta < 0$). This mens that the operator should trust the result by regressing on $x_i$, when the majority of samples are in the treatment group.

When $\mathbf{g}$ and $\mathbf{f}$ is negatively correlated, SLR performs better when a few samples get treatment ($p$ is small, and $\Delta < 0$). This suggests that it is better to perform SLR when only a few samples are in the treatment group, i.e., when the treatment signals are scarce. For demand response, this is a regime of interest, since most customers receive relatively few DR signals, and the correlation between the main effect and treatment effect is negative. For example, considering temperature as the covariate, then the consumption increases together with temperature because of higher cooling needs. However, when temperature is high, people may be more reluctant to reduce consumption (turn off AC's in this case) to respond to DR signal.

From Fig. 2.2, we also observe that $\Delta$ changes sign when altering $p$ and fixing $\Upsilon = 0$.

This is another interesting regime of demand response, when the treatment effect of each unit, i.e., $g_i$, is linear in the covariates, and the normal consumption is a constant ($f_i = f_c$ is a constant). In this case, the linear regression model is expressed in (2.11):

$$y_i = x_i z_i \gamma + f_c + \epsilon_i, \tag{2.11}$$

where $g_i = z_i \gamma$.

This is a regime of interest in demand response. For example, the normal consumption without demand response does not appreciably rely on covariates but the treatment effect may depend on the covariates. In this case, $\Delta = (2p - 3p^2)(\mathrm{Cov}(\mathbf{g}, \mathbf{z}))^2$ meaning that as long as $0 < p < \frac{2}{3}$, MLR is better than SLR.

### *2.5.2 Comparison between SLR/MLR and MCM*

We can also analyze the performance of MCM with SLR and MLR in this specific case. We again restrict ourselves to one dimensional analysis (the covariate $z_i$ is one dimensional), as in last section. The main claim is shown in Remark 1, with the assumption that the covariate follows a Gaussian distribution with unit variance and mean denoted by $\mu$. An illustration of a more general case with multi-dimensional covariate is shown at the end of this section. In addition, we show in Section 5.6 that the intuition built from the analysis here carries over to real world data, whose distribution may not be Gaussian.

**Remark 1.** *Consider the setup in* (2.11)*, where the normal consumption $f_i$ is a constant and the treatment effect to the signal $g_i$ is linear in the covariate $x_i$. Suppose that the covariate $z_i$ follows a Gaussian distribution with mean $\mu$ and unit variance. Then the performances of the three estimators depend both on the value of $p$ and $\mu$. We find that MCM performs the best when $p$ is relatively small and SLR performs the best when $p$ is relatively large. Otherwise, MLR yields the best estimator for ATE, i.e., $\bar{g}$, when $p$ takes on moderate values between 0 and 1. The variance of the proposed linear estimators are shown in* (2.12a)*,* (2.12b) *and*

(2.12c)*:*

$$\begin{aligned} Var(\hat{\bar{g}}_{MCM} - \bar{g}) &= Var((\hat{\gamma} - \gamma)\frac{\sum_i z_i}{N}) \\ &\approx \frac{\gamma^2\mu^2p^2(3+\mu^2)}{Np(1-p)(1+\mu^2)^2}, \end{aligned} \tag{2.12a}$$

$$Var(\hat{\bar{g}}_{SLR} - \bar{g}) = \frac{(1-p)^2\gamma^2}{p(1-p)N}, \tag{2.12b}$$

$$Var(\hat{\bar{g}}_{MLR} - \bar{g}) = \frac{(2p-1)^2\gamma^2}{p(1-p)N}. \tag{2.12c}$$

From the above expressions, we see that MCM performs better when $p$ is relatively small and worse when $p$ is relatively big. To illustrate that the estimators are different, consider the case when $\mu = 1$. We find that when $p$ is close to 1, then SLR performs the best. On the contrary, when $p$ is close to 0, then MCM yields the smallest variance. When $p$ is around 0.5, MLR outperforms both SLR and MCM in terms of variance reduction. Therefore, if the model in (2.11) correctly captures the consumption behavior, when the treatment signal is scarce, it is preferable to use MCM to estimate ATE. A more general case study can be found in [27] for interested readers.

Overall, based on the discussion in Section 2.5, the observation of the variance is summarized as the following:

- If $\mathbf{g}$ and $\mathbf{f}$ is positively correlated, then MLR performs better when $p$ is small.
- If $\mathbf{g}$ and $\mathbf{f}$ is negatively correlated, then MLR performs better when $p$ is large.
- If $\mathbf{g}$ is not correlated with $\mathbf{z}$, then MLR performs better.
- If $\mathbf{f}$ is not correlated with $\mathbf{z}$, then MLR performs better if $p$ is relatively small ($p < \frac{2}{3}$), otherwise SLR performs better.
- If the covariate $z_i$ is one dimensional, $g_i$ is linear in $z_i$, and $f_i$ is a constant across all sample $i$, MCM works better when a few samples get treatment signal, SLR works bet-

ter when many samples get treatment signal, and MLR works better when a moderate number of samples get treatment signal.

## *2.6 Simulation results*

In this section, we conduct experiments on data from three sources: synthetic data, building data, and data from Pecan Street [28].

### *2.6.1 Synthetic Data*

We first generate data from two linear models, with one dimensional covariate $x_i$ drawn from a Gaussian distribution with unit mean and unit variance. The models are:

$$y_i = z_i\gamma_1 + z_i\gamma_2 x_i, \tag{2.13a}$$

$$y_i = \gamma_0 + z_i\gamma_2 x_i. \tag{2.13b}$$

We take $\gamma_1 = 6$ and $\gamma_2 = 20$, so that $\Upsilon = 0.3$ for (2.13a). From Theorem 1, this means that SLR performs better if $p > 0.77$. For (2.13b) $\Upsilon = 0$, since the main effect is a constant. We further set $\gamma_0 = 20$, and the simulated covariate to be centered at 1. This is the regime discussed at in Section 2.5, with the case where main effect $f_i$ is a constant and that treatment effect is linear, i.e., $g_i = z_i\gamma_2$. The results are shown in Fig. 2.3.

As can be seen from Fig. 2.3, the performances of the three estimators depend on both the assignment probability $p$ and the structure of the underlying model. The results from Fig. 2.3(a) supports our claim that when the treatment assignment probability is high, i.e., $p = 0.9$, SLR performs the best with model in (2.13a). As for the model presented in (2.13b), according to the discussions in Section 2.5, MCM is the best estimator with least variance, which is demonstrated in Fig. 2.3(b).

### *2.6.2 Building data*

In this section, we validate the claim via building data generated using EnergyPlus [23]. Using this software, we generate building covariates such as environment temperature, number

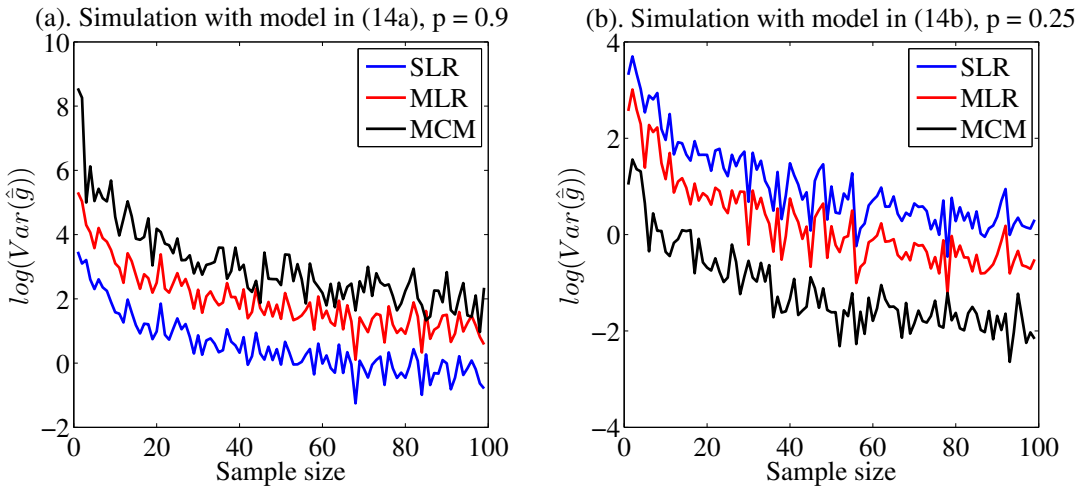


Figure 2.3: Variance of the three estimators of linear model in semi-log scale. Left figure for (2.13a) with $p = 0.9$, right figure for (2.13b) with $p = 0.25$.

of occupants, appliances scheduling, etc. They are denoted by a vector $\mathbf{z}_i$ for each single observation $i$. The building model is illustrated in Fig. 2.1 at Section 2.2. In this specific residential building, there are four floors with eight apartment located at each floor and office located at the first floor. The total floor area is 3135 squared meters. In this dataset, each sample point contains a consumption data point, as well as covariate values. DR signals are randomly assigned in time and the goal is to estimate its impact.

More specifically, the sample index $i$ denotes different time slots of the building consumption model. The treatment $x_i$ is added to $f_i$, so the final output of the simulated building consumption under DR signal is $y_i = f_i + g_i x_i$, where $g_i$ is the treatment effect of building $i$. To validate the claims in this chapter, we consider two scenarios: 1) $g_i$ is a constant (when treatment effect is a constant across all sample points); 2) $g_i$ is linear in $\mathbf{z}_i$ (when treatment effect is linear in the covariates for each sample point). The models that we consider in the simulation are: 1) The linear models, i.e., SLR/MLR/MCM as discussed in this chapter; 2) A neural network, because of its predictive performances [29]. For the purpose of this simulation, the input of the neural network is the covariates as well as the binary treatment

signal for each different sample, the output is the corresponding electricity consumption.

Table 2.2: Var $\hat{\bar{g}}$ (normalized) based on EnergyPlus data, where $p = 0.5$ and $g_i$ is a constant.

| **SLR** | **MLR** | **MCM** | **Neural net** |
|---|---|---|---|
| 1.000 | 0.100 | 1.506 | 1.667 |

The results of the two scenarios are shown in Table 2.2 ($g_i$ is a constant) and Table 2.3 ($g_i$ is linear in $\mathbf{z}_i$). When $g_i$ is a constant, as shown in Table 2.2, MLR performs the best among all the three methods because the variance of ATE is the lowest. This validates the proposed claim in Theorem 1 that as long as $g_i$ is a constant, MLR is always the best linear estimator, for all possible values of $p$. As can be seen from Table 2.2, neural network exhibits a high variance as compared to linear models. This indicates that a neural network is prone to overfit when there is not a large amount of data, even when the actual ground truth is simple, and may not be suitable as a reliable inference method.

Next, we generate another set of DR simulations with $g_i = \mathbf{z}_i^\top \boldsymbol{\gamma}$, i.e., that the treatment effect is linear in the covariates of the particular building $i$. We compare the estimators based on their variance and the results are illustrated in Table 2.3, where the treatment assignment probability $p = 0.15$. From Table 2.3, we observe the opposite as to Table 2.2, that MLR yields the worst performance among all three estimators. In addition, MCM and SLR have similar performances. Therefore, contrary to the case in Table 2.2, the utility company should not blindly trust the results from a seemingly more powerful model, i.e., MLR, and should be careful about the interactions between covariates when modeling consumption behavior. The neural network is a still more complex model, but in this regime, it is still inferior to a simple linear regression model when it comes to estimating ATE, i.e., $\bar{g}$.

In all, the observations from Table 2.2 and Table 2.3 validate the claim in this chapter, that it is not always good to conduct a full linear regression with all the covariates in the model, since the inclusion of those covariates may lead to a larger noise if the linear regression

model is not correctly defined.

Table 2.3: $\operatorname{Var}\hat{\bar{g}}$ (normalized) based on EnergyPlus data, where $p = 0.15$ and $g_i$ is linear in $\mathbf{z}_i$.

| **SLR** | **MLR** | **MCM** | **Neural net** |
|---|---|---|---|
| 1.000 | 3.191 | 1.020 | 5.622 |

### *2.6.3 Pecan Street Data*

In this section, we test the estimators on data from Pecan Street [28], which provides massive real consumption data to researchers. In our tests, we treat the high price signals as treatments and the user index as the sample point index. The outcomes are these users' consumption data. To compose the treatment group and control group, we extract the high price signal and include users whose consumption data is available at that time into the treatment group, and put other users in the control group. For the users in the control group, we find their consumption data at the same hour in the date closest to the high price signal date. This mimics the situation where the signals are randomized assigned, since each user has some chance of receiving a specific signal. As standard practice, we use temperature as the covariate [1]. Other covariates such as appliance information can easily be added.

Since we do not know the true ATE and the true model for observational data, we use $p$-values associated with the $t$-test and the $F$-test to make comparisons with Pecan Street data. These tests are hypothesis tests for linear regression models [30]. The difference between $t$-test and $F$-test is that $t$-test only examines whether including one particular regressor significantly improve the model whereas the $F$-test examines whether including all regressors significantly improve the model. When sample size and the number of covariates are fixed to fit a linear regression model, a lower $p$-value suggests a higher explained variance

of the model [21], which is resulted from higher accuracy in the estimators (lower variance of the estimator). We can thus relate the computed $p$-values to the accuracy of the estimators in our case study here.

Suppose that we just include one covariate into the model, then the regressor becomes $\tilde{\boldsymbol{z}}_i = [x_i - p\ ; z_i\ ; 1]$ and $\boldsymbol{\beta}^\dagger = [\beta\ ; \boldsymbol{\gamma}\ ; \gamma^{(0)}]$. Therefore $\bar{g} = \beta$ is the ATE to a specific DR signal, $x_i - p$ is the centered binary indicator variable for DR signal and $z_i$ is the covariate. The null hypothesis for the $t$-test in this regression model is $H_0 : \beta = 0$ and for the $F$-test is $H_0 : \beta = 0, \boldsymbol{\gamma} = 0$. For both tests, we examine the significance by setting a confidence level $\alpha$, normally taken as 0.05, or more strictly as 0.01. While comparing the values of a certain statistic under different models does not seem intuitive, we can alternatively resort to $p$-value, which is defined as the probability of obtaining the observed(or more extreme) result under the null hypothesis. Higher $p$-values suggest that the null hypothesis is true, whereas smaller $p$-values suggest the opposite. We then can compare the $p$-value to interpret the significance test under different regression models.

In addition, the treatment group has 100 observations and the control group has 500 observations. We want to emphasize here that the data set is not as large as the data set to train prediction models because of the sparsity of DR signals. The estimation of ATE from the three linear models are shown in Table 2.4. As can be seen from Table 2.4, the estimation obtained by MLR is lower than that from SLR, we then perform MCM and its estimation of ATE is again higher than MLR. These results suggest that MLR might have returned an underestimate of ATE, even with extra regressors.

Table 2.4: Estimation results for pecan street data.

| | $\hat{\bar{g}}_{SLR}$ | $\hat{\bar{g}}_{MLR}$ | $\hat{\bar{g}}_{MCM}$ |
|---|---|---|---|
| Estimation of ATE | 1.16 | 0.59 | 0.90 |

We further examine the performance of the models by significance tests. The results

are shown in Table 2.5. From the results in Table 2.5, we can see that the $p$-value with the $F$-test for all methods is generally small, meaning that the consumption data cannot be explained by just an intercept. However, the $p$-value associated with the $t$-test is the highest for MLR, suggesting the insignificance of regressing on the treatment variable if the threshold is 0.01. This is mainly due to the lack of information on how the covariates interact with consumption data and that the treatment group is much bigger than the control group. So if an utility uses MLR to estimate the ATE, it may conclude that the DR program is ineffectual by mistake. It is then beneficial to run more significance tests in SLR and MCM to gain more insights to the significance of the treatment effect. This example also shows that including covariates will improve prediction (smaller $p$-value for the $F$-test), but not necessarily inference.

Table 2.5: Significance results for pecan street data.

| | **SLR** | **MLR** | **MCM** |
|---|---|---|---|
| $p$-value for $t$ test | 2.7e-7 | 1.4e-2 | 2.9e-09 |
| $p$-value for $F$ test | 2.7e-7 | 1.4e-4 | 2.9e-09 |

From Table 2.5 we can see that the $p$-value for $t$-test with MCM is small, suggesting that we should regress on the modified covariate. In this case, the SLR and MCM estimates agree, providing confidence that the ATE is close to 1 rather than the value of 0.59 as suggested by MLR.

## *2.7 Summary*

In this Chapter, we estimate the average treatment effect (ATE) of demand response programs, defined as the average change in consumption when users receive DR signals. We derive linear estimators for ATE through simple linear regression, multiple linear regression

and modified covariate method. The simulation results show that although including more covariates may be good for prediction purposes (as in multiple linear regression), the performance of the estimators depend both on the assignment probability and the correlation between the effect and the covariate. Thus, the interactions between the covariates and the demand response signal must be carefully modeled and we provide practical guidance on which estimators should be used based on both synthetic and real data.

# Chapter 3

# DESIGN THE BEST INCENTIVE – STATIC DEMAND RESPONSE

## *3.1 Introduction and literature review*

In the last Chapter we discuss about the difference between SLR and MLR when randomized assignment is used to estimate DR. Randomized trial is usually thought as the "gold standard" in these types of models mainly due to the fact that randomly assigning treatments to users removes the effect of confounding factors and provides a consistent estimate of the treatment effect. In the presence of many covariates, however, random assignment can be extremely inefficient. In fact, as we show in this chapter, in the high dimensional setting, random assignment *does not reduce the variance* of the estimate of the average treatment effect, even as the number of treatment grows without bound. Instead, following the outline in [31], we design a selection scheme users are picked based on their covariates to be treated.

Suppose there are $N$ total users in the system. Under the linear models considered in this proposal, the best possible lower bound on the rate of variance reduction is $\Omega(1/N)$,[1] given by considering the Fisher information [32]. As discussed later, under high dimensional settings, a randomized algorithm can only achieve $\Omega(1)$, even when there are large number of fraction of users are assigned DR signals. The main contributions of this Chapter are:

1. We show if the number of users selected is a constant fraction of the total number of users, there exists user assignments that achieve a variance reduction rate of $\Theta(1/N)$. This rate is independent of the dimension of the covariates, as long as it is less than $N$.

[1] no estimator can reduce variance faster than $1/N$

2. We develop a tractable user assignment algorithm. This algorithm is obtained by converting the variance reduction problem in a densest-cut problem on a graph [33–36].

Our approach differs from previous effort in learning demand response in one important regard. In previous studies, the focus was on training the best predictive model and subtracting out the predicted consumption from the measured consumption [37, 38]. In our approach, we do not ever learn a predictive model, in the sense that we do not learn the relationship between the covariates and the consumption. Rather, focus on learning a single parameter: the response to the DR signal.

The results in [31] act as an impetus to this work. The main difference is that in [31], the users are assigned a treatment of $\pm 1$, therefore some information is always conveyed by this assignment. In our model, the users are assigned either 1 (receives DR signal) or 0 (no signal). Therefore, for the users assigned 0, we do not obtain any information about the impact of DR signals. This makes the problem much more technically challenging, and consequently we only consider the offline assignment problem whereas [31] also considers the online assignment problem. There are extensive literature on average treatment effect estimation, and the interested reader can refer to [20, 26] and references within.

### *3.2 Preliminaries and problem formulation*

In this Chapter we assume that a user's consumption is given by a linear model. Let $x_i \in \{0, 1\}$ denotes a binary DR signal, where 1 represents that a signal is sent to user $i$ and 0 presents that no signal is sent. A covariate vector $\boldsymbol{z}_i$ is also associated with a user, representing available side information. For example, side information may include local temperature, user's household size, and number of electrical vehicles and so on. We denote the dimension of the covariate vector by $d$, and assume the last component is 1, which is the intercept. Let $y_i$ denote the consumption of user $i$, which is given as

$$y_i = \beta x_i + \boldsymbol{\gamma}^T \boldsymbol{z}_i + \epsilon_i, \tag{3.1}$$

where $\epsilon_i$ is white noise with variance $\sigma^2 = 1$ (for convenience). The coefficient $\beta$ is the impact of the DR signal and estimating it efficiently is the goal of the chapter. The coefficient $\boldsymbol{\gamma}$ represents the effect of the covariate vectors. The main technical challenge is to accurately estimate the coefficient of interest $\beta$, even when $\boldsymbol{\gamma}$ is high dimensional. For analytical simplicity, we assume that the entries of $\boldsymbol{z}_i$ are drawn as i.i.d. Gaussian random variables (possibly after centering and rescaling). In simulations (Section 3.6), we show that the results holds for other types of distributions as well.

We assume there are $N$ total users. In this model, a single user that receives two demand response signals at two different times is equivalent to two users each receiving a demand response signal. Therefore, we suppress the time dimension and label all users by $i$. Note that in (3.1), all users share a common response $\beta$ to DR signals.

We denote the estimate of $\beta$ by $\hat{\beta}$. The value of $\hat{\beta}$ is a function of the DR assignments, that is, the value of the $x_i$'s. Under the linear setting in (3.1), the ordinary least square (ols) estimator $\hat{\beta}$ of $\beta$ is unbiased for all possible allocations of DR assignments, $\hat{\beta}$ is centered at the true value $\beta$. The natural measure of performance is then the variance: $\operatorname{Var}\hat{\beta}$. With some simple linear algebra, the variance of $\hat{\beta}$ is given by [25]:

$$\operatorname{Var}\hat{\beta} = \frac{\sigma^2}{\boldsymbol{x}^{\mathrm{T}} P_{\boldsymbol{Z}^\perp} \boldsymbol{x}}, \tag{3.2}$$

where $P_{\boldsymbol{Z}^\perp} = I - \boldsymbol{Z}(\boldsymbol{Z}^{\mathrm{T}}\boldsymbol{Z})^{-1}\boldsymbol{Z}^{\mathrm{T}}$. The $i$'th row of the data matrix $\boldsymbol{Z}$ is given by $\boldsymbol{z}_i^T$. We adopt the notation that $\boldsymbol{Z}_{N,d}$ denotes a matrix $\boldsymbol{Z}$ that has $N$ rows and $d$ columns, while $\boldsymbol{Z}_{i:j}$ denotes the $i^{th}$ to $j^{th}$ column of a matrix $\boldsymbol{Z}$, where $i \leq j$.

We are primarily interested in the setting where an operator can assign a limited number of $x_i$'s to be 1. This setting reflects the limit in budget of an operator in sending DR signals. Specifically, let $k$ be the total number of DR signal that can be sent. The goal of the operator is to strategically assign $k$ $x_i$'s to be 1 such that the variance of $\hat{\beta}$ is minimized. In particular, we are interested in the rate of reduction of $\hat{\beta}$ as $N$ increases and in settings where $k/N$ is a constant.

From (3.2), minimizing the variance of $\hat{\beta}$ is equivalent to maximizing the quantity $\boldsymbol{x}^{\mathrm{T}} P_{\boldsymbol{Z}^\perp} \boldsymbol{x}$,

and we focus on the latter quantity in the rest of the chapter due to notational convenience. Two types of algorithms are of interest: i) the standard random assignment where each $x_i$ is chosen to be 1 or 0 with probability $k/N$, and ii) an optimal assignment procedure where $x_i$'s are chosen to maximize $\boldsymbol{x}^{\mathrm{T}} P_{\boldsymbol{Z}^{\perp}} \boldsymbol{x}$. Both algorithms face the constrain that only $k$ out of $N$ $x_i$'s can be assigned to be 1. We characterize *growth rate* of quantity $\boldsymbol{x}^{\mathrm{T}} P_{\boldsymbol{Z}^{\perp}} \boldsymbol{x}$ in terms of $k, N$ and $d$, or equivalently, the decay rate of $\mathrm{Var}\,\hat{\beta}$.

We show that when $d$ is relatively small compared to $N$, the two strategies yield similar rates of $\Theta(N)$. In a high dimensional setting where $d$ is comparable to $N$, e.g., $d = N - 1$, however, the random assignment is essentially useless in estimating $\beta$, in the sense that $\boldsymbol{x}^{\mathrm{T}} P_{\boldsymbol{Z}^{\perp}} \boldsymbol{x}$ remains a constant in expectation as $N$ grows. Our proposed strategy, on the other hand, improves the rate to $\Theta(N)$ in this case, as long as $k/N$ is a constant. In Section 3.3, we discuss the randomized strategy. The optimal assignment algorithm is then considered in Section 3.4.

### *3.3 Random assignment*

Random assignment has been extensively studied in literature, mainly because it balances the covariates in two groups and eliminate the influence of confounders [26]. For our model in (3.1), random assignment means that a subset of $k$ $x_i$'s are chosen at random and assigned a value 1. Theorem 2 quantifies the rate of the increase of $\boldsymbol{x}^{\mathrm{T}} P_{\boldsymbol{Z}^{\perp}} \boldsymbol{x}$.

**Theorem 2.** *Random assignment achieves a rate of* $\Theta((N-d)\frac{k(N-k)}{N^2})$. *If* $\frac{k}{N} = p$ *is a constant, then this rate is* $\Theta(N-d)$. ■

Before proving Theorem 2, we discuss the scaling rate under the setting when $k/N = p$ is a constant. In practice, this is the regime of interest since it is reasonable to suppose that a fraction (e.g. 10%) of users receives DR signals. In this case, the rate achieved by random assignment is $\Theta(N-d)$. This rate is $\Theta(N)$ when $d$ is relatively small compared to $N$. However, when $d$ is large, e.g., $d = N - 1$, then this rate becomes $\Theta(1)$. This rate is not desirable as it indicates that the variance of the estimator is not decaying with $N$ even when

$N$ is large. Thus we would like to design an assignment strategy which yields an estimator that still possesses a relatively good performance even when $d$ is very close to $N$. In the next section, we show that with optimal assignment, we achieve the optimal rate $\Theta(N)$ when $\frac{k}{N} = p$. The proof of Theorem 2 follows.

*Proof.* We consider a random assignment where $\Pr\{x_i = 1\} = \frac{k}{N}$. Then the rate becomes:

$$\begin{aligned}
&\mathbb{E}\,\mathrm{tr}\{\boldsymbol{x}^{\mathrm{T}}(I - \boldsymbol{Z}(\boldsymbol{Z}^{\mathrm{T}}\boldsymbol{Z})^{-1}\boldsymbol{Z}^{\mathrm{T}})\boldsymbol{x}\} \\
=&k - \mathbb{E}\,\mathrm{tr}\{\boldsymbol{x}^{\mathrm{T}}\boldsymbol{Z}(\boldsymbol{Z}^{\mathrm{T}}\boldsymbol{Z})^{-1}\boldsymbol{Z}^{\mathrm{T}}\boldsymbol{x}\} \\
\overset{(a)}{=}&k - \mathrm{tr}\{\boldsymbol{Z}(\boldsymbol{Z}^{\mathrm{T}}\boldsymbol{Z})^{-1}\boldsymbol{Z}^{\mathrm{T}}\,\mathbb{E}\,\boldsymbol{x}\boldsymbol{x}^{\mathrm{T}}\} \\
\overset{(b)}{=}&k - \mathrm{tr}\{\boldsymbol{Z}(\boldsymbol{Z}^{\mathrm{T}}\boldsymbol{Z})^{-1}\boldsymbol{Z}^{\mathrm{T}}\,\mathbb{E}(\tilde{\boldsymbol{x}} + \frac{k}{N})(\tilde{\boldsymbol{x}} + \frac{k}{N})^{\mathrm{T}}\} \\
\overset{(c)}{=}&k - \mathrm{tr}\{\boldsymbol{Z}(\boldsymbol{Z}^{\mathrm{T}}\boldsymbol{Z})^{-1}\boldsymbol{Z}^{\mathrm{T}}(\frac{k(N-k)}{N^2}I + 0 + \frac{k^2}{N^2}\mathbf{1}\mathbf{1}^{\mathrm{T}})\} \\
\overset{(d)}{=}&k - d\frac{k(N-k)}{N^2} - \frac{k^2}{N^2}N \\
=&(N-d)k(N-k)/N^2,
\end{aligned} \tag{3.3}$$

where $(a)$ follows from linearity and cyclic permutation of the trace operator; $(b)$ follows from defining $\tilde{\boldsymbol{x}} = \boldsymbol{x} - \frac{k}{N}$; $(c)$ follows from multiplying out each terms inside $(\tilde{\boldsymbol{x}} + \frac{k}{N})(\tilde{\boldsymbol{x}} + \frac{k}{N})^{\mathrm{T}}$ and using the fact that each element in $\tilde{\boldsymbol{x}}$ has a zero mean and a variance as $\frac{k(N-k)}{N^2}$; $(d)$ follows from $\boldsymbol{Z}(\boldsymbol{Z}^{\mathrm{T}}\boldsymbol{Z})^{-1}\boldsymbol{Z}^{\mathrm{T}}$ being a projection matrix onto $\boldsymbol{Z}$. Using the fact that the eigenvalues of a projection matrix are either 0 or 1 and $\boldsymbol{Z}$ has rank $d$ with probability one, then the trace of $\boldsymbol{Z}(\boldsymbol{Z}^{\mathrm{T}}\boldsymbol{Z})^{-1}\boldsymbol{Z}^{\mathrm{T}}$ is $d$ with probability one. In addition, from Lemma 1 (the proof can be found in [39]), it is shown that $\boldsymbol{Z}(\boldsymbol{Z}^{\mathrm{T}}\boldsymbol{Z})^{-1}\boldsymbol{Z}^{\mathrm{T}}\mathbf{1} = \mathbf{1}$ if $\boldsymbol{Z}$ contains one column as intercept, so that the trace of $\boldsymbol{Z}(\boldsymbol{Z}^{\mathrm{T}}\boldsymbol{Z})^{-1}\boldsymbol{Z}^{\mathrm{T}}\mathbf{1}\mathbf{1}^{T} = N$, which completes the equality in $(d)$. □

**Lemma 1.** *If $\boldsymbol{Z}$ is a $N$ by $d$ matrix (where $d < N$) with one column which contains all ones, then $\boldsymbol{Z}(\boldsymbol{Z}^{T}\boldsymbol{Z})^{-1}\boldsymbol{Z}^{T}\mathbf{1} = \mathbf{1}$.* ■

### *3.4 Optimal assignment*

Instead of being randomly assigned into DR programs, users can be optimally allocated to either the treatment group or the control group depending on their covariate information, in order to obtain the best estimator of $\beta$. Mathematically speaking, we optimally assign each $x_i$ to be 0 or 1, in order to minimize the variance of the estimator $\hat{\beta}$. This optimization problem is:

$$\begin{aligned} \underset{\hat{\boldsymbol{x}}}{\text{maximize}} \quad & \boldsymbol{x}^{\mathrm{T}} P_{\boldsymbol{Z}^{\perp}} \boldsymbol{x} \\ \text{subject to} \quad & \sum_{i=1}^{N} x_i = k \\ & x_i \in \{1, 0\}. \end{aligned} \tag{3.4}$$

We first discuss the upper bound on the quantity $\boldsymbol{x}^{\mathrm{T}} P_{\boldsymbol{Z}^{\perp}} \boldsymbol{x}$ (which signifies the lower bound for $\mathrm{Var}\,\hat{\beta}$). We show that it is $\mathrm{O}(N)$. Then we establish that under the regime of $k/N = p$, there exist algorithms that achieve a rate that meets the upper bound of $O(N)$.

#### *3.4.1 Optimal Rate*

Before proceeding on analyzing the rate obtained by the proposed strategy, we first discuss the upper bound on the rate of $\boldsymbol{x}^{\mathrm{T}} P_{\boldsymbol{Z}^{\perp}} \boldsymbol{x}$.

**Proposition 1.** *No assignment can achieve a better rate that $O(N)$ [31].* ■

*Proof.* The basic idea is to derive the Fisher information with the linear regression model in (3.1). The inverse of the Fisher information provides a lower bound for the variance of the estimator obtained by least squares and thus an upper bound for the quantity $\boldsymbol{x}^{\mathrm{T}} P_{\boldsymbol{Z}^{\perp}} \boldsymbol{x}$. For more details, please refer to Proposition 1 in [31]. □

In the next subsection we will show that when $\frac{k}{N} = p$ which is a constant, we achieve this upper bound.

### *3.4.2 Achievability of Optimal Rate*

We first present the main result of this section. We assume that each element of $\boldsymbol{Z}_{1:d-1}$ (excluding the intercept column) is drawn independently from a standard Gaussian distribution. This assumption will facilitate the calculation of the main result shown in Theorem 3. The algorithm associated with Theorem 3 is presented in Algorithm 2.

**Theorem 3.** *Recall that the rate is the growing rate of the inverse of the variance introduced in* (3.2)*. This rate from optimal assignment is of* $\Theta(\frac{k^2 log(\frac{N}{k})}{N})$*, which is independent of the dimension of covariates. More specifically, when* $\frac{k}{N} = p$ *is a constant, then this rate is linear rate, i.e.,* $\Theta(N)$*.* ■

**Algorithm 2** Procedures to obtain the rate shown in Theorem 3.

1: **Input**:Covariates $\boldsymbol{Z}$.
2: **Output**: Rate of optimal assignment and the corresponding optimal assignment strategy when $d = N - 1$.
3: Reduce the optimization problem in (3.4) to (3.6) using Lemma 2.
4: Compute the null space of $\boldsymbol{Z}^{\mathrm{T}}_{N,N-1}$, denote it by $\boldsymbol{\zeta}$. Each element of $\boldsymbol{\zeta}$ should independently follow a standard Gaussian distribution, according to Lemma 3.
5: Find the lower bound for the $k^{th}$ largest element in $\boldsymbol{\zeta}$ (suppose that this element is non negative). This lower bound is shown in Lemma 4.
6: The optimal value of the objective function in (3.6) is at least $\frac{k^2}{N}$ times this lower bound. The rate of this optimal value is stated in Theorem 3. The optimal assignment is to assign those $x_i$'s corresponding to the $k$ largest $\zeta_i$'s in $\boldsymbol{\zeta}$ to be 1's and the rest to be 0's.

Before proving Theorem 3, we first show in Lemma 2 that the worst case scenario for the rate is when $d = N - 1$. This scenario provides a minimum on the quantity $\boldsymbol{x}^{\mathrm{T}} P_{\boldsymbol{Z}^{\perp}} \boldsymbol{x}$ for every $d$ where $d < N$, which provides a maximum for $\mathrm{Var}\,\hat{\beta}$ for every $d < N$. Thus if we can show in Theorem 3 that in the worst case scenario where $d = N - 1$, the growing rate

of quantity $\boldsymbol{x}^{\mathrm{T}} P_{\boldsymbol{Z}^{\perp}} \boldsymbol{x}$ is $\Theta(N)$ when $\frac{k}{N} = p$ is a constant, then this rate holds for all $d$ where $d < N - 1$.

**Lemma 2.** *Var$\hat{\beta}$ is increasing in $d$. Consequently, if $d = N - 1$, the estimator yields the worse case performance [31]:*

$$\inf_{1 \leq d < N} \frac{\boldsymbol{x}^T P_{\boldsymbol{Z}^{\perp}_{N,d}} \boldsymbol{x}}{N} = \frac{\boldsymbol{x}^T P_{\boldsymbol{Z}^{\perp}_{N,N-1}} \boldsymbol{x}}{N} \tag{3.5}$$

■

*Proof.* This is a general result about linear estimation and the interested reader can refer to Lemma 5 in [31]. □

When $d = N - 1$, the rank of $\boldsymbol{Z}_{N,N-1}$ is one with probability one, thus we write $P_{\boldsymbol{Z}^{\perp}_{N,d}} = \frac{\boldsymbol{\zeta}\boldsymbol{\zeta}^{\mathrm{T}}}{||\boldsymbol{\zeta}||^2}$, where $\boldsymbol{\zeta}$ is in the null space of $\boldsymbol{Z}^{\mathrm{T}}_{N,N-1}$ [31], i.e., $\boldsymbol{Z}^{\mathrm{T}}_{N,N-1}\boldsymbol{\zeta} = \boldsymbol{0}$. Based on this observation, $\boldsymbol{x}^{\mathrm{T}} P_{\boldsymbol{Z}^{\perp}} \boldsymbol{x}$ is written into a simpler form as $\frac{\boldsymbol{x}^{\mathrm{T}}\boldsymbol{\zeta}\boldsymbol{\zeta}^{\mathrm{T}}\boldsymbol{x}}{||\boldsymbol{\zeta}||_2^2} = \frac{(\boldsymbol{\zeta}^{\mathrm{T}}\boldsymbol{x})^2}{||\boldsymbol{\zeta}||^2}$. The problem is then to maximize $\frac{(\boldsymbol{\zeta}^{\mathrm{T}}\boldsymbol{x})^2}{||\boldsymbol{\zeta}||^2}$ under the constraint that we only get to assign $k$ $x_i$'s to be 1's and the rest to be 0's. The optimization problem is:

$$\begin{aligned} \underset{\hat{\boldsymbol{x}}}{\text{maximize}} \quad & \frac{(\boldsymbol{\zeta}^{\mathrm{T}}\boldsymbol{x})^2}{||\boldsymbol{\zeta}||^2} \\ \text{subject to} \quad & \sum_{i=1}^{N} x_i = k \\ & x_i \in \{1, 0\}. \end{aligned} \tag{3.6}$$

To solve the optimization problem in (3.6), we need to find $k$ $\zeta_i$'s in $\boldsymbol{\zeta}$ such that their sum is maximized, where $\zeta_i$ is the $i^{th}$ element of the vector $\boldsymbol{\zeta}$. We observe that it actually suffices to provide a lower bound on this maximum sum to prove the rate.

To provide this lower bound we need to know the structure of $\boldsymbol{\zeta}$. We then show in Lemma 3 that if $\boldsymbol{\zeta}$ is in the null space of $\boldsymbol{Z}_{N,N-1}$, then each $\zeta_i$ can be constructed to be drawn from an i.i.d. standard Gaussian distribution. Based on this observation, the problem is further reduced to find the lower bound on the $k^{th}$ largest $\zeta_i$, assuming that $2k$ is smaller than $N$ to ensure that with overwhelming probability the $k^{th}$ largest $\zeta_i$ is non negative. Let us refer

to this statistic as the $(N-k+1)^{th}$ order statistic of $\boldsymbol{\zeta}$ and denote it by $\zeta_{(N-k+1)}$ such that $\zeta_{(1)} \leq \zeta_{(2)} \leq \cdots \leq \zeta_{(N)}$. We present a lower bound for $\zeta_{(N-k+1)}$ in Lemma 4 when $k$ is smaller than $\frac{N}{2}$. This lower bound facilitates the final proof for Theorem 3. The proof of Lemma 3 and Lemma 4 is in the longer version at [39].

**Lemma 3.** *The basis of the null space of $\boldsymbol{Z}_{N,N-1}^T$ can be constructed as an i.i.d. standard Gaussian vector with length $N$, when each element of $\boldsymbol{Z}_{1:N-2}$ is independently drawn from a standard Gaussian distribution and the last column of $\boldsymbol{Z}$ is an all one column.* ■

**Lemma 4.** *Let $\boldsymbol{\zeta}$ satisfies $\boldsymbol{Z}_{N,N-1}^T \boldsymbol{\zeta} = 0$. If each $\zeta_i$ is independent and follows standard Gaussian distribution, then $\mathbb{E}\,\zeta_{(N-k+1)} \geq C\sqrt{\log \frac{N}{k}}$, where $C$ is a positive constant and $\frac{k}{N} < \frac{1}{2}$.* ■

Now we can use the introduced lemmas to prove Theorem 3. A summary is presented in Algorithm 2, illustrating the procedures to obtaining the rate stated in Theorem 3 using the proposed lemmas. This algorithm also provides the optimal assignment strategy when $d = N-1$.

*Proof of Theorem 3.* We will focus on the case when $d = N-1$ since it provides the worst case rate for every $d < N$, as stated in Lemma 2.

From lemma 3, we know that $\boldsymbol{\zeta} \sim N(0, \mathrm{I}_N)$, we then obtain the following results:

$$
\begin{aligned}
&\max_{\boldsymbol{x}, x_i \in \{1,0\}, \sum x_i = k} \mathbb{E}\,\frac{(\boldsymbol{\zeta}^{\mathrm{T}}\boldsymbol{x})^2}{||\boldsymbol{\zeta}||_2^2} \\
&\geq \mathbb{E}\,\frac{\{(\zeta_{(N)} + \ldots + \zeta_{(N-k+1)})^2\}}{||\boldsymbol{\zeta}||_2^2} \\
&\overset{(a)}{=} \frac{\mathbb{E}\{(\zeta_{(N)} + \ldots + \zeta_{(N-k+1)})^2\}}{\mathbb{E}\,||\boldsymbol{\zeta}||_2^2} + O(\frac{1}{N}) \\
&\geq \frac{\mathbb{E}\{(k\zeta_{(N-k+1)})^2\}}{N} + O(\frac{1}{N}) \\
&= k^2 \frac{\mathbb{E}\{\zeta_{(N-k+1)}^2\}}{N} + O(\frac{1}{N}) \\
&\overset{(b)}{\geq} k^2 \frac{(\mathbb{E}\,\zeta_{(N-k+1)})^2}{N} + O(\frac{1}{N}) \\
&\overset{(c)}{\geq} k^2 \frac{C^2 log\frac{N}{k}}{N} + O(\frac{1}{N}),
\end{aligned}
\tag{3.7}
$$

where $(a)$ is based on the multivariate delta method [40], $(b)$ comes from Jensen's inequality and $(c)$ is based on Lemma 3 and Lemma 4.

Specifically, if $\frac{k}{N} = p$, then (3.7) can be written as:

$$k^2 \frac{C^2 log \frac{N}{k}}{N} = C^2 p^2 \log(p^{-1}) N = \Theta(N). \tag{3.8}$$

Another interesting case is when $k = \log N$, (3.7) can be written as:

$$k^2 \frac{C^2 \log \frac{N}{k}}{N} = C^2 (\log N - \log \log N) = \Theta(\log N). \tag{3.9}$$

□

As can be seen from Theorem 3, we will obtain the optimal rate $\Theta(N)$ by replacing $\frac{k}{N}$ as a constant. This indicates that with optimal assignment, the estimation variance will indeed decay with $N$ instead of being a constant as shown in Theorem 1, when the dimension of the covariates $d$ is comparable to $N$. This is very interesting as it indicates that even in a high dimensional setting, the variance of the estimator will decay optimally by solving the variance minimization problem.

### *3.5 A tractable alternative*

Algorithm 2 provides a simple way to find the optimal assignment when $d = N - 1$. When $d$ is less than $N - 1$, this algorithm cannot be applied. In fact, the optimization problem in (3.4) is a nonconvex quadratic optimization problem which can be NP-hard. In this section, we present a tractable approximate algorithm by relaxing the original combinatorial optimization problem into and semidefinite program. We then demonstrate that this SDP problem approximates the original problem with a performance ratio that is better than $\frac{k}{N}$ when $\frac{k}{N}$ is in the range of $(0.2, 0.9995)$. This procedure follows the results established in [35].

We first revisit the original variance minimization problem in (3.4) and transform $\boldsymbol{x}$ into $\boldsymbol{x} = (\hat{\boldsymbol{x}}+1)/2$. Denote each element in $\hat{\boldsymbol{x}}$ as $\hat{x}_i$, then each $\hat{x}_i$ takes value in $\{-1, 1\}$. Therefore

the variance minimization problem is written as:

$$\begin{aligned} \underset{\hat{\boldsymbol{x}}}{\text{maximize}} \quad & \frac{1}{4}(\hat{\boldsymbol{x}}+1)^{\mathrm{T}} P_{\boldsymbol{Z}^{\perp}}(\hat{\boldsymbol{x}}+1) \\ \text{subject to} \quad & \sum_{i=1}^{N} \hat{x}_i = 2k - N \\ & \hat{x}_i \in \{1, -1\}. \end{aligned} \tag{3.10}$$

This is a Dense-$k$-Subgraph (DSP) problem with existence of self edges. To illustrate this, let element at row $i$ and column $j$ in matrix $P_{\boldsymbol{Z}^{\perp}}$ be denoted as edge weight $w_{ij}$ (except that $w_{ii}$ is half of the value on the diagonals) associated with vertex $i$ and vertex $j$, then (3.10) is trying to find a set of $k$ vertices such that the sum of edge weights induced by these vertices are maximized. Since the problem presented in (3.10) contains binary variables, we relax this problem into a SDP formulation:

$$\begin{aligned} \underset{\boldsymbol{X},\hat{\boldsymbol{x}}}{\text{maximize}} \quad & \frac{1}{4}\sum_i \sum_j w_{ij}(1 + \hat{x}_i + \hat{x}_j + X_{ij}) \\ \text{subject to} \quad & \sum_i \hat{x}_i = 2k - N \\ & X_{ii} = 1 \\ & \sum_i \sum_j X_{i,j} = (2k-N)^2 \\ & \begin{bmatrix} 1 & \hat{\boldsymbol{x}}^{\mathrm{T}} \\ \hat{\boldsymbol{x}} & \boldsymbol{X} \end{bmatrix} \succeq 0. \end{aligned} \tag{3.11}$$

The original problem in (3.10) is hard, we will only obtain a surrogate solution in polynomial time. We thus adopt Algorithm 3 to obtain an approximate solution from SDP formulation. Let us denote this solution by $\hat{\boldsymbol{x}}^*$ based on Algorithm 3. The performance of the approximation from SDP is evaluated by the performance ratio $r$ which satisfies:

$$\mathbb{E}\,\frac{1}{4}(\hat{\boldsymbol{x}}^*+1)^{\mathrm{T}} P_{\boldsymbol{Z}^{\perp}}(\hat{\boldsymbol{x}}^*+1) \geq r w^*. \tag{3.12}$$

Here the randomness in $\hat{\boldsymbol{x}}^*$ is introduced by the random rounding procedure shown in Algorithm 3 and $w^*$ is the optimal value of the objective function shown in (3.10). Perfor-

mance ratio $r$ can be used to quantify how close the solution from Algorithm 3 is to the optimal solution by solving the original hard problem.

There exists a fruitful line of work on the approximation algorithms using either greedy algorithm or LP/SDP relaxation for DSP problems [33–36, 41–45]. Most recent research has improved the performance ratio to $O(N^{-\frac{1}{4}+\epsilon})$ with LP relaxation in [45]. However, if $\frac{k}{N}$ is not decaying with $N$, i.e., a constant, then this ratio is not desirable since it is decreasing in $N$. The authors in [35] propose an improved performance ratio that is better than $\frac{k}{N}$ for a wide range of $\frac{k}{N}$. We will adopt the approximation procedure in [35] and argue that the performance ratio is valid in our case here as well. In the following, we will first present the general algorithm and then show that the performance ratio in [35] is still applicable in our case.

The approximation procedure in [35] is presented in Algorithm 3, including three main procedures:

- Solve SDP problem in (3.11) (step 1). After this procedure we can obtain the optimal continuous solution for (3.11) and the optimal value of the objective function is denote by $w^{SDP}$.

- Construct initial $S$, where $S$ represents the initial subgraph and is a set of indices (step 2 through step 4). The $\hat{x}_i$'s take value 1 such that $i \in S$ and the rest -1. Let us denote them by $\hat{\boldsymbol{x}}^0$. The value of the objective function in (3.11) is written as $w(S) = \frac{1}{4}\sum_i \sum_j w_{ij}(1 + \hat{x}_i^0 + \hat{x}_j^0 + \hat{x}_i^0\hat{x}_j^0) = \frac{1}{4}(\hat{\boldsymbol{x}}^0 + 1)^{\mathrm{T}} P_{\boldsymbol{Z}^\perp}(\hat{\boldsymbol{x}}^0 + 1)$. Here $w(S)$ is the total weights of edges in the subgraph induced by $S$. At this point the cardinality of $S$ is not necessarily $k$.

- Resize $S$ to $\tilde{S}$ such that $\tilde{S}$ contains exactly $k$ vertices (step 5 through step 16). The final assignment of $\hat{x}_i$'s is that $\{\hat{x}_i = 1, \hat{x}_j = -1 | i \in \tilde{S}, j \notin \tilde{S}\}$. Let us denote them by $\hat{\boldsymbol{x}}^*$. The value of the objective function is $w(\tilde{S}) = \frac{1}{4}(\hat{\boldsymbol{x}}^* + 1)^{\mathrm{T}} P_{\boldsymbol{Z}^\perp}(\hat{\boldsymbol{x}}^* + 1)$ and is the total weights of the edges induced by $\tilde{S}$.

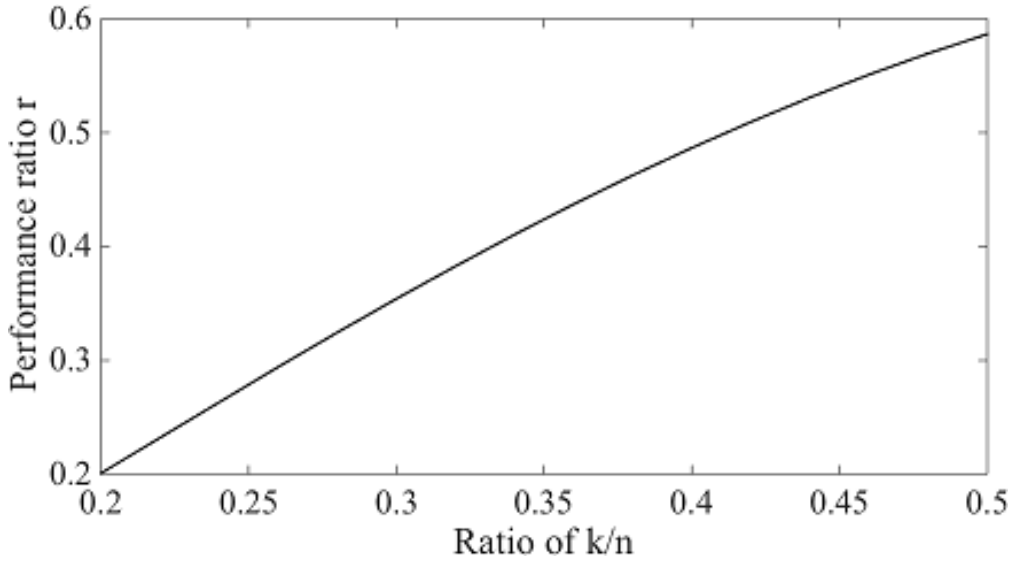


Figure 3.1: Performance ratio from Algorithm 3 for $\frac{k}{N} \in [0.2, 0.5]$.

We now demonstrate that Algorithm 3 achieves the performance ratio shown in Proposition 2.

**Proposition 2.** *The performance ratio $r$ from Algorithm 3 defined as:*

$$\mathbb{E}\, w(\tilde{S}) \geq r w^* \tag{3.13}$$

*satisfies the conditions presented in Proposition 2 in [35] and is plotted in Fig. 3.1, where $w^*$ is the optimal value of the objective function in problem* (3.10)*. When $k$ is large, this ratio is better than either $O(N^{-(\frac{1}{3}-\epsilon)})$ or $O(N^{-(\frac{1}{4}-\epsilon)})$ obtained by LP relaxation.* ■

As can be seen from Proposition 2, the performance ratio $r$ quantifies the gap between the approximated solution obtained by Algorithm 3 and the optimal solution from the original problem shown in (3.10). This ratio $r$ is the direct result from the random rounding procedure and the resizing procedure shown in Algorithm 3. The ratios associated with these two procedures are presented in (3.14) and (3.15):

$$\mathbb{E}\, w(S) \geq \alpha w^*, \tag{3.14}$$

and

$$w(\tilde{S}) \geq \xi w(S). \tag{3.15}$$

In [35], the authors well define the parameter $\alpha$ (which depends on $k$ and $N$) and $\xi$ (depends on $k$ and $S$ obtained from the random rounding procedure) so that the performance ratio $r$ satisfies Proposition 2 where there are no self edges, i.e., $w_{ii} = 0$. However, in our case, the $w'_{ii}s$ are the diagonal elements of $\boldsymbol{P}_{\boldsymbol{Z}^\perp}$ and they are not necessarily zero, so the graph in our case contains non trivial self edges. If we show that the presence of self edges does not change the values of $\alpha$ and $\xi$, then Proposition 2 naturally holds in our case as well.

Let us first discuss (3.14). From [35], parameter $\alpha$ does not depend on whether there are self edges in the graph, so (3.14) directly applies.

Next we need to check if the same $\xi$ applies at the presence of self edges. When there are no self edges, i.e., $w_{ii} = 0$, the authors in [35] show that $\xi = \frac{k(k-1)}{|S|(|S|-1)}$ when $|S| > k$ and $\xi = 1$ otherwise. We show that the same condition for $\xi$ holds even with the presence of non negative self edges, as stated in Lemma 5.

**Lemma 5.** *Let $S$ and $\tilde{S}$ be obtained from random rounding procedure and resizing procedure in Algorithm 3 from a graph with non negative self edges, i.e., $w_{ii} \geq 0$. Then we have:*

$$w(\tilde{S}) = \begin{cases} \frac{k(k-1)}{|S|(|S|-1)} w(S), & \text{if } |S| > k \\ 1, & \text{otherwise} \end{cases}$$

■

Proof of Lemma 5 is given in Section B.1. Lemma 5 validates the $\alpha$ and $\xi$ with the presence of non negative self edges, thus the performance ratio $r$ stated in Proposition 2 is valid. A list of performance ratio $r$'s for different values of $\frac{k}{N}$ is shown in [35] and is plotted in Fig. 3.1. This rate is satisfactory since it has a rate of $O(\frac{k}{N})$ but strictly larger than $\frac{k}{N}$ [35]. It is better than $\mathrm{O}(N^{-\frac{1}{4}+\epsilon})$ when $\frac{k}{N}$ is not decaying faster than $O(N^{-\frac{1}{4}+\epsilon})$. In fact, as long as $\frac{k}{N}$ lies within some constant range, then $\frac{k}{N}$ can be seen as a varying constant thus is not decaying as a function of $N$.

## *3.6 Simulation*

In this section we show the comparison results between random assignment and optimal assignment. We simulate the covariates from two different distributions, i.e., Gaussian distribution and uniform distribution. We also validate the claim by simulated building data from [23].

### *3.6.1 Gaussian Ensemble*

We first generate the covariates as they are drawn from i.i.d. Gaussian ensemble, i.e., $N(\mathbf{0}, I)$. We compare two cases where $N = 3k$ and $N = 5k$ in Fig. 3.2. Note that Fig. 3.2 is shown in semilogarithmic plot where the $y$-axis has a logarithmic scale and the $x$-axis has a linear scale. In addition, we adopt the value of $\theta$ in [35], i.e., 0.9 for $N = 3k$ and 0.94 for $N = 5k$. We let $d = N - 1$ to obtain the worst case performance.

In addition, we use the result from branch and bound (upper bound) to serve as the reference in order to compare the random assignment and the proposed optimal assignment. The duality gap for branch and bound is set to be 0.05 for all $N$ when $N = 3k$. Due to computational complexity and time constraints, we set this gap to be around 0.25 when $N$ is big in the case of $N = 5k$.

In Fig. 3.2, we see that the semilog plot on $\mathrm{Var}^{-1}\,\hat{\beta}$ $(\boldsymbol{x}^{\mathrm{T}} P_{\boldsymbol{Z}^{\perp}_{N,N-1}} \boldsymbol{x})$ is growing with $N$ and similar to $\log N$. This suggests that $\mathrm{Var}^{-1}\,\hat{\beta}$ is linear in $N$, as we stated in Section 3.4. In addition, It is very close to the solution obtained by branch and bound, meaning that the result from SDP relaxation is close to the optimal solution in (3.10). The empirical performance ratio from SDP relaxation is shown in Table 3.1.

From Table 3.1, we see that the performance ratio for $N$ between 10 and 200 is actually greater than $\frac{k}{N}$, which is even better than the theoretical bound in Proposition 2. In addition, if we decrease $k$ with respect to $N$, i.e., change $k$ from $\frac{N}{3}$ to $\frac{N}{5}$, then the performance ratio is reduced. This is due to the fact we need to do more eliminations during the resizing procedure in Algorithm 3 and the deterioration increases. However, if $\frac{k}{N}$ is well defined

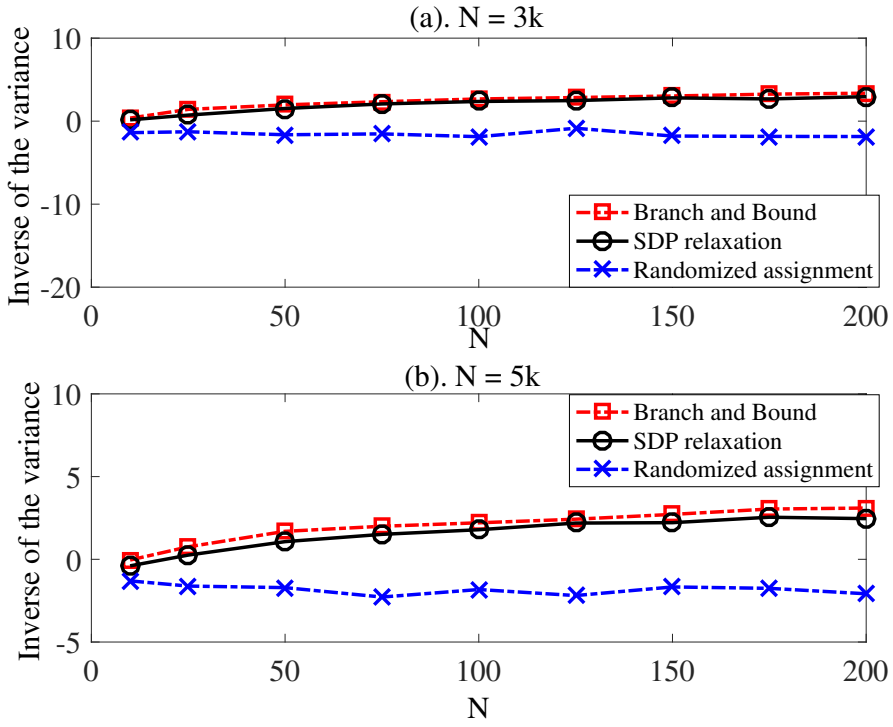


Figure 3.2: Semilogarithmic plot on the inverse of Var $\hat{\beta}$, i.e., $\boldsymbol{x}^{\mathrm{T}} P_{\boldsymbol{Z}_{N,N-1}^{\perp}} \boldsymbol{x}$, assuming Gaussian distribution of $\boldsymbol{Z}_{1:N-2}$. The $y$-axis is shown in a logarithmic scale and the $x$-axis is shown in a linear scale. Upper plot shows the rate when $N = 3k$, lower plot shows the corresponding rate when $N = 5k$.

within a range, then this deterioration is controlled and does not change the statement in Proposition 2.

On the other hand, the semilog plot on $\mathrm{Var}^{-1}\,\hat{\beta}$ from random assignment is a constant on average across different values of $N$, whether $k$ is small or large. This validates Theorem 2 as it states that the rate is $\Theta(1)$ when $d = N - 1$. In this case, we cannot obtain an efficient estimator since the variance is not decaying even when $N$ is big.

Table 3.1: Empirical performance ratio for Gaussian ensemble with different values for $\frac{k}{N}$ and varying $N$.

| $p = \frac{k}{N}$ | $N = \mathbf{10}$ | $N = \mathbf{50}$ | $N = \mathbf{100}$ | $N = \mathbf{200}$ |
|---|---|---|---|---|
| $\frac{1}{3}$ | 0.8131 | 0.6486 | 0.7416 | 0.6588 |
| $\frac{1}{5}$ | 0.7026 | 0.5362 | 0. 6577 | 0.5273 |

### *3.6.2 Uniform Ensemble*

Although we discuss the rate of quantity $\boldsymbol{x}^{\mathrm{T}} P_{\boldsymbol{Z}_{N,N-1}^{\perp}} \boldsymbol{x}$ with respect to Gaussian ensemble, we also simulate the covariates where the elements are drawn from a uniform distribution in an interval [-1,1]. The results are shown in Fig. 3.3. Fig. 3.3 is again a semilogarithmic graph. We again take $\theta$ to be 0.9 when $N = 3k$ and 0.94 when $N = 5k$. The duality gap is 0.05 when $N = 3k$. When $N = 5k$, the duality gap is around 0.1 to 0.2 for $N$ greater than 100 and is 0.25 for $N = 200$. The comparison result is shown in Fig. 3.3 and the performance ratio by SDP relaxation is shown in Table 3.2.

Table 3.2: Empirical performance ratio for uniform ensemble with different values for $\frac{k}{N}$ and varying $N$.

| $p = \frac{k}{N}$ | $N = \mathbf{10}$ | $N = \mathbf{50}$ | $N = \mathbf{100}$ | $N = \mathbf{200}$ |
|---|---|---|---|---|
| $\frac{1}{3}$ | 0.6961 | 0.6755 | 0.8068 | 0.8094 |
| $\frac{1}{5}$ | 0.6101 | 0.6113 | 0.4799 | 0.5145 |

The observation from Fig. 3.3 and Table 3.2 is similar to the analysis in the case of Gaussian ensemble, that the solution obtained from SDP relaxation is still within a constant of the branch and bound solution for $10 \leq N \leq 200$. The performance ratio is again

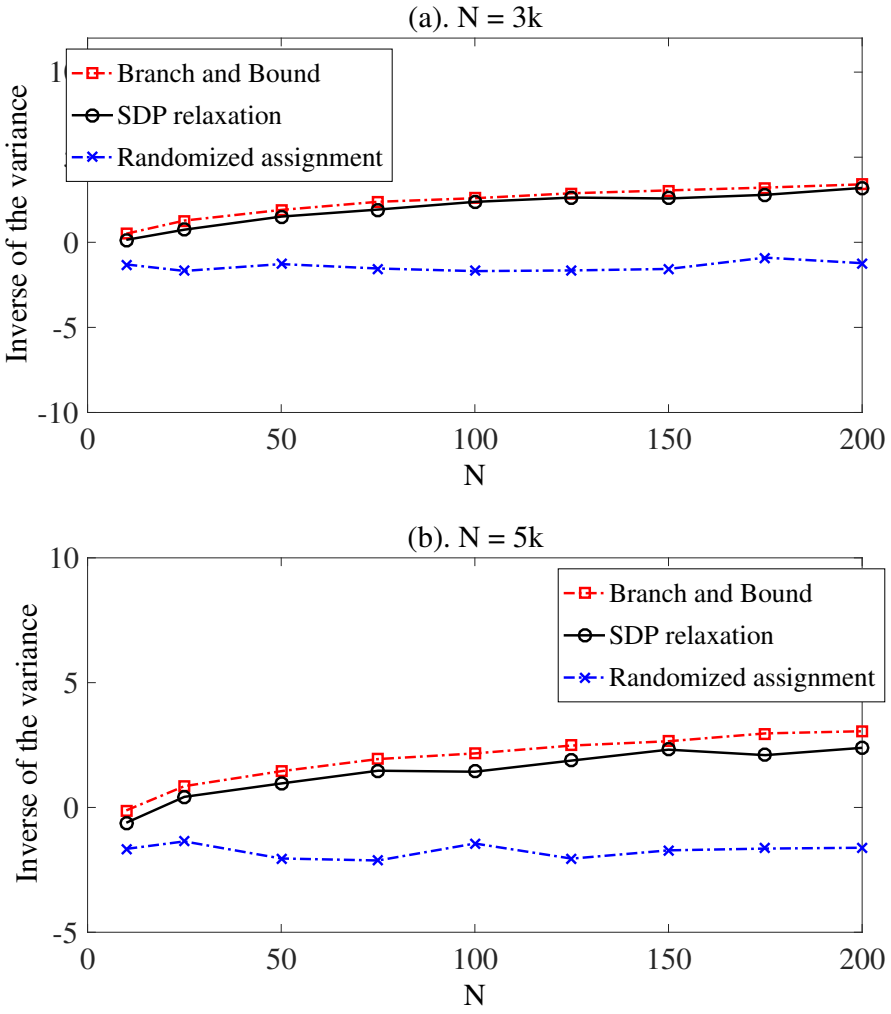


Figure 3.3: Semilogarithmic plot on the inverse of Var $\hat{\beta}$, i.e., $\boldsymbol{x}^{\mathrm{T}} P_{\boldsymbol{Z}_{N,N-1}^{\perp}} \boldsymbol{x}$, assuming uniform distribution of $\boldsymbol{Z}_{1:N-2}$. Upper plot shows the rate when $N = 3k$, lower plot shows the corresponding rate when $N = 5k$.

decreased when we decrease $k$, which indicates the similar deterioration occurred during the resizing procedure.

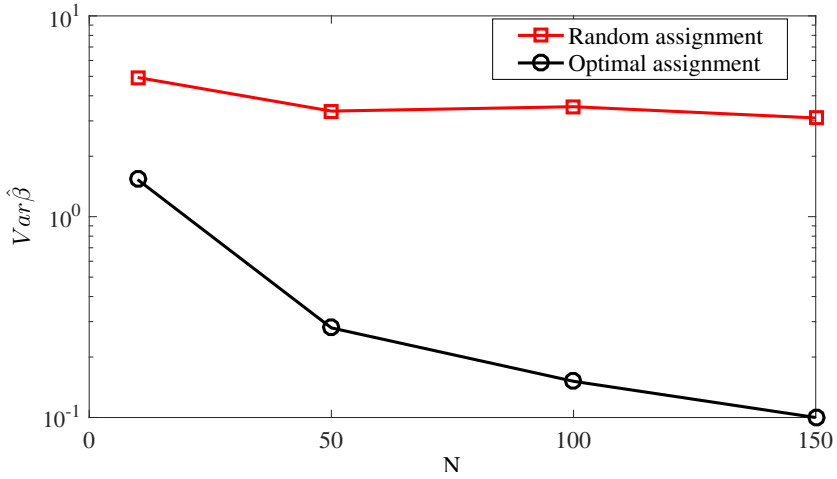


Figure 3.4: Variance of $\hat{\beta}$ as a function of $N$ when $d = N - 1$, simulated from building data, with two different assignment strategies.

### *3.6.3 Building data*

We also validate the claim in the chapter by simulated building data obtained from [23]. Using this software, we can generate building covariates such as environment temperature, number of occupants, appliances scheduling, etc. The software outputs the energy consumption based on the covariates that we generate. The buildings vary from a small postal office, to a large commercial hotel, with different number of covariates involved in the modeling.

For the purpose of this chapter, we include significant covariates into the linear regression model and the number of those covariates are comparable to the number of users in the simulation. The values of the covariates are whitened by the covariance matrix so that the covariates have zero mean and unit variance [46]. The details of this procedure is given in [39]. In addition, we fix $k = \frac{1}{3}N$ in the simulation.

The simulation results are shown in Fig. 3.4 and Fig. 3.5.

In Fig. 3.4, we observe that $\mathrm{Var}\,\hat{\beta}$ is decaying very fast with the optimal assignment strategy, whereas the variance stays unchanged if adopting a random assignment strategy.

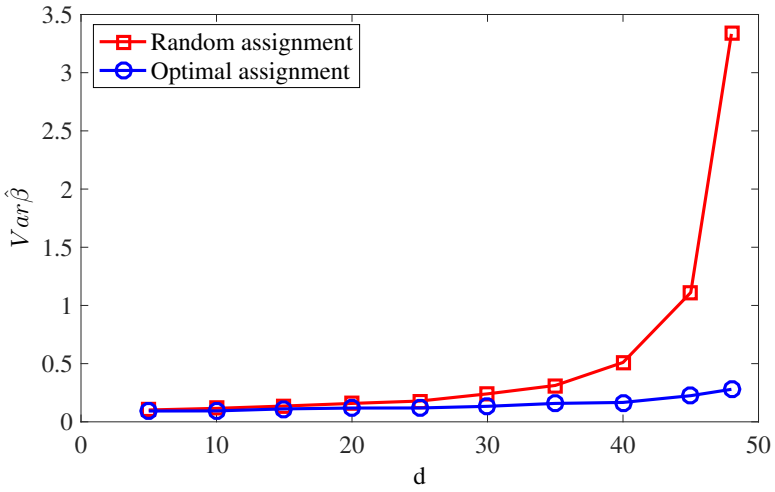


Figure 3.5: Variance of $\hat{\beta}$ as a function of $d$ when $N$ is fixed, simulated from building data, with two different assignment strategies.

The variance $\mathrm{Var}\,\hat{\beta}$ is a varying quantity in terms of the dimension of the covariates, i.e., $d-1$. Assume that the number of users are fixed, i.e., $N$ is fixed, and that $\rho$ is a constant. According to Theorem 2 and in Theorem 3, with random assignment the variance decays with $N-d$ whereas with optimal assignment the worse case scenario with $d=N-1$ yields a decay rate of $N$.

In Fig. 3.5, we show how $\mathrm{Var}\,\hat{\beta}$ varies with an increasing $d$ and a fixed $N=50$. As can be seen from Fig. 3.5, the increasing $d$ deteriorates the variance much severely from random assignment than that from the proposed optimal assignment. This again validates the efficiency of the proposed strategy in improving estimation accuracy, especially in a high dimensional setting where $d$ is comparable to $N$.

### *3.7 Summary*

In this Chapter, we discuss about the performance of random treatment assignment and optimal treatment assignment, especially in the case of high dimensional covariates. We show that in this special case, random treatment assignment fails to obtain an efficient estimator

of treatment effect in terms of variance. The proposed optimal assignment strategy is able to obtain the best estimator and matches lower bound from fisher information. We use simulation data from EnergyPlus to validate the statement.

**Algorithm 3** Approximation algorithm with SDP relaxation in (3.11), adopted from [35].

**Input**:$w_{ij}, k, N$

Solve SDP in (3.11), obtain $\boldsymbol{X}, \hat{\boldsymbol{x}}$.

Construct $\bar{\boldsymbol{X}} = \begin{bmatrix} 1 & \hat{\boldsymbol{x}}^{\mathrm{T}} \\ \hat{\boldsymbol{x}} & \boldsymbol{X} \end{bmatrix}$.

Construct covariance matrix $Y = \theta\bar{\boldsymbol{X}} + (1-\theta)\boldsymbol{P}$, where: $0 \leq \theta \leq 1$, $\boldsymbol{P} = \begin{bmatrix} 1 & \chi & \chi & \cdots & \chi \\ \chi & 1 & \chi^2 & \cdots & \chi^2 \\ \vdots & \vdots & \vdots & \ddots & \vdots \\ \chi & \chi^2 & \cdots & \chi^2 & 1 \end{bmatrix}$, $\chi = 2\frac{k}{N} - 1$.

Generate $\boldsymbol{u} \sim N(0, \boldsymbol{Y})$, $\tilde{\boldsymbol{x}} = sign(\boldsymbol{u})$, $S = \{i \geq 2 : \tilde{x}_i = \tilde{x}_1\}$.

Let $\tilde{S} = S$.

**if** $|\tilde{S}| = k$ **then**

    Output $\tilde{S}$

**if** $|\tilde{S}| < k$ **then**

    arbitrarily add $k - |\tilde{S}|$ nodes into $\tilde{S}$. **Output** $\tilde{S}$.

**while** $|\tilde{S}| > k$ **do**

    **for** each $i \in \tilde{S}$ **do**

        $\eta_i = \sum_{j \in \tilde{S}} w_{ij}$.

        Rearrange $\tilde{S} = \{i_1, i_2, \ldots, i_{|\tilde{S}|}\}$, where $\eta_{i_1} \geq \eta_{i_2} \geq \cdots \geq \eta_{i_{|\tilde{S}|}}$. Remove $i_{|\tilde{S}|}$ and reset $\tilde{S} = \{i_1, i_2, \ldots, i_{|\tilde{S}|-1}\}$.

        **Output** $\tilde{S}$.

**Output**:$S$

# Chapter 4

# OPERATOR'S PERSPECTIVE – ONLINE DEMAND RESPONSE

## *4.1 Introduction*

Besides accurately estimating the impact of a static DR signal, it is also crucial to consider DR signal assignment in a real system setting. In a real power system, a utility (or system operator) manages a certain amount of flexible consumers. What is more, the utility faces uncertainty and limited communication. Specifically, the aggregator does not know the cost function of consumers and cannot have multiple rounds of information exchange with consumers. We formulate an optimization problem for the utility to minimize its operational cost considering time-varying demand response targets and responses of consumers. We develop a joint online learning and pricing algorithm. In each time slot, the utility sends out a price signal to all consumers and estimates the cost functions of consumers based on their noisy responses. We measure the performance of our algorithm using regret analysis and show that our online algorithm achieves logarithmic regret with respect to the operating horizon.

The problem of private customer information is not new in demand response. A standard approach to address this challenge is to adopt a "negotiation" process between the customers and the utility. For example, at time $t$, suppose the utility wishes to elicit some change from the customers but do not know their individual cost functions. By repeatedly probing the customer with different prices, the optimal price–i.e., same price as if the utility had full information–can be agreed upon as long as the cost functions satisfy some technical constraints [5]. However, in practice, this strategy may be difficult to implement in some settings. Firstly, some systems still lack real-time two-way communication between customers

and utilities, which makes multiple rounds of information exchange in a short time difficult. Secondly, many customers do not actively engage in the process and tend to change their consumption just based on the first price they observe. For example, many companies use text-based notifications [47, 48], and it is unrealistic to assume customers would manually negotiate with the companies. In this dissertation, we move away from this setting by assuming that at any time $t$, a customer changes its consumption after it receives a price and does not undergo a negotiation process. Therefore any information the utility learns from the price and customers' responses at time $t$ will only be useful the next time demand response is called. Thus some loss relative to the case where the utility has full information, or *regret*, is inevitable. Our contribution is in describing an algorithm that minimizes the regret.

Specifically, we consider the following optimization problem. An utility has a *time-varying* demand response target at each time $t$ and manages $N$ users. Each of the users has a quadratic cost function that is not known to the utility. To achieve its desired target, the utility sends out a price signal to the users. Interpreting this price as payment, the users solve an optimization problem to determine their changes in demand. The utility observes the response of the customers. The two key difficulties of the problem are: 1) the utility *commits* to the price at the beginning of a time slot and can only use its observations for the next time; and 2) the demand response target changes throughout time. Therefore the price must be determined in an online fashion, optimized using historical prices and responses.

To measure the performance of an online problem, we adopt the standard metric of *regret*, which measures the difference between the performance of the online scheme and the performance of an optimal offline scheme that has the full information. Normally regret is reported as the sum of the differences between the online and offline versions as a function of the total number of time steps $T$. A regret *sublinear in* $T$ is consider to be a "good" regret, since a trivial online algorithm has regret that is proportional to $T$. In a seminal work, the authors in [49] showed that under broad conditions, no online algorithm can achieve a better regret than $\log(T)$. In this dissertation, we present an algorithm that meets this lower bound. Throughout the dissertation, we assume that the utility has a quadratic penalty if it receives

a different demand response amount than its target and each user has a convex quadratic cost function. We do not explicitly model power flow, and view the aggregate demand response received by the utility as the sum of the response of each user. We believe losses can be include into the framework by accounting for the topology of the power network.

### *4.2 Literature Review*

Demand response was first proposed as a load control mechanism and gained popularity in both academia and industry in the past decade because of the advancement of smartgrid [2, 50,51]. The setting of where utility does not have (or only has partial) customer information was considered by authors in [5, 17, 52]. Most of these studies assumed that the utility and users conduct a negotiation process before committing to a decision. This process is typically modeled as implementing a distributed optimization algorithm [53–55].

Recently, a series of papers investigated the setting where the utility must commit to its decision under uncertainty about its users. The authors in [56] considered using reinforcement learning to learn the home appliances of a single household, and the related work of designing an automated system in [57] include energy scheduling under uncertainty in price. The authors in [58] considered a data-driven approach to learn customer behavior using historical consumption profile. The authors in [59] considered a two-stage market where the demand is modeled by a Markov jump process. Our work differs from these in that we focus on the problem from the utility's point of view, focus on the uncertainty in the response of the customers, and do not require extensive data on historical consumption profiles. The work in [60] is closest to our model, although under a different setup where the authors consider risk in learning and not directly focused on cost of the utility.

### *4.3 Problem setup*

We consider a demand response system shown in Fig. 4.1. An utility coordinates a set of users $i = 1, ..., N$ to provide demand response service to the power grid over a time horizon $t = 1, ..., T$. At time $t$, the utility broadcasts a price $\lambda_t$ to all users, and each user $i$ responds

to the price and changes its consumption by some amount. We assume that there are no iterative communications between users and the utility in a single time period. That is, a user responds at the time he/she receives the price signal without any negotiations. In the following, we will present the models for both utility and users and formulate the demand response optimization problem and its offline optimal solution.

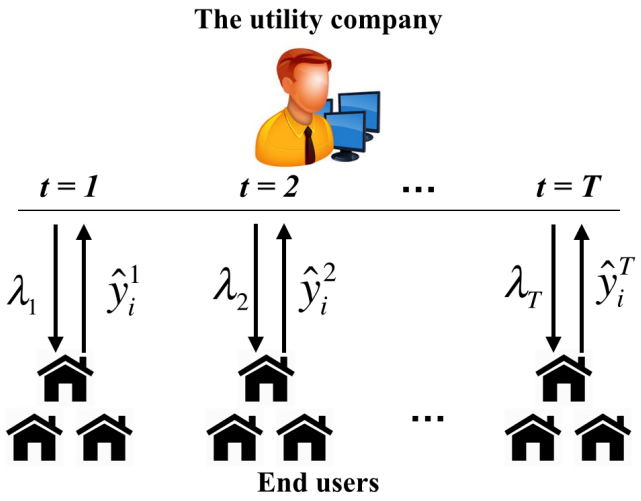


Figure 4.1: Interactions between the utility and users: $\lambda_t$ is the price at time $t$ and $\hat{y}_i^t$ is the change in demand of user $i$ at time $t$.

### *4.3.1 Utility Cost Model*

The utility aggregates power consumption changes from all the users to provide demand response service to the power grid [5]. The utility seeks to minimize its cost or maximize its profits by calling a certain amount of demand responses from users. We assume that the power grid specifies a normalized amount of demand reduction denoted as $d_t$ at the beginning of time slot $t$. The utility determines its capacity of demand response $Y$ and provides a response of $Yd_t$. We assume that the utility receives revenue proportional to a price $\theta$. The capacity $Y$ captures size of the utility, that is, the number of customers

an utility can call to provide demand response. However, if the actual aggregated demand reduction deviates from the committed reduction $Yd_t$, the utility will suffer a penalty as its cost. Let $y_i^t$ denote the response of user $i$ at time $t$. Then the utility's profit in time slot $t$ is modeled as

$$\theta Y - \frac{1}{2}\left(\sum_{i=1}^{N} y_i^t - Yd_t\right)^2. \tag{4.1}$$

The first term $\theta Y$ is the revenue from providing demand reduction at capacity $Y$. where $\theta$ is the unit price of a standardized size of demand reduction (denoted by $d_t$) and $Y$ is a scaling factor showing how many standardized demand reduction the utility provides. The second term is the penalty of deviation between actual aggregated demand reduction $\sum_{i=1}^{N} y_i^t$ from the committed reduction $Yd_t$.

### *4.3.2 User Model*

We model users' response to the broadcasted price as solving an optimization problem to balance their reward from responding with respect to their cost functions [5, 50]. Here we consider the following quadratic cost function $u_i(\cdot)$ for user $i$:

$$u_i(y_i^t) = \frac{1}{2}\beta_i(y_i^t)^2 + \alpha_i y_i^t, \tag{4.2}$$

where $y_i^t$ is user $i$'s response in consumption at time $t$.

Note that both $\beta_i$ and $\alpha_i$ are unknown parameters to the utility. The price signal serves as a reward to users for their consumption reduction. Specifically, for those users who adjust their consumption by $y_i^t$, they will receive payment $\lambda_t' y_i^t$ from the utility in time slot $t$, where $\lambda_t'$ is the price in unit consumption. Since users aim to minimize their net cost from reducing consumption, we have the cost minimization problem for each user $i$:

$$\min_{y_i^t} \quad u_i(y_i^t) - \lambda_t' y_i^t. \tag{4.3}$$

Note that this optimization problem is operationally the same as $\min_{y_i^t} \frac{u_i(y_i^t)}{N} - \lambda_t y_i^t$, where $\lambda_t = \frac{\lambda_t'}{N}$. This is in accordance with the optimization that is introduced later in Section 4.3.3,

when the costs are divided by $N$. To be consistent, we refer to $\lambda_t$ as the price signal that stimulates consumption.

In practice, there is always some noise associated with the response of users. For example, users (or more likely their home management systems) can relax the temperature tolerance of their homes, but the actual power consumption reduction would be somewhat random [61]. Therefore, we assume that the actual response of the users is a noisy version of the optimal solution to (4.3). Then user $i$'s consumption change is given by

$$\hat{y}_i^t = y_i^t + \epsilon_i^t, \tag{4.4}$$

where $\epsilon_i^t$ is the noise in observation and is independent and identically distributed. We assume the noise is Gaussian in this section, although the results extend to other types of noises.

### *4.3.3 Problem Formulation*

The operator aims to minimize the following expected average cost over the time horizon:

$$\begin{aligned} &\min_{Y} \ \min_{\boldsymbol{y}} \sum_{t=1}^{T} \sum_{i=1}^{N} \frac{1}{N} \mathbb{E}\left[\frac{1}{2}\beta_i(y_i^t+\epsilon_i^t)^2 + \alpha_i(y_i^t+\epsilon_i^t)\right] \\ &+ \sum_{t=1}^{T} \frac{1}{2N} \mathbb{E}\left[\left(\sum_{i=1}^{N}(y_i^t+\epsilon_i^t) - Y d_t\right)^2\right] - \frac{\theta Y T}{N} \\ =&\min_{Y} \ \min_{\boldsymbol{y}} \mathbb{E} \sum_{t=1}^{T} C(\hat{\boldsymbol{y}}_t, Y) - \frac{\theta Y T}{N} \end{aligned} \tag{4.5}$$

where the expectation is taken over the noise $\epsilon_i^t$ in user's response. The cost function $C(\hat{\boldsymbol{y}}_t, Y)$ involves two terms: the quadratic cost of users' response in consumption, i.e., $\hat{\boldsymbol{y}}_t$, and the cost of mismatch between the sum of user consumption and the target consumption. Here, $\hat{\boldsymbol{y}}_t$ is a vector storing each user's consumption $\hat{y}_i^t$ at time $t$. The last term $\frac{\theta Y T}{N}$ is the revenue of the utility. The utility determines the optimal capacity of demand response $Y$ at the beginning of the time horizon, and the optimal responses $y_i^t$'s are determined in every time

period. Since $\lambda^t$ uniquely determines the responses (up to the random noises), we sometimes write them as $\hat{y}_i^t(\lambda^t)$.

The optimization problem (4.5) is not difficult to solve if $\beta_i$ and $\alpha_i$ are known to the utility. It suffices to solve a convex quadratic programming in a centralized manner. Alternatively, if the users can iteratively communicate with the utility in a time step, a decentralized algorithm can also be deployed. However, utilities generally do not have information about the cost coefficients of the users [62, 63], and often do not engage in multi-round communication with users [60]. In the next section, we present the main results, which describes how (4.5) can be solved when the utility needs to learn and optimize demand response of users in an online fashion.

### *4.3.4 Online Algorithm and Regret*

When the utility does not know the parameters of the cost function and wants to solve the optimization problem in (4.5), it needs to solve two problems at the same time: 1) learn the cost function, and 2) design proper price signals to obtain desired aggregated responses from end users. These two problems are solved in an *online fashion*, where the utility determines current price $\lambda_t$ based on partial information, i.e., the past sequence of prices $\{\lambda_1, \lambda_2, ..., \lambda_{t-1}\}$, and the past responses from users $\{\hat{y}_i^s(\lambda_s), 1 \leq i \leq N, 1 \leq s \leq t-1\}$ . The online strategy is a policy that maps the history observation $\mathcal{H}_t = \{\lambda_s, \hat{y}_i^s(\lambda_s), 1 \leq i \leq N, 1 \leq s \leq t-1\}$ to $\lambda_t$, denoted by $\lambda_t = f(\mathcal{H}_t)$. The function $f(\cdot)$ is called a policy, or more specifically, an online learning algorithm that uses information from the past to make sequential decisions without knowing the future information. The main result is that there is an online policy that will eventually *find the correct price*, with a small regret.

We adopt the notion of regret to evaluate the performance of an online pricing strategy $\lambda_t$. Regret is widely used in literature to evaluate an online decision process, for example in online convex problems [64] and in multi-arm bandit problems [65]. In this dissertation, it is defined as the expected difference between the costs obtained by the online strategy with unknown $\alpha_i$ and $\beta_i$, and the optimal solution of when all parameters are known in advance.

More specifically, regret $R$ over horizon $1, 2, ..., T$ is defined as:

$$R = \mathbb{E}\{\sum_{t=1}^{T} C(\hat{\boldsymbol{y}}_t(\lambda_t), Y)\} - \mathbb{E}\{\sum_{t=1}^{T} C(\hat{\boldsymbol{y}}_t(\lambda_t^*), Y)\}, \tag{4.6}$$

where $Y$ is the capacity predetermined beforehand for the demand response program. The expectation is taken over the randomness from $\hat{\boldsymbol{y}}_t(\lambda_t)$, when users' consumption is noisy.

In addition, $\lambda_t^*$ is the optimal reward signal if given full information (values of $\alpha_i$, $\beta_i$), and $\lambda_t$ is the online pricing signal obtained from online strategy. We stack all users' response $y_i^t$ as a vector $\hat{\boldsymbol{y}}_t(\lambda_t)$ at time $t$ stimulated with price $\lambda_t$. The regret can be decomposed as across each time period as:

$$\begin{aligned} R &= \sum_{t=1}^{T} \{\mathbb{E}\{C(\hat{\boldsymbol{y}}_t(\lambda_t), Y)\} - \mathbb{E}\{C(\hat{\boldsymbol{y}}_t(\lambda_t^*), Y)\}\} \\ &= \sum_{t} R_t. \end{aligned} \tag{4.7}$$

### *4.3.5 Summary of main results*

We now state the main theorem in this dissertation, that quantifies the performance of the online strategy. The details of the learning strategy are illustrated in Section 4.5.

The main theorem of this dissertation is:

**Theorem 4.** *There is an algorithm where the gap $R_t$ between online strategy and optimal offline solution decays as $1/t$ and the algorithm achieves $\log T$-regret.*

Theorem 4 states that the gap $R_t$ is diminishing with time $t$ and has a rate $\frac{1}{t}$, as shown in Fig. 4.2. This gives an overall regret in the order of $\log(T)$ over at total of $T$ time periods. This is actually the best one can hope for, because of a celebrate result in online optimization that states no online algorithm can do better [49].

In Section 4.5, we aim to find an algorithm such that this bound of the regret is achieved. The existence of such an algorithm validates the statement in Theorem 4, and the proof on the convergence of the algorithm is left to the appendices for interested readers.

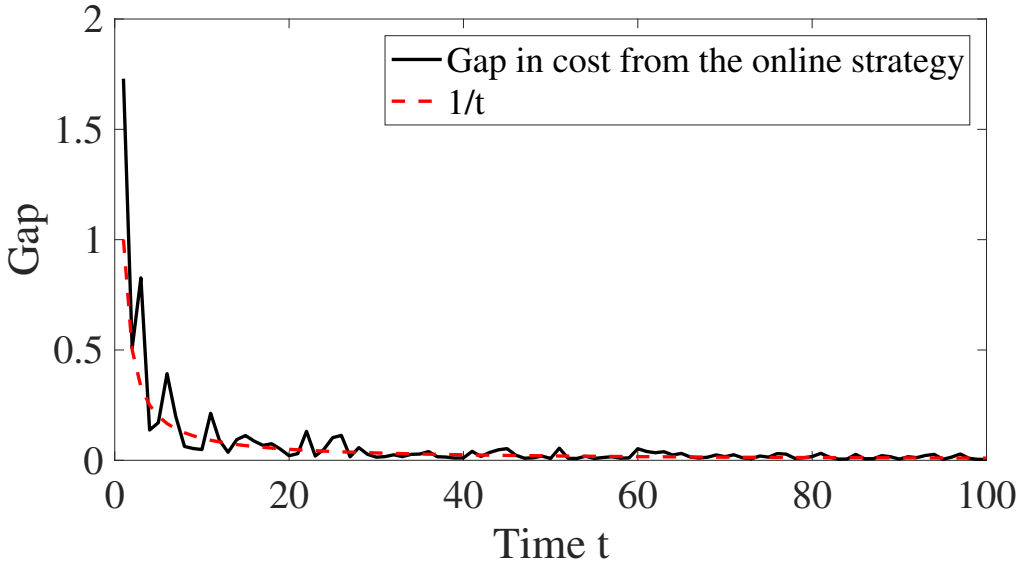


Figure 4.2: Gap between the online cost and optimal cost over time, accumulated over 100 users for 100 time slots. Detailed parameters in the model are illustrated in Section 4.6.

### *4.4 Offline optimal solution*

In this section, we characterize the offline optimal solution, which provides insights for designing the online strategy in Section 4.5.

Suppose that the utility knows the value of $\alpha_i$ and $\beta_i$ of all users. To solve (4.5), we start by solving the inner minimization problem, assuming that the optimal capacity $Y^*$ has been determined beforehand. Then we solve the following problem to derive the optimal demand response of all the users $i = 1, 2, ..., N$ over time slots $t = 1, 2, .., T$, with $Y^*$ as a parameter:

$$\begin{aligned}\min_{\boldsymbol{y}} \sum_{t=1}^{T}\sum_{i=1}^{N} \frac{1}{N}\mathbb{E}\left(\frac{1}{2}\beta_i(y_i^t+\epsilon_i^t)^2+\alpha_i(y_i^t+\epsilon_i^t)\right)\\ +\sum_{t=1}^{T}\frac{1}{2N}\mathbb{E}\left[(\sum_{i=1}^{N} y_i^t+\epsilon_i^t-Y^*d_t)^2\right]\end{aligned} \tag{4.8}$$

Since $Y^*$ is a predefined scaling factor, each time period is decoupled. The optimal

scheduling for each user $i$ at each time $t$ is computed as the solution from (4.8):

$$y_i^{t,*} = \frac{N\frac{Y^* d_t + \sum_{i=1}^N \frac{\alpha_i}{\beta_i}}{N + \sum_{i=1}^N \frac{N}{\beta_i}} - \alpha_i}{\beta_i}, \tag{4.9}$$

where we used the fact that the noise is zero mean and independent to everything [66].

In the online setting, the utility can only influence the users through a price. Therefore here we look at the price signals that would realize the desired changes in (4.9). To design this price, we introduce an ancillary variable $D_t$, which is the sum of responses from users into problem in (4.8):

$$\begin{aligned} \min_{\boldsymbol{D},\boldsymbol{y}} & \sum_{t=1}^{T}\sum_{i=1}^{N} \frac{1}{N}\,\mathbb{E}\left(\frac{1}{2}\beta_i(y_i^t+\epsilon_i^t)^2 + \alpha_i(y_i^t+\epsilon_i^t)\right) \\ & + \sum_{t=1}^{T}\frac{1}{2N}\,\mathbb{E}\left[\left(D_t + \sum_{i=1}^{N}\epsilon_i^t - Y^* d_t\right)^2\right] \\ \text{s.t. } & D_t - \sum_{i=1}^{N} y_i^t = 0. \end{aligned} \tag{4.10}$$

The problem in (4.10) is a constrained convex problem [67] that solves exactly the same problem as presented in (4.8). We introduce a dual variable $\lambda_t$ for the equality constraint $D_t - \sum_{i\in\mathcal{N}} y_i^t = 0$ and use KKT conditions [67] to solve the optimal solution in a closed form as:

$$y_i^{t,*} = y_i^t(\lambda_t^*) = \frac{N\lambda_t^* - \alpha_i}{\beta_i}, \tag{4.11}$$

and

$$\lambda_t^* = \frac{Y^* d_t + \sum_{i=1}^N \frac{\alpha_i}{\beta_i}}{N + \sum_{i=1}^N \frac{N}{\beta_i}}, \tag{4.12}$$

where $\lambda_t^*$ is the optimal value of the dual variable associated with the equality constraint in (4.10) and can be interpreted as optimal price incentive that the utility needs to incentivize users to achieve the optimal consumption change as in centralized control in (4.8). Note that since each cost term in (4.8) is divided by a factor of $N$, $\lambda_t$ and $\lambda_t'$ (defined in (4.3)) differs with a scaling factor of $\frac{1}{N}$ as well.

After solving the optimal demand change of users $\boldsymbol{y}^* = \{y_i^{t,*},\ \forall i,\ \forall t\}$, we substitute the optimal solution obtained in (4.9) as a function of $Y$ into (4.8) and solve the optimal solution for $Y^*$ as

$$Y^* = \frac{T\theta(1+\sum_i \frac{1}{\beta_i})^2 - \sum_t(\sum_i \frac{\alpha_i}{\beta_i})(1+\sum_i \frac{1}{\beta_i})d_t}{\sum_t d_t^2(1+\sum_i \frac{1}{\beta_i})}, \tag{4.13}$$

which depicts the optimal "capacity" in demand reduction during demand response programs.

### *4.5 Online strategy and regret analysis*

Now we proceed to design an optimal online pricing strategy that achieves the regret as mentioned in Theorem 4, given that the parameters are not unknown to the utility. There are two questions: 1) does the utility need to estimate each individual $\alpha_i$ and $\beta_i$ to design such a price, and 2) does the noisy observation from the users' consumption data affect the estimating procedure.

First, given full information, the optimal price signal presented in (4.12) only involves the terms $\sum_i \frac{1}{\beta_i}$ and $\sum_i \frac{\alpha_i}{\beta_i}$, given that $Y^*$ is set to some predefined value. This suggests that if $\alpha_i$ and $\beta_i$ are not known to the utility, only those two aggregated terms $\sum_i \frac{1}{\beta_i}$ and $\sum_i \frac{\alpha_i}{\beta_i}$ need to be computed. The dimension of the parameter space reduces from $2N$ to 2, which reduces the information needed to compute the online price. More specifically, it is sufficient for the utility to observe the aggregated consumption:

$$\sum_i \hat{y}_i^t = \sum_i \frac{N}{\beta_i}\lambda_t - \sum_i \frac{\alpha_i}{\beta_i} + \sum_i \epsilon_i^t \tag{4.14}$$

where we restate that $\lambda_t$ is the designed price signal at time $t$ that is based on past observation. Since the noise for each user is independent and follows standard gaussian distribution, the aggregated noise $\sum_i \epsilon_i^t$ follows a gaussian distribution with variance equals to $N$.

Second, note that the observation of the aggregated consumption in (4.14) follows a gaussian distribution and the expected value of the observation is linear in the parameter $\sum_i \frac{N}{\beta_i}$ and $\sum_i \frac{\alpha_i}{\beta_i}$ . Since least square estimator is the Best Linear Unbiased Estimator

(BLUE) [68], we therefore adopt the least square approach to estimate $\sum_i \frac{N}{\beta_i}$ and $\sum_i \frac{\alpha_i}{\beta_i}$ using a linear regression model.

With the clarification of the two questions, we elaborate the formulation of the regret introduced in Section 4.4 and propose an iterative linear regression estimator in Algo. 4 to design online price strategy. In the following subsections, we first give more details on the formulation of the regret. Then we introduce the proposed online learning strategy for pricing $\lambda_t$ based on historical observation. We also state the performance of the online strategy and leave the detailed analysis on the order of the regret (Theorem 5) to the appendices.

### *4.5.1 Regret formulation*

As stated in Section 4.3.4, we evaluate an online pricing strategy by regret. We let $\hat{y}_i^{t*} = y_i^{t*} + \epsilon_i^t$ and $\hat{D}_t^* = \sum_i \hat{y}_i^{t*}$ denote the optimal response with noise and optimal aggregated response, respectively. Since each time $t$ is decoupled and for simplicity reasons, the regret for one step (gap $R_t$) can be computed as the following (details shown in [69]):

$$\begin{aligned} R_t =& \mathbb{E}\{C(\hat{\boldsymbol{y}}_t(\lambda_t), Y^*)\} - \mathbb{E}\{C(\hat{\boldsymbol{y}}_t(\lambda_t^*), Y^*)\} \\ =& A_1(\mathbb{E}\,\lambda_t^2 - (\mathbb{E}\,\lambda_t)^2) + A_1(\mathbb{E}\,\lambda_t - \lambda_t^*)^2 + A_2(\mathbb{E}\,\lambda_t - \lambda_t^*). \end{aligned} \tag{4.15}$$

where

$$A_1 = \frac{N}{2}\left(\sum_{i=1}^{N}\frac{1}{\beta_i} + (\sum_{i=1}^{N}\frac{1}{\beta_i})^2\right),$$

and

$$A_2 = \sum_{i=1}^{N}\frac{\alpha_i}{\beta_i}\left(\sum_{i=1}^{N}\frac{1}{\beta_i} - 1\right)$$

are some constant coefficients that do not evolve with time $t$.

From (4.15), we observe that the regret consists of variance, bias and squared bias of $\lambda_t$, respectively. This suggests that it is preferable to have a pricing strategy that achieves both small variance and bias, or can tradeoff two.

### *4.5.2 Online learning procedure*

The online learning strategy for optimal prices is presented in Fig. 4.3. We denote $\gamma_1 \triangleq \sum_i \frac{1}{\beta_i}$ and $\gamma_2 \triangleq -\sum_i \frac{\alpha_i}{\beta_i}$. Since at each time period the users' response is linear in the price signal, we propose to estimate the unknown parameters through linear regression based on history using least squares. The parameters to estimate are: $\gamma_1, \gamma_2$. The estimation of $\gamma_1$ and $\gamma_2$ at time $t$ are denoted by $\hat{\gamma}_1^t$ and $\hat{\gamma}_2^t$, respectively.

The online learning algorithm shown in Fig. 4.3 consists of several steps: first, the utility collects history observation until the current time point; then it adopts the decision from Algo. 4 (linear regression) to design the price signal and broadcast it to the end users. Finally, the users' consumption based on this price signal is reported back to the utility and the process repeats.

The core of the online algorithm is in Algo. 4, which determines the performance of the algorithm. In Algo. 4 we estimate the unknown parameters $\gamma_1$ and $\gamma_2$ by the least square method[1]. What is more, the whole procedure is done iteratively by adding more samples into the model, which means that as $t$ gets bigger, we accumulate more samples to train the model and iterate. We thus call Algo.4 *iterative linear regression*. Its details are illustrated in the next subsection.

The performance of the algorithm in Fig. 4.3 is evaluated by regret. Recall that Theorem 4 states there exists an algorithm that the regret $R$ is growing logarithmically with time horizon $T$. We use Theorem 5 to show that the proposed algorithm in Fig. 4.3 achieves this rate.

Moreover, we adopt the following asymptotic bound notations. These notations facilitate the analysis to compare the orders of quantities of interest [70].

**Definition 1.** *$f(n) = \Theta(g(n))$ means there are positive constants $k_1$, $k_2$, and $n_0$, such that $0 \leq k_1 g(n) \leq f(n) \leq k_2 g(n), \forall n \geq n_0$.*

[1]When $t = 1$ and 2, since there are no enough data points to derive least square estimator from the linear regression model, we impose a prior information on the parameters and estimation is done as ridge regression.

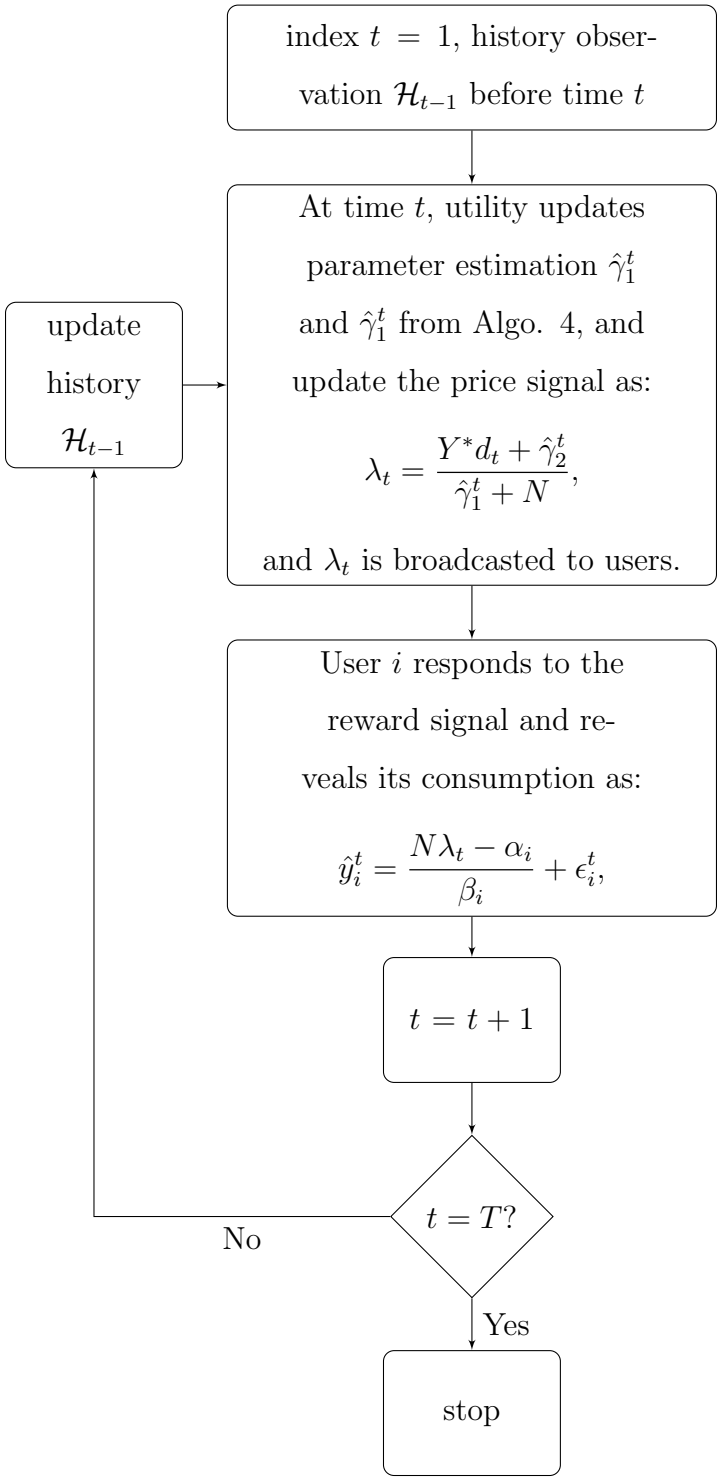


Figure 4.3: Online learning algorithm for pricing.

**Definition 2.** *$f(n) = O(g(n))$ means there are positive constants $k$, and $n_0$, such that $f(n) \leq k_2 g(n), \forall n \geq n_0$.*

With these notations, we state Theorem 5 as below.

**Theorem 5.** *The algorithm presented in Fig. 4.3 achieves $\Theta(\log T)$-regret.*

In addition, recall that, if $f(n) = \Theta(g(n))$ then $f(n) = O(g(n))$, the proposed algorithm at the same time achieves a regret of $O(\log T)$ as well. Therefore, proving Theorem 5 infers Theorem 4. The detailed proof of Theorem 2 can be found at Appendix. Here we provide a sketch of the proof to Theorem 2.

*Sketch of proof to Theorem 5 .* We want to show that at each time $t$, the gap between the offline optimal strategy and online strategy is bounded by $\frac{1}{t}$. Then following the fact that $\sum_t \frac{1}{t} = \log T$ for $T$ time slots, the regret is $\log T$. To show that the gap is $\frac{1}{t}$, from (4.15) it suffices to show that the variance and the bias (with a multiplicative term $C_1$ and $C_2$) of the price estimate $\lambda_t$ is decaying at a rate of $\frac{1}{t}$ at each time slot $t$. In the detailed proof shown in the Appendix, we show that this rate indeed holds. □

### *4.5.3 Iterative linear regression*

As can be seen from Fig. 4.3, the performance of the algorithm in Fig. 4.3 largely depends on the estimator of $\gamma_1$ and $\gamma_2$ obtained by the least square from Algo. 4, since they influence variance and bias of $\lambda_t$ which determine the regret. Algo.4 is shown with one step iteration.

There are a few points to note. First, the estimators from Algo. 4 are consistent but not unbiased. This is because that the online prices $\lambda_t$ that we generate based on the estimates from Algo. 4 is correlated with past noise. These $\lambda_t$'s are again fed into Algo. 4 as regressors to train the linear regression model. However, the bias is of lower orders compared to the order of the estimator and is decaying with the number of time periods, we approximate the estimators as well as their variance and expectation by assuming that they are unbiased estimators. This approximation is validated by simulation results.

**Algorithm 4** Iterative linear regression (one step)

1: **Input**: History $\mathcal{H}_{t-1}$ which includes price history $\lambda_s$ and response history sequence $\sum_i \hat{y}_i^s$ for $s = 1, 2, ..., t-1$ and $t$ is the current time stamp.

2: The linear regression model is:

$$\sum_i \hat{y}_i^s = N\lambda_s\gamma_1 + \gamma_2 + \sum_i \epsilon_i^s, s \in \{1, 2, ..., t-1\}. \tag{4.16}$$

3: Do a least square estimate in the linear regression model of $\sum_i \hat{y}_i^t$ on $N\lambda_t$ plus an intercept.

4: **Output**: Least square estimate $\hat{\gamma}_1^t$ and $\hat{\gamma}_2^t$.

Second, one thing that might hinder one from using iterated linear regression in online learning algorithms is that it may happen that the observations are not exploring the linear regression model. For example $\lambda_t$ is the same for all $t \in \{1, 2, ..., s\}$. If so, the linear regression is not efficient because the two regressors ($\lambda_t$ and the intercept) is the same which renders infinite variance in the estimator. This problem is addressed in [60, 71].

However, with the assumption that $d_t$ is randomly spread between $[d_{min}, d_{max}]$, (4.12) suggests that $\lambda_t$ will also be much different across different time $t$. Then we can sufficiently explore the structure of the linear regression model and that the estimation from least square is efficient. In the simulation, we show that even some of the $d_t$'s are similar, the exploration of the linear regression model is still effective, such that the regret is still in order $\log T$.

## *4.6 Simulation*

### *4.6.1 Parameter set up*

In the simulation, we generate a random price at $t_1 = 1$ to start the online algorithm. For practical purposes, we introduce ridge regression estimators in the linear regression model [72]. The influence of $\lambda$ on the estimator will decay fast as more samples are included into the model.

The parameters of the system are shown in Table 4.1, where $d_t$ are the normalized demand reduction and $c$ is a constant bounded away from zero. The iteration of Monte Carlo simulation for the responses of users is set to be 1000 and the regularization parameter in the ridge regression is set to be 0.001. In addition, there are totally 100 different users.

Table 4.1: Parameters. Intervals indicate the uniform distribution. $c$ is some constant. We simulate two sets of parameters and compare the results.

| $\theta$ | $\alpha_i$ | $\beta_i$ | $d_t$ |
|---|---|---|---|
| $c\max\{d_t\}$ | [1,2] | [4,8] | [3,6] |
| $c\max\{d_t\}$ | [1,3] | [3,10] | [2,5] |

### *4.6.2 Pricing strategy*

We first validate the online pricing strategy discussed in Section 4.5. The comparisons between the optimal pricing and online pricing are shown in Fig.4.4a and Fig. 4.4b. As can be seen from Fig.4.4a and Fig. 4.4b, at the first few time steps, the online algorithm is still learning the parameters given very few sample points, and the online price deviates a lot from the optimal pricing. This deviation in price also drives the aggregated response to be suboptimal. However, the estimation accuracy is greatly improved given just a few more sample points, and as we can see from Fig.4.4a and Fig. 4.4b, the online price tracks the optimal price after less than 50 time steps, so does the aggregated response. This means that after a few time steps, the aggregated response is able to achieve the demand response requirement by the utility, even the utility does not know the user's parameters in advance.

The comparison is clearer when we explicitly compute the difference between aggregated online response and optimal response, shown in Fig. 4.5. As can be seen from Fig. 4.5, the aggregated response $\sum_i \hat{y}_i^t(\lambda_t)$ induced by the proposed online pricing strategy $\lambda_t$ is

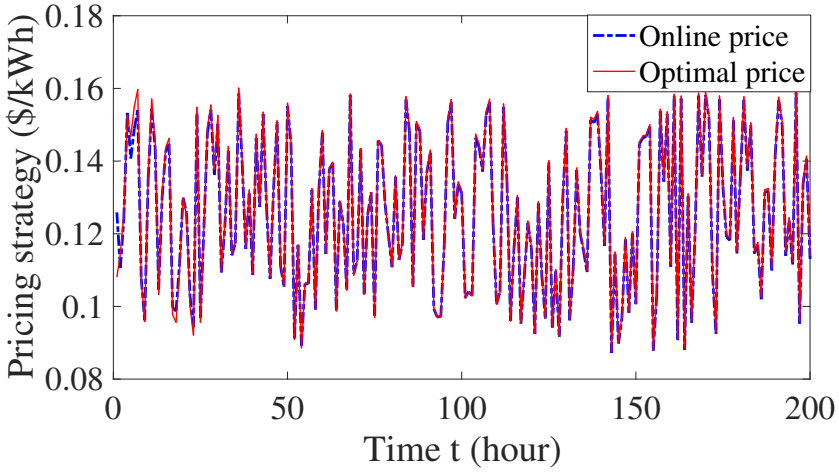


(a) Optimal pricing and online pricing.

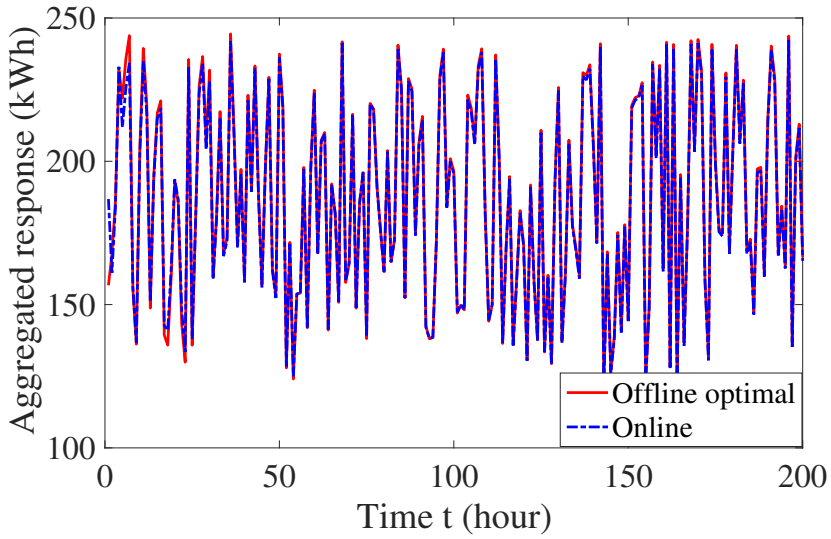


(b) Optimal response and online response (aggregated).

Figure 4.4: Comparison between optimal pricing (aggregated response) and online pricing.

approaching the optimal response $\sum_i \hat{y}_i^t(\lambda_t^*)$. The difference between the two responses is diminishing and becomes zero as time goes on.

The variance and the bias of online price $\lambda_t$ is shown in Fig. 4.6a and Fig. 4.6b. As we

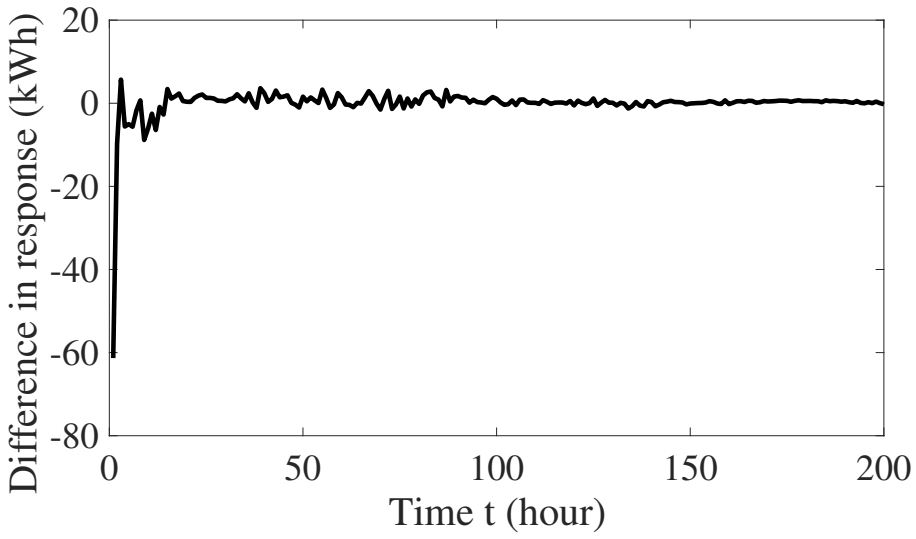


Figure 4.5: Difference between the aggregated response induced by online pricing and optimal pricing.

can see, at first the bias is huge because $\lambda_1$ is randomly initialized, so it is not accurate. As long as the learning procedure begins, the bias drops drastically. The variance of $\lambda_t$ has a much slower decay rate of $\frac{1}{t}$, as has been discussed in Section 4.5. Comparing the orders, the squared bias is much smaller than the variance. Therefore the tradeoff between variance and squared bias is dominated by variance.

### *4.6.3 Regret Analysis*

We then analyze the regret for the online pricing strategy. The gap $R_t$ between online cost and offline cost is shown in Fig. 4.2 in Section 4.3.5 and the regret is shown in Fig. 4.7.

From Fig. 4.2, we observe that the gap decays fast with time with a rate of $\frac{1}{t}$, which means the cost obtained from online price signals $\lambda_t$ approaches the true cost to the system quickly with time. The regret is the sum of the gaps during all time periods and is in order $\log T$ as shown in Fig. 4.7. As can be seen from Fig. 4.7, the regret is within some bounds of $\log t$, which validates Theorem 5. What is more, from Fig.4.7, we find that the algorithm

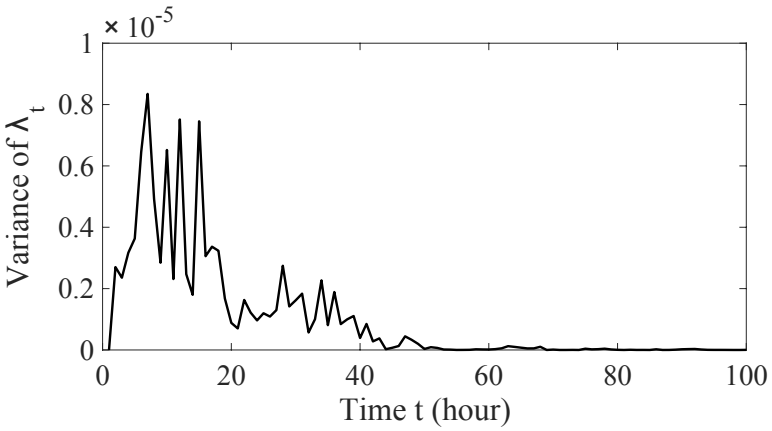


(a) Variance of $\lambda_t$

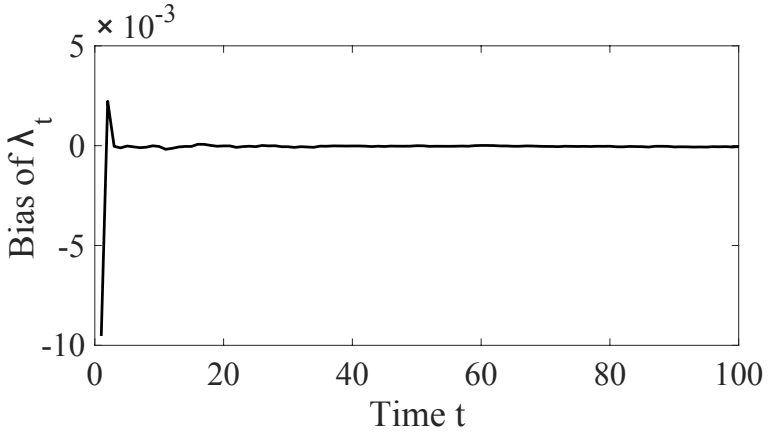


(b) Bias of $\lambda_t$

Figure 4.6: Variance and bias of online price $\lambda_t$.

works for different sets of parameters.

### *4.6.4 Performance of the algorithm subject to same consecutive requirement over time*

As has been pointed out in [60], an iterated linear regression may not well explore the model. This results in a larger variance in the estimator $\hat{\gamma}_1$ and $\hat{\gamma}_2$, and thus deteriorates the estimation of price, i.e., $\lambda_t$, which may lead to a regret worse than $O(\log T)$.

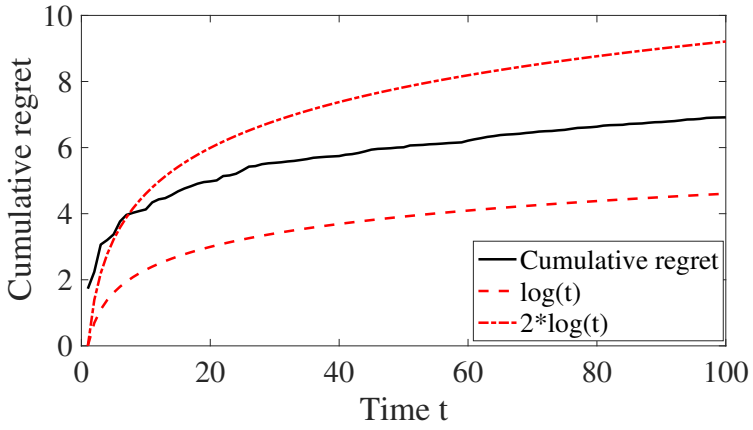


(a) $\alpha_i \sim [1, 2]$, $\beta_i \sim [4, 8]$, $d_t \sim [3, 6]$.

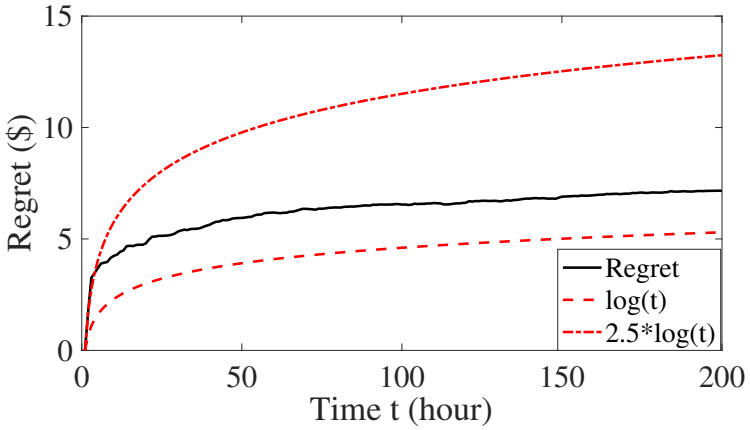


(b) $\alpha_i \sim [1, 3]$, $\beta_i \sim [3, 10]$, $d_t \sim [2, 5]$.

Figure 4.7: Regret over time with different parameters.

With a more careful scrutiny, we find that this situation only happens when the regressors $\lambda_t$'s are highly correlated. We have argued in Section 4.5 that this situation is avoided with the assumption that $d_t$'s are different across time, or there are sufficiently many $d_t$'s that are not the same to each other.

To state this clearer, we first set up a sequence of $d_t$'s in which 20 %, 30% and 40% of

them are identical. The result is shown in Fig. 4.8.

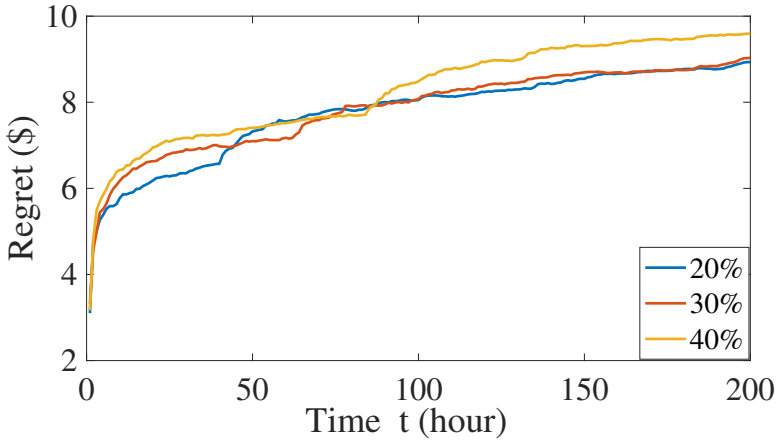


Figure 4.8: Regret $R$ over time where 20 %, 30% and 40% of $d_t$'s are the same. Cost function is quadratic and linear.

From Fig. 4.8, we see that the regret is still sub-linear, i.e., $\Theta(\log t)$, in time $t$. This suggests that even with some portion of same $d_t$'s in the system, the proposed algorithm still works effectively.

We also test against a case where each time period is short, i.e., $t$ represent fifteen minute-level observation. Suppose that the demand response requirement only get changed every hour, which means that $d_t$ remains the same for every four time slots. In total, 25% of all the $d_t$'s are the same. The results are shown in Fig. 4.9 and Fig. 4.10.

As can be seen from Fig.4.9, the response now is smoother than that shown in Fig. 4.4b, since the observation is more frequent. The online aggregated response is again able to achieve the optimal response, after roughly 50 time slots.

The regret is shown in Fig. 4.10. It is clearly within the bounds of $\log T$, which validates the statement that the algorithm remains effective with some amount of repetitive pattern in $d_t$.

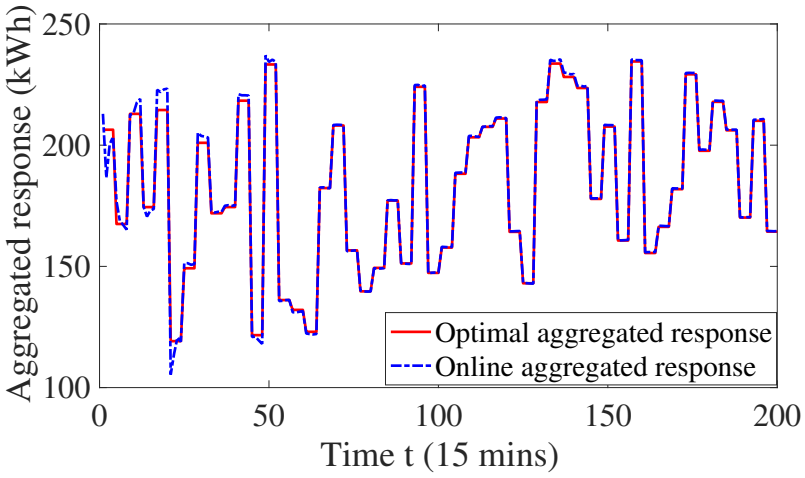


Figure 4.9: Comparison of the optimal aggregated response and online aggregated response, where $d_t$ is the same every four time slots.

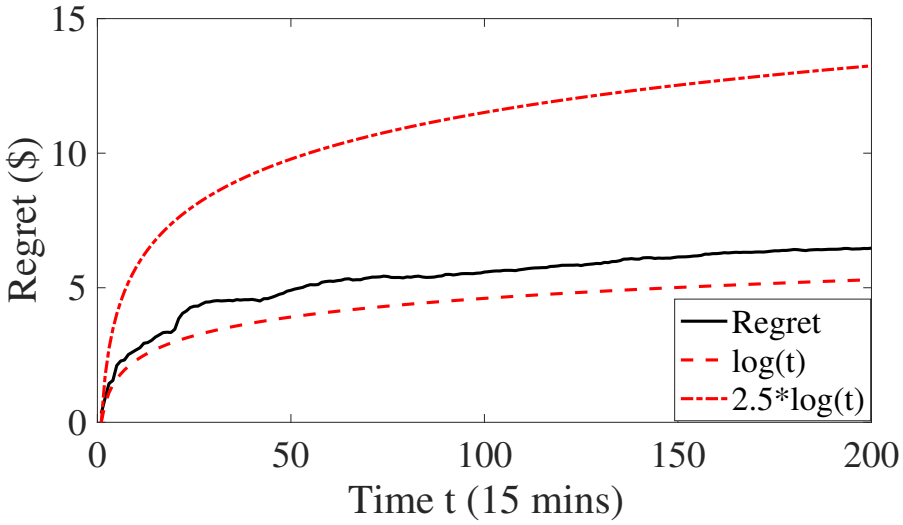


Figure 4.10: Regret $R$ where $d_t$ is the same every four time slots.

### *4.7 Summary*

In this Chapter, we consider a scenario where the utility(system operator) interacts with users through demand response signals (prices) and try to reduce satisfactory amount of

electricity at each time period. We propose a distributed online pricing strategy for the utility to optimize the users' response as well as to assign optimal prices on a fly. We show that the proposed price updating strategy obtains a logarithmic regret and is able to find optimal prices after a few updates. Simulation results validate the statement that the regret converges in a logarithmic rate, and is robust to a wide range of parameters as well as different resolution in consumption data.

# Chapter 5

# PLANNING OF RENEWABLE ENERGY RESOURCES – CAPACITY INVESTMENT GAME

## *5.1 Introduction and literature review*

The proliferation of distributed renewable generators (especially PV) has allowed for a much more flexible system, but also led to operational complexities because they are often not coordinated [73]. Recently, there has been strong regulatory and academic push to allow these individual generators to participate in a market, hoping to achieve a more efficient and streamlined management structure [74,75]. Therefore, in this chapter we study an investment game where individual firms decide their installation capacities of PV panels and compete to serve the load.

Currently, there are several lines of fruitful research on the investment of solar energy resources. The common challenge in these works is to address the *pricing* of solar energy, since once installed, power can be produced at near zero operational cost. In [76], feed-in tariffs (fixed prices) are used to guide the investment decisions. In [77, 78], risks about future uncertainties in prices are taken into account, although these prices are assumed to be independent of the investment decisions. Instead of exogenously determined feed-in tariffs, [79–81] study incentive based pricing, arguing that the price of solar energies should match their market value, which is the revenue that those resources can earn in markets, without the income from subsidies. However, the investment question of how to decide the capacity of each solar installation is not considered.

A common assumption made in existing studies is that an operator (or utility) makes centralized decisions about the capacity of the solar installation at different sites [82, 83], although each installation may participate in a market to determine the exact pricing of

energy. It is rare that the two problems–capacity investment and pricing–are considered at the same time. On the other hand, as these markets continue to evolve, academics and regulators [74, 75, 84, 85] have increasingly argued in favor of a more decentralized operation, i.e., allowing for direct economic transactions between producers and consumers of electricity. The call for decentralization has been primarily driven by the rapid proliferation of renewable sources of energy, which in turn has led to a shift from large-scale generators to decentralized producers. For example, photovoltaic (PV) cells can be installed at a low cost on the rooftops of buildings, and the excess generation can be 'sold to the grid' [7]. The environmental benefits of renewable sources are well-understood; equally important are the notions that such markets can deliver energy at a much lower cost than conventional sources of energy, and distributed sources lead to greater resilience in the power grid. Indeed, the paradigm shift towards distributed renewables is poised to benefit society both environmentally and economically.

The competition between individual producers in a decentralized market for electricity is normally studied either via the Cournot model or the Bertrand model [86]. In the former, the producers compete via quantity, while in the latter they compete via price. In this work, we adopt the Bertrand competition to model price bidding since it is a more natural process in the distribution system, where there is no natural inverse demand function (required by the Cournot competition model) [87,88]. Then the investment game becomes a *two-level* game as shown in Fig. 5.1b. For any given capacities, the producers compete through the Bertrand model to determine their prices to satisfy the demand in the system. Then the outcome of this game feeds into an upper level capacity game, where each producer determines its investment capacities to maximize its *expected profit*.

This type of two-level game was studied in [89] in the context of communication network expansion. They showed that Nash equilibria exist, but the efficiency of any of these equilibria are bad compared to the social planner's (or operator's) solution. More precisely, as the number of players grows, the social cost of all of the equilibria grow with respect to the cost of the social planner's problem. Therefore, instead of increasing efficiencies, competition

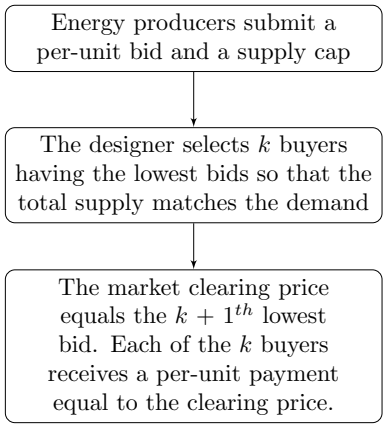


(a) Centralized mechanism where a central authority sets the market clearing price.

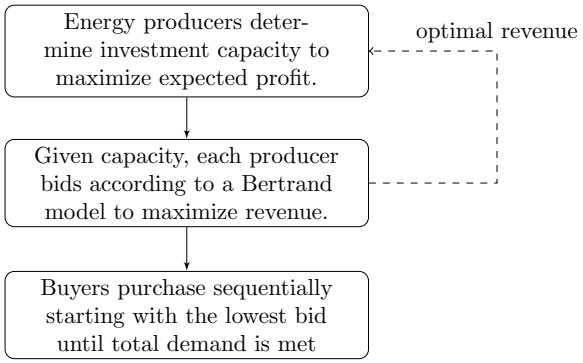


(b) Decentralized mechanism where each producer decides on the price at which they sell the good.

Figure 5.1: Centralized vs. decentralized market mechanisms.

can be arbitrarily bad. A similar intuition has existed in traditional power system investment problems, where the market power of the generators is highly regulated and closely monitored [90].

## *5.2 Contribution*

The central question of decentralized market involving uncertain renewable resources is:

> *Can we design a market mechanism for distributed renewable energy that maximizes social welfare at equilibrium without comprising on buyer surplus?*

In this chapter, we show that contrary to the result in [89], *the investment game between renewable producers leads to efficient outcomes under mild assumptions.* More precisely, 1) the investment capacity decisions made by the individual producers match the capacity decisions that would be made by a social planner; 2) as the number of producers increases, the

equilibria of the price game approaches a price level that allows the producers to just recover their investment costs. The key difference comes from the fact that renewables are *inherently random*. Therefore instead of trying to exploit the "corner cases" in a deterministic setting as in [89, 90], the uncertainties in renewable production naturally induces conservatism into the behavior of the producers, leading to a drastic improvement of the Nash equilibria in terms of efficiency. Therefore, uncertainty helps rather than hinders the efficiency of the system.

To analyze the equilibria of the game, our work builds on the results in [91]. In [91], the authors discuss the price bidding strategies in markets with exactly two renewable energy producers. They show that a unique mixed pricing strategy always exists given that the capacity of those producers are fixed beforehand. They extend it to a storage competition problem in later work [92]. However, this work did not address the strategic nature of the capacity investment decisions, nor did it consider markets with more than two producers.

In our setting, we explicitly consider the joint competition for capacity considering each player's investment cost, as well as the bidding strategy to sell generated energy. This problem is neither studied in traditional capacity investment games (randomness is not considered) [93, 94][1] nor in competition of renewable resources (investment strategy is considered) [79, 97]. To characterize the Nash equilibria in the two level capacity-pricing game, we consider two performance metrics. The first is social cost, which is the total cost of a Nash equilibrium solution with respect to the social planner's objective. The second is market efficiency, which measures the market power of the energy producers. As a comparison, the results in [89] show that in a deterministic capacity-pricing game, as the number of producers grows, *neither the social cost nor the efficiency improves at equilibrium.* In contrast, we show that a little bit of randomness leads to improvements on both metrics. Specifically, we make the following two contributions:

1. We consider a two level capacity-pricing game between multiple renewable energy pro-

[1]The work in [95, 96] studies an investment game where the demand curve is uncertain, but under a very different context than ours

ducers with random production. We show that contrary to commonly held belief, randomness improves the quality of the Nash equilibria.[2]

2. We explicitly characterize the Nash equilibria and show that the social cost and efficiency improve as the number of producers grows.

The rest of the chapter is organized as follows. Section 5.3 motivates the problem set up and details the modeling of both the decentralized and centralized market. Section 5.4 formally introduces the evaluation metrics for our setting. Section 5.5 presents the main results of this chapter, i.e., the relationship between the proposed decentralized market and the social planner's problem, and the analysis on the efficiency of the game in the decentralized market. Proofs for the main theorems are left in the appendices for interested readers. The simulation results are shown in Section 5.6 followed by the conclusion in Section 5.7.

## *5.3 Technical preliminaries*

### *5.3.1 Motivation*

Traditionally, power systems are often built and operated in a centralized fashion. The system operator acts as the social planner by aggregating the producers and makes centralized decisions on investment and scheduling (as shown in Fig. 5.2a). The goal of the social planner is to maximize the overall welfare of the whole system— this includes optimizing the costs incurred due to the investment and installation, and the cost paid by the consumers.

However, as distributed energy resources (DERs) start to disperse across the power distribution network, the centralized setup becomes difficult to maintain and manage. DERs such as rooftop PV cells are small, numerous, and owned by individuals, allowing them to act as producers and choose their own capacities and prices. Consequently, managing these

[2]This is conceptually similar to the results obtained in [98], where randomness increases the efficiency of Cournot competition.

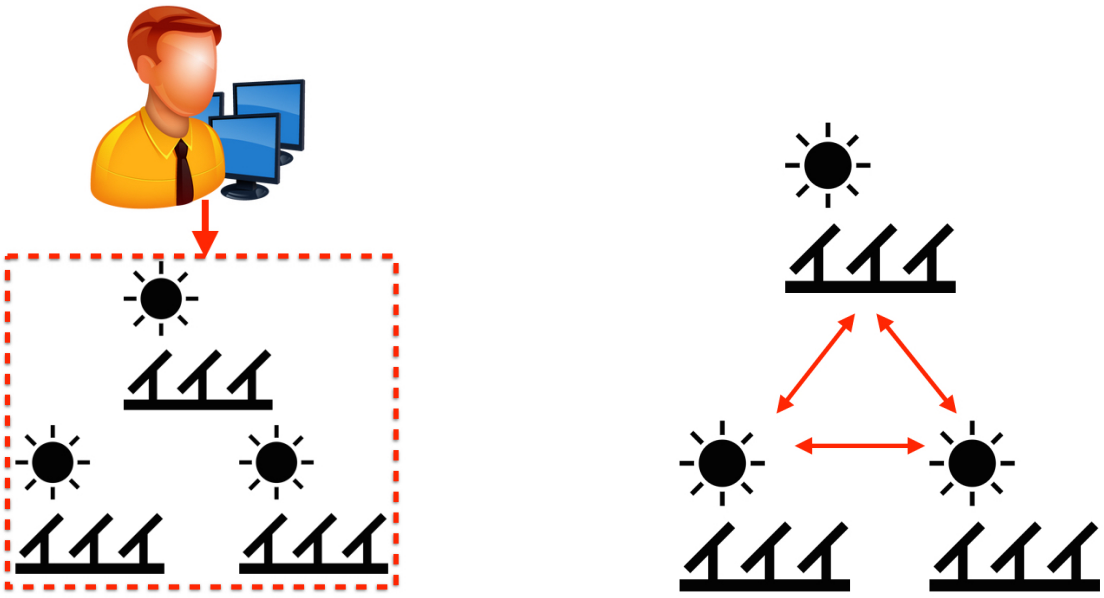

(a) Centralized. (b) Decentralized.

Figure 5.2: Centralized vs. decentralized market setup.

resources through a decentralized market (as shown in Fig. 5.2b) is starting to gain significant traction in the power distribution system.

Several issues arise in a decentralized market. Chief among them is that it is not clear whether the decentralized market achieves the same decision as if there were a central planner maximizing social welfare. The competition between energy producers is suboptimal if the following occurs:

- If the investment decisions by the competing producers deviate from the social planner's decision: this means that the competition is sub-optimal when it comes to finding a socially desirable investment plan.

- If the bidding strategy leads to a higher payment from electricity consumers than that from the social planner's decision, it means that the energy resource producers are

taking advantage of the buyers and the market is not efficient.

Both of these adverse phenomena can happen in decentralized markets in the absence of uncertainty [89, 99, 100], even when there are a large number of individual players. However, the rest of this chapter shows that neither of them occur in a decentralized market with renewables resources having random generation. We show that the inherent *uncertainty* in the production naturally improves the quality of competition. We start by formally introducing the game in the next section.

### *5.3.2 Renewable Production Model*

The nomenclatures used in this Chapter is shown in Appendix A.3.

**Renewable Production Model:** When producer $i$ invests in a capacity of $C_i$, its actual generation of energy is a random variable given by $C_i U_i \leq C_i$. That is, due to the randomness associated with renewables, its realized production may not equal its maximum capacity.

We make the following assumption on the $U_i$'s:

**[A1]** We assume that the random variable $U_i$ has support $[0, 1]$ and its density function is bounded and continuous on its domain. This assumption is mainly made for analytical convenience and captures a wide range of probabilistic distributions used in practice, e.g., truncated normal distribution and uniform distribution. Furthermore, we assume that $U_i$ is not a constant, so $\mathbb{E}(U_i - \mathbb{E}\, U_i)^2 = \sigma_i^2 > 0$.

### *5.3.3 Competition in decentralized markets*

Consider $N$ renewable producers who compete in a decentralized market. Each producer needs to decide two quantities: capacity (sizing) and the corresponding everyday price bidding strategy. To make this decision, each producer needs to take into consideration the fact that larger capacities lead to higher investment costs but may also result in enhanced revenue due to increased sales. If the invested capacity is low, then the investment cost is low but the producer risks staying out of the market because of less capability to provide energy. There-

fore competition requires non-trivial decision making by the decentralized stakeholders. In this chapter, we consider the case where each producer has the same investment cost, that is, $\gamma_i = \gamma$ for all $i$. This assumption is true to the first order since the solar installation cost in an area is roughly the same for all the consumers. Since the producers need to compete for capacity based on revenue (which is determined by optimal bidding), we refer to the capacity competition—how much to invest—as the *capacity game* and the pricing competition, i.e., how much to bid, as the *price sub-game*.

### *5.3.4 Capacity game*

The ultimate decision for the producers is to determine the optimal capacity to invest in. Suppose that the capacity is denoted by $C_i$ for each producer $i$, then each producer's objective is to maximize its profit, which is specified as:

$$\text{(Profit)} \quad \pi_i(\boldsymbol{C}_i, C_{-i}) - \gamma C_i, \forall i, \tag{5.1}$$

where $\pi_i(\boldsymbol{C}_i, C_{-i})$ is the payment (revenue) from consumers to producer $i$ when its capacity is fixed at $C_i$ and the others' capacities are fixed at $C_{-i}$. This payment is determined by the price sub-game given that a capacity decision is already made, i.e., $\boldsymbol{C} = [C_1, C_2, ..., C_N]$: we leave a detailed discussion of the revenue and the price sub-game to Section 5.3.5. The term $\gamma C_i$ represents the investment cost.

Since we are in a game-theoretic scenario, the appropriate solution concept is that of a Nash equilibrium. Specifically, a capacity vector $\boldsymbol{C}^\diamond = [C_1^\diamond, C_2^\diamond, ..., C_N^\diamond]$ is said to be a Nash equilibrium if:

$$C_i^\diamond = \arg\max_{C_i \geq 0} \pi_i(\boldsymbol{C}_i, C_{-i}^\diamond) - \gamma C_i, \forall i, \tag{5.2}$$

The Nash equilibrium shown in (5.2) is interpreted as the following: each producer $i$ chooses a capacity $C_i$ such that given the optimal capacity strategy of the others, there is no incentive for this producer to deviate from this capacity $C_i$. Note that while choosing its capacity, each producer implicitly assumes that its resulting revenue is decided by the solution obtained via the price sub-game.

### *5.3.5 Price sub-game*

In this section, we explicitly characterize the payment function $\pi_i(\boldsymbol{C}_i, C_{-i})$ at the equilibrium solution of the price sub-game for a fixed capacity vector $(C_i)_{1\leq i\leq N}$. The producers now compete to sell energy at some price $p_i$. This is known as the Bertrand price competition model, where the consumer prefers to buy energy at low prices. In this model, consumers resort to buying at a higher price only when the capacity of all the lower-priced producers are exhausted. Suppose that the profit for producer $i$ when the producers bid at $\boldsymbol{p} = [p_1, p_2, ..., p_N] = [p_i, \boldsymbol{p}_{-i}]$ is denoted by $\pi_i(C_i, \boldsymbol{C}_{-i}, p_i, \boldsymbol{p}_{-i})$. We make the following assumption about the prices:

**[A2]** The customers have the options to buy energy at unit price from the main grid.

This assumption follows the current structure of a distribution system, where customers have access to the main grid at a fixed price, and here we normalize the price to 1. Equivalently, this can be thought as the value of the lost load in a microgrid without a connection to the bulk electric system [101].

As shown in [89, 91], there is no pure Nash equilibrium on $p$ for the price sub-game. Intuitively, this means that no player can bid at a single deterministic price and achieve the most revenue, since the other players can undercut by a tiny amount and sell all their generation. Therefore no player settles on a pure strategy. Such a situation particularly arises where each producer is small ($C_i \leq D, \forall i$), but the aggregate is large ($\sum_i C_i > D$, where $D$ denotes the total demand in the market).

However, there exists a *mixed Nash equilibrium on price p*, where the optimal bids follow a distribution such that the bids of each DER are independent of the rest. Informally, this implies that each producer $i$ draws its price $p_i$ from a distribution $\mathcal{P}_i^*$, which maximizes its expected revenue given the distributions of the other producers. For example, the price distribution of a two player Bertrand model is given in [91]. For our purpose, the exact form of the optimal price distribution is not of particular interest. The quantity of interest is the form of the revenue function , i.e., the expected payment, resulting from this random

price bidding. Let us denote the expected payment to producer $i$ based on the optimal random price by $\pi_i(C_i, \boldsymbol{C}_{-i}) = \mathbb{E}_{\boldsymbol{p}\sim\mathcal{P}_1^*\times\ldots\times\mathcal{P}_N^*}\,\pi_i(C_i, \boldsymbol{C}_{-i}, p_i, \boldsymbol{p}_{-i})$. Proposition 3 characterizes the optimal payment to each producer:

**Proposition 3.** *Given any solution $(C_1, C_2, \ldots, C_N)$ having $C_1 \leq C_2 \leq \ldots \leq C_N$, the expected payment received by producer $i$ in the equilibrium of the pricing sub-game is given by:*

$$\pi_i(C_1, \ldots, C_N) = \pi_N(C_1, \ldots, C_N)\frac{C_i E[\min(U_i, \frac{D}{C_i})]}{C_N E[\min(U_N, \frac{D}{C_N})]}. \tag{5.3}$$

*Moreover, if the capacity is symmetric, i.e., $C_i = C_j, \forall j \neq i \in \{1, 2, ..., N\}$, then:*

$$\pi_i(C_i, \boldsymbol{C}_{-i}) = \mathbb{E}_{U_{-i}}\mathbb{E}_{U_i}\min\{(D - \sum_{j\neq i} U_j C_j)^+, U_i C_i\}. \tag{5.4}$$

A complete proof of Proposition 3 is deferred to the Appendix. Let us now understand Proposition 3 for the symmetric investment solution. Equation (5.4) denotes the payment received by producer $i$ when it bids deterministically at price $p_i = 1$ and all of the other producers bid according to their mixed pricing strategy. By assumption A2, this player bids at the highest possible price. Then the amount of energy sold equals the minimum of the leftover-demand from the market ($(D - \sum_{j\neq i} U_j C_j)^+$) and the player's actual production ($C_i U_i$). Since $p_i = 1$ belongs to the support of the mixed pricing strategy adopted by this player, one can use well known properties of mixed Nash equilibrium [89, 91] to argue that producer $i$'s payment at this price equals the expected payment received by this producer at the equilibrium for the pricing sub-game.

## *5.4 Evaluation metrics*

### *5.4.1 Social planner's problem*

One essential characteristic of a game is its cost as compared to a centralized decision. In this section, we present the benchmark cost that we consider; in particular, we focus on the

social cost minimization achieved by a social planner controlling the producers. In Section 5.4.2 we give more details on the definition of game efficiency as compared to this benchmark.

Suppose that these producers are managed by a social planner in a centralized manner. The purpose of the social planner is to fulfill demand while minimizing the total cost by deciding the investment capacities of the producers. The social planner thus wants to minimize *social cost* in the following form:

$$\boldsymbol{C}^* = \underset{C_i \geq 0, \forall i \in \{1,2,...,N\}}{\arg\min} \sum_{i=1}^{N} \gamma C_i + \mathbb{E}\{(D - \sum_{i=1}^{N} Z_i C_i)^+\}, \tag{5.5}$$

where $\boldsymbol{C}^* = [C_1^*, C_2^*, ..., C_N^*]$ is the optimal capacity decision from the social planner for each producer $i$. The social cost presented in (5.5) is composed of two terms. The first term is the total investment cost which is linear in the capacities, and the second term is the imbalance cost in buying energy from electricity grid if the renewables cannot satisfy the demand. These two terms represent the tradeoff between investing energy resources and buying energy from conventional generators in order to meet the electricity demand.

### *5.4.2 Performance of the decentralized market*

Given the definition of the equilibrium solutions due to both price and capacity competition, a natural question is to evaluate the performance of the decentralized market: i.e., *does competition result in efficiency?*. As mentioned previously, we measure this efficiency via two metrics: the social cost of the decentralized capacity investment compared to that achieved by the social planner, and the total investment cost compared to the payments made by the demand. An simple example of a one-player case is shown in [102], which suggests that the producer is exploiting its market power to considerably improve its profit and the benefits of renewables are not being transferred to the consumers.

**Market Efficiency** As noticed in the above example, inefficiency arises due to the high prices felt by the demand in the decentralized market. Formally, we define market efficiency as the ratio between the investment cost paid by the producers to the total payment received

by the producers at any equilibrium of the capacity price game. Therefore, efficiency takes the following form:

$$\xi = \frac{\gamma \sum_{i=1}^{N} C_i^{\diamond}}{\sum_{i=1}^{N} \pi(C_i^{\diamond}, \boldsymbol{C}_{-i}^{\diamond})}. \tag{5.6}$$

A "healthier" game should achieve a higher $\xi$ that is as close as to 1. This means that the producers should bid at the prices that cover their investment cost, so that bidding is efficient and does not take advantage of the electricity consumers. A particularly interesting question is whether competition leads to increased efficiency as the number of producers in the market increases. We formalize this notion below.

**Definition 3.** *We define the efficiency of a Nash equilibrium in a capacity game illustrated in* (5.1) *by* $\xi$*. The capacity game is asymptotically efficient when* $\xi \to 1$ *as* $N \to \infty$ *for every Nash equilibrium.*

Now the question of interest is 1) whether uncertainty in generation deteriorates or improves the market efficiency of the game, and 2) whether efficiency increases as the number of players in the game increases. In the following sections, we will see that without randomness in the generation, the producers are able to charge a relatively high price for energy, which makes the game less efficient. Interestingly, when producer's generation becomes uncertain, the game becomes more efficient as more producers are involved in the decentralized market.

*Inefficiency due to Social Cost:* When there are multiple producers, it is possible that even the investment decisions may not coincide with that of the social planner. Therefore, a second source of inefficiency is the social cost due to the capacity investment, as defined in (5.5). More concretely, we compare the social cost of the equilibrium solution ($C_i^{\diamond}$) with that of the social cost of the planner's optimal capacity ($C_i^{*}$)— clearly, the latter cost is smaller than or equal to the former.

### *5.4.3 Deterministic game*

Before moving on to the main results, we highlight the (in)efficiency of the equilibrium in the *deterministic* version of the capacity game, i.e., one without production uncertainty where

$U_i = 1$ with probability one. Understanding the inefficiency of this deterministic game is the starting point for us to better gauge the effects of uncertainty in investment games.

We begin with the social planner's problem, which in the absence of uncertainty can be formulated as follows:

$$\min_{C_i \geq 0, \forall i \in \{1,2,\ldots,N\}} \gamma \sum_{i=1}^{N} C_i + (D - \sum_{i=1}^{N} C_i)^+. \tag{5.7}$$

Every solution with non-negative capacities that satisfies $\sum_{i=1}^{N} C_i^* = D$ optimizes the above objective — this includes the symmetric solution $C_1^* = C_2^* = \cdots = C_N^* = \frac{D}{N}$. Moving on to the decentralized game with deterministic energy generation, we can directly characterize the equilibrium solutions using the results from [89]. Specifically, by applying Proposition 13 in that paper, we get although there are multiple equilibrium solutions, every such solution $(C_i)_{1 \leq i \leq N}$ satisfies $(i)$ $\sum_{i=1}^{N} C_i = D$, and $(ii)$ $\pi_i(C_i, \boldsymbol{C}_{-i}) = C_i$. The second result implies that at every equilibrium, each producer charges a price that is equal to the electricity price of one from the main grid. Finally, by applying (5.6), we can characterize the efficiency in terms of the investment cost $\gamma$:

$$\xi = \frac{\gamma D}{D} = \gamma. \tag{5.8}$$

*Why is this result undesirable?* First note that when $\gamma < 1$, (5.8) implies that the deterministic game is inefficient at *every Nash equilibrium*. In fact, using the results from [89], one can deduce that the system is inefficient even when different producers have different investment costs. Perhaps more importantly, the costs of investment as well as the market price of renewable energy have dropped consistently over the past decade and are expected to continue doing so in the future [103–105]. In this context, Equation (5.8) has some stark implications, namely that *as $\gamma$ (the investment price) drops in the long-run, the efficiency actually becomes worse ($\xi \to 0$ as $\gamma \to 0$)*, i.e., the improvements in renewable technologies do not benefit the electricity consumers.

## *5.5 Main results*

In this section, we first characterize the capacity decision from the social planner's problem. We then illustrate the relationship between the decentralized market, and the social planner's problem in the centralized market. We also give a thorough analysis on the efficiency of the decentralized market. We begin by considering the case where the capacity generated by the producers are independent of each other and then move on to the correlated case. All of the proofs from this section can be found in the appendix.

### *5.5.1 Social planner's optimal decision*

An immediate observation of the socially optimal capacity as described in (5.5) is that if the randomness is independent and identical across different producers, the socially optimal capacity is symmetric:

**Theorem 6.** *If the random variables $U_i$ are i.i.d. and satisfy assumption A1, then the optimal capacity obtained by* (5.5) *is symmetric, i.e., $C_1^* = C_2^* = \cdots = C_N^* = C^*$.*

Theorem 6 states that when the investment cost per unit capacity is the same across all producers, and the random variable is i.i.d., then the optimal decision for the social planner is to treat all producers equally and invest the same amount of capacity for each producer. In reality, the randomness due to renewable sources can be correlated and Section 5.5.4 shows that Theorem 6 stills holds under some conditions on the nature of the correlation.

### *5.5.2 Existence and Social Cost*

Now that we have captured the structure of the socially optimal capacity decision, we want to address the issue of whether or not the capacity price game admits Nash equilibrium solutions in the decentralized market. A second question concerns the social cost of Nash equilibria when compared to the optimum investment decision adopted by a social planner. As discussed in Section 5.4.2, one of the two sources of inefficiency in decentralized stems

from the fact that the social cost of equilibrium solutions may be larger than that of the central planner's solution. Theorem 7 addresses both of these questions by proving the existence of a Nash equilibrium that coincides with the socially optimal capacity decision.

**Theorem 7.** *There is a Nash equilibrium that satisfies* (5.2)*, which also minimizes the social cost. That is,* $(C^*, C^*, \ldots, C^*)$ *is a Nash equilibrium.*

Therefore, existence is always guaranteed in our setting. More importantly, Theorem 7 provides an interesting relationship between the centralized decision that minimizes social cost, and the decentralized decision where producers seek to maximize profit. It states that the game yields a socially optimal capacity investment solution as if there were a social planner controlling the producers. In addition, as we will show later in Section 5.5.5, this Nash equilibrium is the unique symmetric equilibrium in the capacity game. For the following sections, we use $C^*$ to denote both the socially optimal capacity decision and this Nash equilibrium.

### *5.5.3 Efficiency of Nash equilibrium*

Although the capacity price game studied this work admits a Nash equilibrium that minimizes the social planner's objective, there may also exist other equilibria that result in sub-optimal capacity investments. How do these (potential) multiple equilibria look like from the consumers' perspective, i.e., is the price charged to consumers larger than the investment? In this section, we show a surprising result: the two-level capacity-pricing game is asymptotically efficient. That is, as $N \to \infty$, the total payment made to the producers approaches the investment costs for *every Nash equilibrium*. The reason for this startling effect is that as the number of producers competing against each other in the market increases, with the presence of uncertainty, the market power of these producers decreases and the efficiency of the game equilibrium increases. We first present our main theorem with i.i.d. generation.

**Theorem 8.** *Let $(C_1^\diamond, C_2^\diamond, \ldots, C_N^\diamond)$ denote any Nash equilibrium solution in an instance with $N$ producers and $N > \frac{1}{\gamma}$. Then, as long as the $U_i$'s are i.i.d and satisfy assumption A1, we have that:*

$$\sum_{i=1}^{N} \pi_i(C_1^\diamond, C_2^\diamond, \ldots, C_N^\diamond) \leq \gamma \sum_{i=1}^{N} C_i^\diamond + \alpha N^{-c},$$

*where $\alpha, c > 0$ are constants that are independent of $N$. Therefore, as $N \to \infty$, $\xi \to 1$, where $\xi$ denotes the market efficiency due to* any *Nash equilibrium solution.*

Combining Theorems 7 and 8 yields that if we restrict the game to only have the symmetric equilibrium, then the equilibrium minimizes the social cost and the game is asymptotically efficient. Moving beyond the symmetric equilibrium, Theorem 8 states that any Nash equilibrium obtained from the capacity game is efficient, that the collected payment (revenue) tends to exactly cover the investment cost. This further suggests that the capacity game described in (5.1) elicits the true incentive for the producers to generate energy.

### *5.5.4 Correlated generation*

In reality, renewable generation due to multiple entities in a power distribution network is usually correlated with each other because of geographical adjacencies. We assume that the randomness of each producer's generation can be captured as an additive model written as the following:

$$U_i = \hat{U}_i + \bar{U}. \tag{5.9}$$

The model in (5.9) captures the nature of renewable generation. We can interpret $\bar{U}$ as the shared random variable for a specific region. For example, the average solar radiation for a region should be common to every PV output in that region. On the other hand, $\hat{U}_i$ can be seen as the individual-level random variable for the particular location of each PV plant $i$, and this random variable can be seen as i.i.d. across different locations.

For analytical convenience, we make the following assumptions on $U_i$:

**[A3]** Both $\bar{U}$ and $\hat{U}_i$ in (5.9) satisfy assumption A1, the $\hat{U}_i$'s are i.i.d, and are independent of $\bar{U}$ for all $i$.

If the correlation is captured as in (5.9), the optimal capacity decision is still symmetric, i.e., $C_i^* = C_j^*, \forall i \neq j$ is a valid solution to (5.5). This is stated in Theorem 9.

**Theorem 9.** *If the random variable $U_i$ is captured as in* (5.9) *and assumption A3 is satisfied, then the optimal capacity vector that minimizes the planner's social cost is symmetric, i.e., $C_1^* = C_2^* = \cdots = C_N^* = C^*$.*

In addition, note that Theorem 7 does not require the i.i.d assumption on $U_i$. Therefore, we infer that the symmetric solution that minimizes social cost is a Nash equilibrium even when the generation is correlated. In what follows, we further show that correlation does not tamper the efficiency of any Nash equilibria in the capacity game.

**Theorem 10.** *Suppose that $(C_1^\diamond, C_2^\diamond, \ldots, C_N^\diamond)$ denotes any Nash equilibrium solution in an instance with $N$ producers and $N > \frac{1}{\gamma}$. Then, as long as the random variable $U_i$, is captured in* (5.9)*, and assumption A3 is satisfied, we have that:*

$$\sum_{i=1}^{N} \pi_i(C_1^\diamond, C_2^\diamond, \ldots, C_N^\diamond) \leq \gamma \sum_{i=1}^{N} C_i^\diamond + \alpha N^{-c},$$

*where $\alpha, c > 0$ are constants that are independent of $N$.*

Theorem 10 extends the statement in Theorem 8 from i.i.d. random variables to correlated random variables. This indicates that if the randomness of each producer is captured by an additive model interpreted as the sum of shared randomness and individual-level randomness, then the decentralized market is efficient and that both producers and electricity users benefit from this market.

### *5.5.5 Uniqueness of the Symmetric Equilibrium*

Although our setting could admit many equilibrium solutions, we know that one of these solutions must always be symmetric, i.e., every producer has the same investment level. This solution is of particular interest as it minimizes the social cost. We now show that the symmetric Nash equilibrium $C_1^*, C_2^*, \ldots, C_N^*$ is unique in Theorem 11.

**Theorem 11.** *Under assumption A1, the symmetric Nash equilibrium in the capacity game* (5.1) *is unique.*

Theorem 11 states that there is only one symmetric Nash equilibrium in the capacity game. This indicates that if the decentralized market is regulated such that each producer behaves similarly in the presence of uncertainty, then it is guaranteed that the competition is both efficient and socially optimal in the investment decision.

## *5.6 Simulation*

In this section, we validate the statements by providing simulation results based on both synthetic data and real PV generation data. For convenience, we use the symmetric Nash equilibrium as the solution of interest in our simulations.

### *5.6.1 Two-player game*

Let us assume that the generation distribution is uniform, i.e., $U_i \sim \text{unif}(0,1)$. Suppose that the investment price is the same for all players, i.e., $\gamma = 0.25$, then following the analysis in Section 5.5, we know that the optimal capacity satisfies $C_1^* = C_2^*$. Assuming that the demand is normalized to 1, we solve the social optimization in (5.5) with equal investment price $\gamma$. The optimal solution leads to a total capacity of $C_{tot}^* = C_1^* + C_2^* = 1.71$, where $C_1^* = C_2^* = 0.855$. The result is shown in Fig. 5.3.

To verify that $C_1^* = C_2^* = 0.855$ is indeed a symmetric Nash equilibrium, we vary the capacity from $C_1^*$ and study how player 1's profit changes. The analysis for player 2 proceeds in the same way because of symmetry. We show the result of optimality for player 1 in Fig. 5.4 in terms of profit, with a fixed capacity for player 2 where $C_2 = C_2^* = 0.855$.

As can be seen from Fig. 5.4, the profit for player 1—when the other player's capacity is fixed at $C_2^*$—peaks at $C_1 = C_1^*$. By symmetry, we can argue that player 2's profit is maximized at $C_2^*$ when player 1's capacity remains fixed. Therefore, $(C_1^*, C_2^*)$ is indeed a Nash equilibrium as neither player has any incentive to deviate from its investment strategy.

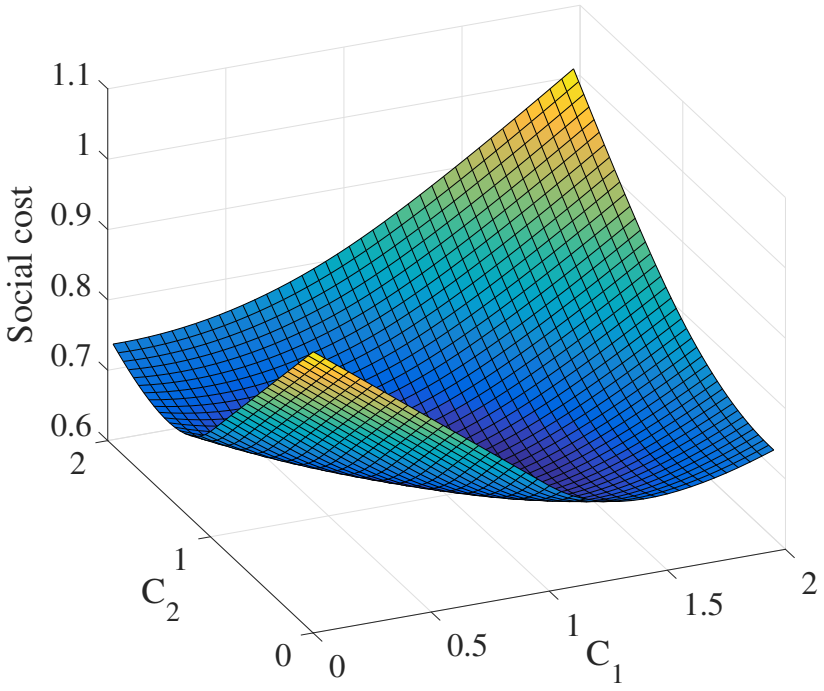


Figure 5.3: Social cost with respect to total capacity when investment price is the same.

In other words, the socially optimal capacity is also a Nash equilibrium for the game shown in (5.1).

### *5.6.2 N-player game*

To illustrate that the Nash equilibrium is efficient with respect to the metric defined in (5.6), we need to show that the payment collected from users in the game exactly covers the investment costs of the producers when the number of producers increases. We therefore simulate the capacity game with identical players ($\gamma_i = 0.25, \forall i$) with i.i.d. generation (uniform distribution). We then compute the efficiency $\xi$ when there are $10, 50, 100, 150, 200, 250, 300$ players in the game. The results are shown in Fig. 5.5.

In Fig. 5.5, we see that the efficiency is growing with the number of players in the game.

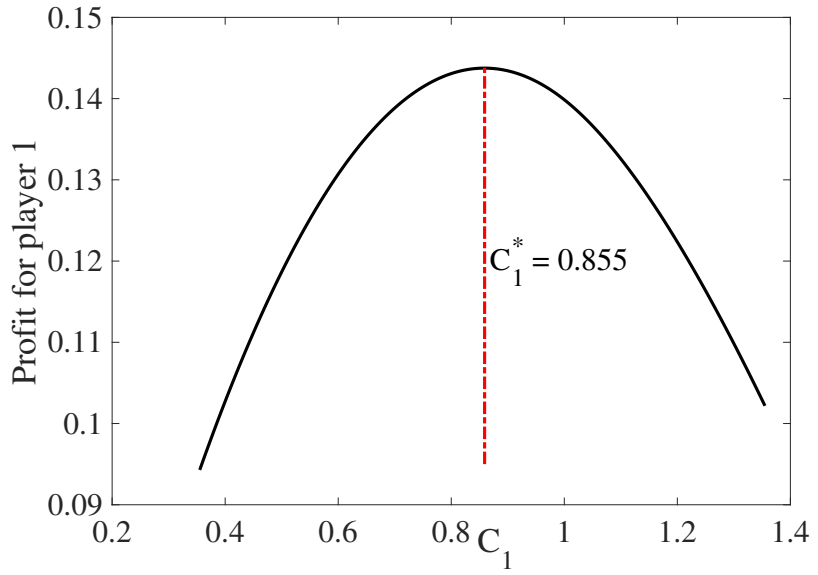


Figure 5.4: Profit for player 1 when its capacity deviates from $C_1^*$.

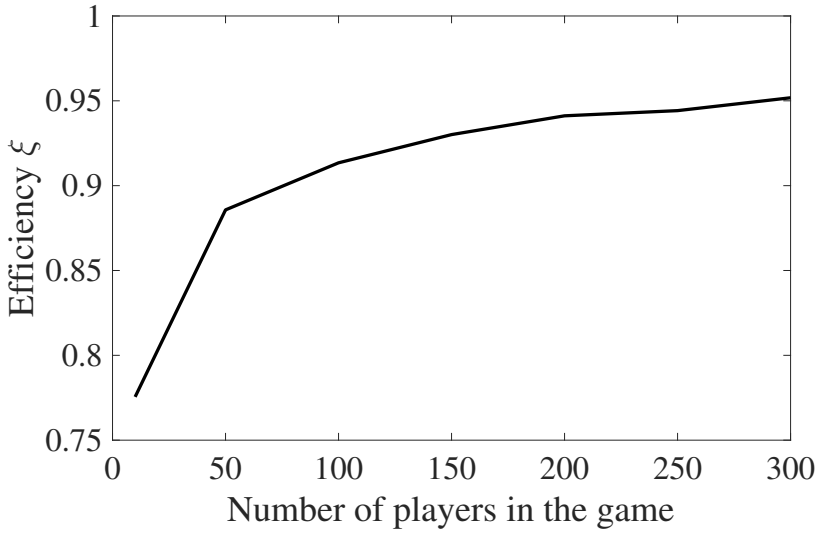


Figure 5.5: Efficiency of the symmetric Nash equilibrium in the game as a function of number of players.

We therefore infer that the competition is healthy as the producers only bid their true costs and do not exploit the consumers of electricity.

### *5.6.3 Case study using real data*

In this section, we simulate the efficiency of the game equilibrium using a real PV generation profile obtained from the National renewable energy laboratory [106]. Our data comes from distributed PVs located in California with a 5 minute resolution. Typical PV profiles after normalization are shown in Fig. 5.6. From Fig. 5.6, we see that the randomness of PV generation from different locations is strongly correlated. The correlation between those PV profiles is also symmetric across different PV plants, as shown in Fig. 5.7.

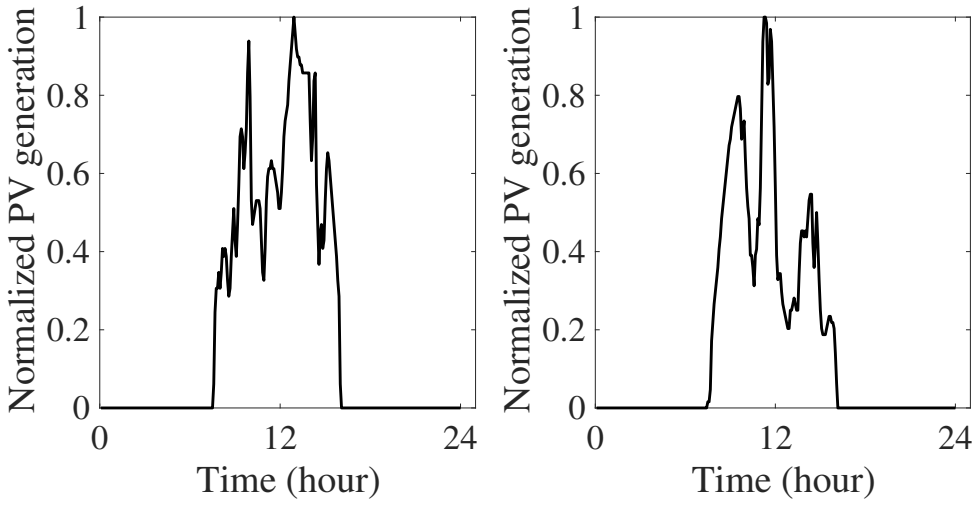


Figure 5.6: PV generation profile in different locations.

We then use these PV profiles to obtain the game equilibrium as we vary the number of PV participants. The result is shown in Table 5.1, with the assumption that $\gamma = 0.15$. As we can see from Table 5.1, in the absence of randomness when the producers are assumed to generate energy deterministically, the efficiency is the investment price as described in Equation (5.8). On the other hand, the efficiency of the game with uncertainty improves as

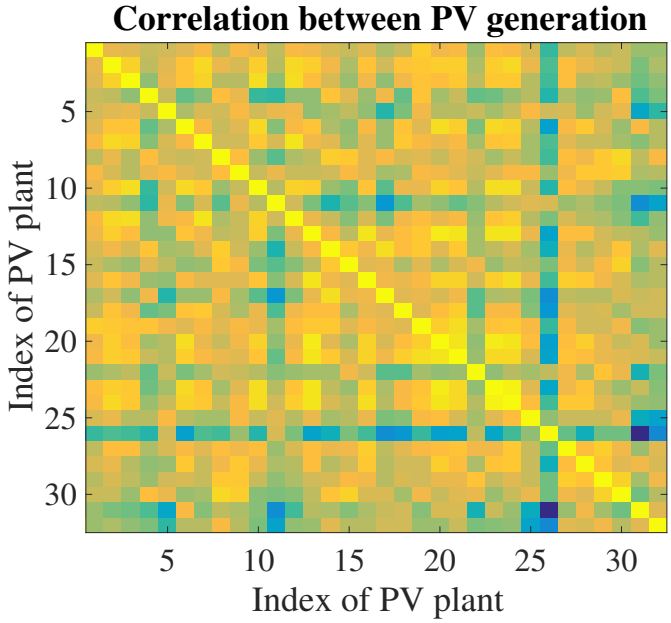


Figure 5.7: Correlation of PV generation in different locations. A lighter color (yellow) represents stronger correlation and dark colors (blue) represent weak correlation.

the numbers of producers in the market increases.

Table 5.1: Game efficiency with different number of producers, when investment price is 0.15 and demand $D = 5$.

| **Number of producers** | **5** | **30** | **120** |
|---|---|---|---|
| Efficiency of deterministic producers | 0.15 | 0.15 | 0.15 |
| Efficiency of random producers | 0.83 | 0.96 | 0.98 |

In addition, in a deterministic game, the total capacity is always the same as the market demand because there is no randomness in generation. In the capacity game with uncertainty, since each producer faces randomness in its own production as well as the random generation

from the other producers, the total invested capacity is greater than demand as illustrated in Table. 5.2. This means that in the capacity game with uncertainty, the total capacity exceeds market demand, which elicits competition among producers.

Table 5.2: The ratio between total capacity and market demand , i.e., $\sum_i C_i^*/D$, when investment price is 0.15 and demand $D = 5$.

| **Number of producers** | **5** | **30** | **120** |
|---|---|---|---|
| $\sum_i C_i^*/D$ with deterministic producers | 1 | 1 | 1 |
| $\sum_i C_i^*/D$ with random producers | 1.26 | 1.32 | 1.30 |

### *5.7 Summary*

In this chapter, we consider a scenario where many distributed energy resources compete to invest and sell energy in a decentralized electricity market especially when uncertainty is present. Each energy producer optimizes its profit by selling energy. We show that such a competitive game has a Nash equilibrium that coincides with the solution from a social welfare optimization problem. In addition, we show that all Nash equilibria are efficient, in the sense that the collected payment to the energy producers approaches their investment costs. Our statement is validated both by theoretical proofs and simulation studies.

# Chapter 6

# STATIC SECURITY – VOLTAGE CONTROL

## *6.1 Introduction and literature review*

Voltage control is crucial to secured operation of power distribution systems, where it is used to maintain acceptable voltages at all buses under different operating conditions [8]. To control voltage, reactive power is traditionally regulated through tap-changing transformers and switched capacitors [9]. With recent advances in cyber-infrastructure for communication and control, it is also possible to utilize distributed energy resources (DERs, i.e., electric vehicles [107], PV panels [10, 11]) to provide voltage regulation. There exists an extensive literature in controlling voltage in a distribution network, some of them focus on centralized control [12, 13], while the others address distributed algorithm [8, 9, 14, 15].

In this chapter, we focus the problem of *voltage control under uncertainties*. In addition to voltage control capabilities, DERs bring significant uncertainty and fast variations to the distribution system [11, 108, 109]. Since most distribution systems do not yet have real-time communication capabilities, a decision made must be valid for a set of possible conditions. For example, the solar PVs in a distribution system may communicate with the feeder (or some other controller) every 5 minutes to receive a command for setting its reactive power, but the changes in solar radiation result in sub-minute timescales changes in its active power. In this chapter, we overcome these fast variations using a centralized control framework, where a central controller sends out regulation signals to DERs periodically, where the control signals are designed to regulate voltages for the entirety of the period in the presence of randomness.

A natural framework to handle the uncertainties introduced by the fast variation in the output of the DERs is through chance constraints since they can be used to bound the probability of voltage constraint violations. Chance constraints have been used extensively

in power system operations, including [110–113]. A challenge in using these constraints is that they may result in difficult optimization problems, requiring algorithms to be designed on a case-by-case basis. The global optimality or even convergence of these algorithms are often hard to guarantee. A second challenge is that the actual probability distribution of the uncertainties are almost never known in practice and has to be estimated or approximated using historical samples, adding to the computational challenge [114].

In this chapter, we first propose a chance constrained optimization framework for the voltage regulation problem. Then we show how the problem can be solved efficiently using historical samples without explicitly estimating or approximating the probability distribution. Lastly, we provide (minor) conditions on which the algorithm will be guaranteed to be optimal.

Formally, we think about the voltage regulation problem as a chance constrained cost minimization problem.[1] Unlike most of the existing literature, we propose to impose a single chance constraint on the whole system. This is different from the standard practice where chance constraints are placed on every bus of the network [110, 111]. Putting constraints on each single bus simplifies the problem, but suggests that the uncertainty at each bus is unrelated. However, the randomness across the DERs can be very correlated in practice. In this work, we show how a single constraint can be used to capture uncertainties from all buses in the system using the linearized DistFlow model introduced in [115].

We show that our proposed voltage control problem can be solved without the need to deploy mixed integer programming (MIP), which is usually used in scenario approximation of chance constraints [116]. Even if the distribution of the uncertainty is unknown, we provide an algorithm that computes a descent direction using historical samples, and moving along this direction would lead to a local minimum. In addition, we show that if the true underlying uncertainty follows a wide family of probability distributions, the proposed algorithm will find the global optimal solution. In summary, we make the following contributions to voltage

[1] Our framework allows a variety of costs, for example, conservative voltage reduction [14].

control in distribution systems:

- The uncertainties of the DER generations are correlated and expressed as a single chance constraint imposed onto the whole system.

- We propose an efficient and tractable descent algorithm by finding a valid descent direction at each iteration using historical samples, therefore avoids MIP formulation and cumbersome integral computation.

- We show that if the uncertainty in the DERs come from a log-concave distribution, the optimization problem is actually convex and our algorithm is guaranteed to be global optimal.

The rest of the chapter is organized as follows. Section 6.2 presents the modeling of the distribution network. Section 6.3 proceeds with the formulation of the voltage control problem and demonstrate the robustness of the proposed framework with an illustrating example. In Section 6.4, we present the proposed descent algorithm to solve the optimization problem efficiently with samples. Section 6.5 states that the problem is convex for a wide range of probabilistic distributions. Section 6.6 validates the statement by simulation results. Finally Section 6.7 concludes the chapter.

## *6.2 Preliminary: Distribution network*

In this section we present the modeling of components in a radial distribution network in power systems. For interested readers, please refer to [117, 118] for more details.

We consider a distribution network with $N+1$ buses collected in the set $\{0, 1, ..., N\}$. We also denote a line in the network by the pair $(i, k)$ of buses it connects. Bus 0 is the feeder (reference bus). For each line $(i, k)$ in the network, its impedance is denoted by $z_{ik} = r_{ik} + \mathrm{j}x_{ik}$, where $r_{ik}$ and $x_{ik}$ is its resistance and reactance. For each bus $i$, let $V_i$ be the voltage magnitude at bus $i$ and $s_i = P_i + \mathrm{j}Q_i$ be the complex power injection, i.e., the generation minus consumption. In addition, the subset $\mathcal{N}_k$ denotes bus $k$'s neighboring

buses that are further down from the feeder head. A linear approximation of the power flow equations can be constructed [115]. Assume that the losses is negligible and the voltage at each bus is close to 1. This enables us to approximate $V_i^2 - V_k^2$ by $2(V_i - V_k)$ [14]. The linearized power flow model is given by [119]:

$$P_{ik} - \sum_{l \in \mathcal{N}_k} P_{kl} = -P_k, \tag{6.1a}$$

$$Q_{ik} - \sum_{l \in \mathcal{N}_k} Q_{kl} = -Q_k, \tag{6.1b}$$

$$V_i - V_k = r_{ik} P_{ik} + x_{ik} Q_{ik}. \tag{6.1c}$$

From (6.1), we can write the voltage magnitude $\boldsymbol{V} = [V_1, \ldots, V_N]^\top$ in terms of reactive power injection $\boldsymbol{Q} = [Q_1, \ldots, Q_N]^\top$ and real power injection $\boldsymbol{P} = [P_1, \ldots, P_N]^\top$, and the reference voltage $V_0$ at the feeder:

$$\boldsymbol{V} = \boldsymbol{R}\boldsymbol{P} + \boldsymbol{X}\boldsymbol{Q} + V_0 \tag{6.2}$$

where $\boldsymbol{R}, \boldsymbol{X} \in \mathbb{R}^{N \times N}$ are matrices with $R_{ik}$ and $X_{ik}$ as the element in $i^{th}$ row and $k^{th}$ column, respectively. The voltage profile at bus $1, ..., N$ is denoted by $\boldsymbol{V} \in \mathbb{R}^N$.

Following the findings in [8], we give the expressions of $R_{ik}$ and $X_{ik}$ in terms of line resistance $r_{ik}$ and reactance $x_{ik}$:

$$R_{ik} = \sum_{(h,l) \in \mathcal{P}_i \cap \mathcal{P}_k} r_{hl}, \; X_{ik} = \sum_{(h,l) \in \mathcal{P}_i \cap \mathcal{P}_k} x_{hl}, \tag{6.3}$$

where $\mathcal{P}_i$ is the set of lines on the unique path from bus 0 to bus $i$.

### *6.3 Voltage regulation with reactive power injection*

To facilitate analysis, rewrite $\boldsymbol{V}$ as the difference between the bus voltage and reference voltage $V_0$, then (6.2) becomes:

$$\boldsymbol{V} = \boldsymbol{R}\boldsymbol{P} + \boldsymbol{X}\boldsymbol{Q}. \tag{6.4}$$

As renewables introduce uncertainty in the bus voltages, the voltage profile is reformulated into the following form:

$$\boldsymbol{V} = \boldsymbol{R}\boldsymbol{P} + \boldsymbol{X}\boldsymbol{Q} + \boldsymbol{\epsilon}, \tag{6.5}$$

where $\boldsymbol{\epsilon}$ is the uncertainty with zero mean and covariance matrix $\boldsymbol{\Sigma}$. WLOG, we assume that $\boldsymbol{\epsilon}$ has a continuous density distribution. The covariance matrix $\boldsymbol{\Sigma}$ is not necessarily a diagonal matrix since the uncertainty is rarely independent of each other across buses. For example, uncertainty can be a result of randomness from renewables at various buses in the distribution network. The randomness is highly correlated across buses because of geometrical adjacency. In this case, every bus is dependent of each other due to correlated randomness and $\boldsymbol{\epsilon}$ captures the uncertainty of the whole system.

Ideally, the voltages in the system should be maintained within a tight region (e.g., plus/minus 5% of nominal). With uncertainties introduced by the operation of the DERs, we model this constraint in a probabilistic fashion. We use the following chance constraints which bounds the probability of the voltages staying in the prescribed bounds:

$$\Pr\{\underline{\boldsymbol{V}} \leq \boldsymbol{V} \leq \overline{\boldsymbol{V}}\} \geq \alpha, \tag{6.6}$$

which is equivalent to be written as:

$$\Pr\{\underline{\boldsymbol{V}} \leq \boldsymbol{RP} + \boldsymbol{XQ} + \boldsymbol{\epsilon} \leq \overline{\boldsymbol{V}}\} \geq \alpha, \tag{6.7}$$

where $\underline{\boldsymbol{V}}$ and $\overline{\boldsymbol{V}}$ are the voltage bounds. The value of $\alpha$ is a parameter that can be chosen to indicate the probability that event $\underline{\boldsymbol{V}} \leq \boldsymbol{RP} + \boldsymbol{XQ} + \boldsymbol{\epsilon} \leq \overline{\boldsymbol{V}}$ occurs.

### *6.3.1 Main Optimization Problem*

In this chapter we only consider reactive power regulation and assume that active load injection $\boldsymbol{P}$ is determined exogenously and the controllable variable is the reactive power injection $\boldsymbol{Q}$. Denote $\Pr\{\underline{\boldsymbol{V}} \leq \boldsymbol{RP} + \boldsymbol{XQ} + \boldsymbol{\epsilon} \leq \overline{\boldsymbol{V}}\}$ by $\psi(\boldsymbol{Q})$, for a given tolerance level $\alpha$, the centralized voltage regulation problem is then captured as the following:

$$\min_{\boldsymbol{Q}} \; C(\boldsymbol{Q}) \tag{6.8a}$$

$$\text{s.t. } \psi(\boldsymbol{Q}) \geq \alpha, \tag{6.8b}$$

$$\underline{\boldsymbol{Q}} \leq \boldsymbol{Q} \leq \overline{\boldsymbol{Q}}, \tag{6.8c}$$

where the cost function $C(\boldsymbol{Q})$ can be any convex cost function, for example, the 2 norm deviation of reactive power support $\|\boldsymbol{Q}\|_2$ as discussed in [120]. This cost function encourages small amount of reactive power support to maintain the acceptable voltage deviation due to uncertainty.

The value of $\alpha$ indicates how the voltage profile behaves within the prescribed bounds. *Risk level* is the usual adopted term with chance constrained optimization and it is equal to $1-\alpha$, representing the severity of the system state.

### *6.3.2 Existing Benchmark: Per-Bus Constraints*

Our approach is different from the existing literature when dealing with chance constraints. In most existing literature with randomness in the distribution network, chance constraints are introduced in [110, 111, 114, 121] separately for each dimension of the system as:

$$\begin{aligned} &\Pr\{\underline{V}_i \le V_i \le \overline{V}_i\} \\ =&\Pr\{\underline{V}_i \le \boldsymbol{R}_i^\top \boldsymbol{P} + \boldsymbol{X}_i^\top \boldsymbol{Q} + \epsilon_i \le \overline{V}_i\} \ge \eta_i, \end{aligned} \tag{6.9}$$

where $\boldsymbol{R}_i^\top$ and $\boldsymbol{X}_i^\top$ extracts the $i$th row in respective matrices. The chance constraint at bus $i$ is associated with prescribed tolerance $\eta_i$. Assuming that each bus has the same tolerance, the optimization problem that incorporates per-bus chance constraint is in the following form:

$$\min_{\boldsymbol{Q}} \ \frac{1}{2}\|\boldsymbol{Q}\|_2^2 \tag{6.10a}$$

$$s.t.\ \psi_i(\boldsymbol{Q}) \ge \eta, \forall i \tag{6.10b}$$

$$\underline{\boldsymbol{Q}} \le \boldsymbol{Q} \le \overline{\boldsymbol{Q}}, \tag{6.10c}$$

where $\psi_i(\boldsymbol{Q}) \triangleq \Pr\{\underline{V}_i \le \boldsymbol{R}_i^\top \boldsymbol{P} + \boldsymbol{X}_i^\top \boldsymbol{Q} + \epsilon_i \le \overline{V}_i\}$.

This per-bus framework is not the same as having a single constraint on the whole system, i.e., the feasible region described by (6.10b) is different from (6.8b). The small example below illustrates that the proposed single system chance constraint framework, captures the coupling between buses and is therefore more realistic and applicable. In addition, as we

show in Section 6.5, the optimization problem can be solved efficiently, negating some of the computational difficulties with higher dimensional chance constraints.

**Toy Example** Consider a line network with 3 buses. Suppose that the reactive power injections at bus 1 and 2 are limited to 0.1 p.u., we have a linear constraint as $-0.1 \leq Q_1, Q_2 \leq 0.1$. Then our proposed framework solves the following optimization problem:

$$\begin{aligned} \min_{\boldsymbol{Q}} \ & \frac{1}{2}\|\boldsymbol{Q}\|_2^2 \\ s.t. \ & \psi(\boldsymbol{Q}) \geq \alpha, \\ & -0.1 \leq Q_j \leq 0.1, \forall j \in \{1,2\} \end{aligned} \tag{6.11}$$

and its optimal solution is denoted by $\boldsymbol{Q}_a^*$. Here we take $\alpha$ to be 0.9.

The per-bus formulation is the following optimization problem:

$$\begin{aligned} \min_{\boldsymbol{Q}} \ & \frac{1}{2}\|\boldsymbol{Q}\|_2^2 \\ s.t. \ & \psi_i(\boldsymbol{Q}) \geq \eta, \forall i \in \{1,2\} \\ & -0.1 \leq Q_j \leq 0.1, \forall j \in \{1,2\} \end{aligned} \tag{6.12}$$

and its optimal solution of (6.12) by $\boldsymbol{Q}_p^*$. Suppose that the randomness $\boldsymbol{\epsilon}$ follows a Gaussian distribution with $\boldsymbol{\mu} = \begin{bmatrix} 0 \\ 0 \end{bmatrix}, \boldsymbol{\Sigma} = \begin{bmatrix} 0.002 & 0.0014 \\ 0.0014 & 0.006 \end{bmatrix}$, and $\boldsymbol{P}$ is randomly picked between 0.3 and $-0.3$ p.u. Unlike the problem in (6.11), setting a "right" $\eta$ in (6.12) is not straightforward. Suppose we want to achieve the same level confidence as (6.11) where the system operates within the prescribed bounds with probability at least 0.9, then what is the right $\eta$ to take? As suggested by previous studies [9], a natural candidate for $\eta$ is to set it equal to $\sqrt[2]{0.9} = 0.949$ by thinking of each bus as independent to each other. A second candidate is simply to set it at 0.9, the same as $\alpha$.

The main results of the three-bus line network are shown in Table 6.1, where $\boldsymbol{Q}^*$ denotes the optimal solution for perspective frameworks. The value $\psi(\boldsymbol{Q}^*)$ denotes the probability $\Pr\{\underline{\boldsymbol{V}} \leq \boldsymbol{RP} + \boldsymbol{XQ}^* + \boldsymbol{\epsilon} \leq \overline{\boldsymbol{V}}\}$ and is the figure of merit we compare the solutions with. The

bound on the voltage deviation is denoted by $\overline{\boldsymbol{V}} = [\ 0.05\ 0.05]^\top$ and $\underline{\boldsymbol{V}} = [\ -0.05\ \ -0.05]^\top$. As can be seen from Table 6.1, setting $\eta = \sqrt[2]{0.9}$ drives the optimization problem with the per-bus constraint infeasible. The second value of $\eta = 0.9$ makes the problem feasible, but at the cost of lowering the joint probability $\psi(\boldsymbol{Q}^*)$ to be 0.86. This result shows that it is difficult to set the correct tolerance level in the per-bus chance constraints.

Table 6.1: The value of $\psi(\boldsymbol{Q}^*)$ under different frameworks.

| **Framework** | (6.11), $\alpha = 0.9$ | (6.12), $\eta = \sqrt[2]{0.9}$ | (6.12), $\eta = 0.9$ |
|---|---|---|---|
| $\psi(\boldsymbol{Q}^*)$ | 0.9 | Infeasible | 0.86 |

To better understand the feasible region of $\boldsymbol{Q}$ under the three different cases in Table 6.1, let us consider the following region for $\boldsymbol{Q}$ (dropping the box constraint on $\boldsymbol{Q}$ for convenience in comparison):

- $A_1 = \{\boldsymbol{Q} : \psi(\boldsymbol{Q}) \geq \alpha\}$.
- $A_2 = \{\boldsymbol{Q} : \psi_i(\boldsymbol{Q}) \geq \sqrt{\alpha}, i = \{1, 2\}\}$.
- $A_3 = \{\boldsymbol{Q} : \psi_i(\boldsymbol{Q}) \geq \alpha, i = \{1, 2\}\}$.

Table 6.1 shows that when $\alpha = 0.9$, $A_2 = \emptyset$. In Fig.6.1, we relax the value of $\alpha$ to 0.7 and show the difference between $A_1, A_2$ and $A_3$.

As can be seen from Fig. 6.1, the region of interest, i.e., $A_1$, is not depicted well by the per-bus constraints $A_2$ and $A_3$. By setting up a strict threshold, i.e., $\eta = \sqrt{\alpha}$ for each bus, we are being conservative about the feasible region of $\boldsymbol{Q}$ and therefore if $\alpha$ is close to 1, $A_2$ disappears even if $A_1$ is still a non-empty set. On the other hand, setting a loose threshold ($\eta = \alpha$ for each bus) makes the feasible region bigger than it should be (comparing $A_3$ to $A_1$), therefore cannot guarantee the desired risk level required by $A_1$.

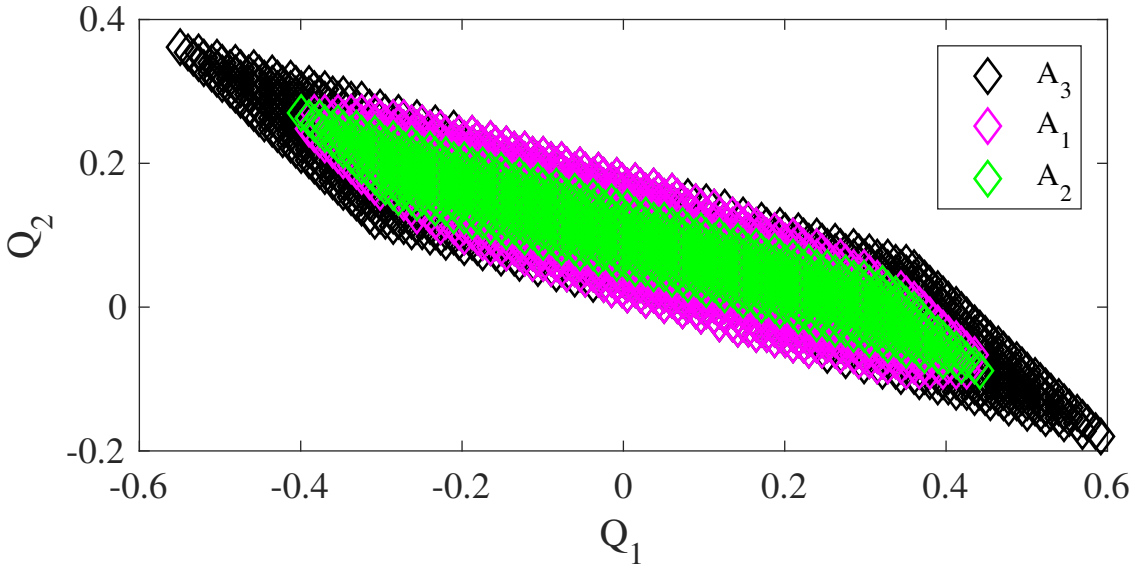


Figure 6.1: Comparison of $A_1, A_2, A_3$ when $\alpha = 0.7$.

This result shows the difficult of using the per bus constraint, where it is difficult to set the correct tolerance level in order to be not overly pessimistic or optimistic. Of course, one could vary $\eta$ and resolve (6.10b), but the procedure is cumbersome (especially for large networks) and the best $\eta$ does not guarantee that the overall probability of violation is the lowest.

In the following section, we elaborate on the framework based on (6.8) and show that it can be solved efficiently using samples.

### *6.4 Sample-Based Descent Algorithm*

The proposed optimization problem in (6.8) has a convex objective, a box constraint and a chance constraint. However, this chance constraint is not easy to deal with. In addition, the probabilistic distribution of the uncertainties in the system is usually not directly known. Instead, *historical observation samples* of the uncertainties (e.g., recorded solar generation values) are available. These samples can be used to find a probability distribution, but this

approach is cumbersome to implement because of two reasons: 1) it is not obvious how to find a good parameterization of the probability distribution to learn from the existing samples; and 2) even if the distribution is given, solving problem (6.8) with the chance constraint is non-trivial.

In this section, we present a sample-based algorithm that can efficiently solve the problem in (6.8) directly from a set of historical samples, without the need to fit a distribution. Let $\mathcal{S}$ denote the set of samples for the random variable $\boldsymbol{\epsilon}$, which we sometimes write as $\boldsymbol{\epsilon}^{(s)}, s \in \mathcal{S} = \{1, 2, \cdots, S\}$. In the rest of the section, we first provide the algorithm then show it is a descent algorithm. Throughout this section, we use $\hat{(\cdot)}$ to represent the approximation of a quantity.

### *6.4.1 Find a descent direction*

The first step in solving the optimization problem in (6.8) is to relax the constraints using the log barrier method [67]:

$$\begin{aligned} \min_{\boldsymbol{Q}} \ & \mathcal{L}(\boldsymbol{Q}) = \frac{1}{2}\|\boldsymbol{Q}\|_2^2 - \frac{1}{t} log(-\alpha + \psi(\boldsymbol{Q})) - \\ & \sum_i \frac{1}{t}\left( log(\overline{\boldsymbol{Q}}_i - \boldsymbol{Q}_i) + log(\boldsymbol{Q}_i - \underline{\boldsymbol{Q}}_i) \right), \end{aligned} \tag{6.13}$$

where $t$ is a tunable parameter, $(\cdot)_i$ represents the $i$th element of a vector, and $\psi(\boldsymbol{Q})$ is the chance constraint $\Pr\{\underline{\boldsymbol{V}} \leq \boldsymbol{RP} + \boldsymbol{XQ} + \boldsymbol{\epsilon} \leq \overline{\boldsymbol{V}}\}$. This optimization problem guarantees that the solution is always feasible to (6.8) and the problem is equivalent to (6.8) if we take $t \to \infty$.

To solve (6.13), the natural method to use is gradient descent. The gradient of $\mathcal{L}(\boldsymbol{Q})$ is:

$$\begin{aligned} \nabla \mathcal{L}(\boldsymbol{Q}) = \boldsymbol{Q} & - \frac{1}{t}\nabla(\log(\psi(\boldsymbol{Q}) - \alpha)) \\ & + \frac{1}{t}(\overline{\boldsymbol{Q}} - \boldsymbol{Q})^{-1} - \frac{1}{t}(\boldsymbol{Q} - \underline{\boldsymbol{Q}})^{-1}. \end{aligned} \tag{6.14}$$

It turns out that directly using (6.14) to solve (6.13) is difficult since there is no easy way to find the gradient of the $(\log(\psi(\boldsymbol{Q}) - \alpha))$. In fact, even if the true distribution of $\boldsymbol{\epsilon}$

is known, finding $\nabla(\log(\psi(\boldsymbol{Q}) - \alpha))$ requires evaluating multidimensional integrals, which is intractable for most distributions. The key step to mitigate this difficulty is to find some descent direction which approximates the gradient using historical samples, rather than trying to compute the exact gradient. In this section we first describe how to find a proxy for $\nabla \log(\psi(\boldsymbol{Q}) - \alpha)$. Then in Section 6.4.2, we show how it can be calculated from the samples.

The idea to find a descent direction is simple. Given any differentiable function $f : \mathbb{R}^N \to \mathbb{R}$, let $\boldsymbol{e}$ be a random unit vector in $\mathbb{R}^N$ and let $\Delta$ be a positive number. Then for any $\boldsymbol{x}$ in the domain of $f$, we can compute

$$\boldsymbol{p} = \frac{f(\boldsymbol{x} + \Delta \cdot \boldsymbol{e}) - f(\boldsymbol{x})}{\Delta} \boldsymbol{e}. \tag{6.15}$$

We can think of $\boldsymbol{p}$ as a random version of the gradient and will be taken as the direction of update in an optimization problem. To be a valid direction, we need to show that $\boldsymbol{p}$ is aligned (making an angle of less than 90°) with the actual gradient of $f$. This is given by the next theorem:

**Theorem 12.** *Let $f(\boldsymbol{x}) : \mathbb{R}^N \to \mathbb{R}$ be a differentiable function, $\boldsymbol{e}$ be a random unit vector in $\mathbb{R}^N$ and $\Delta$ be a positive scalar. Define $\boldsymbol{p} = \frac{f(\boldsymbol{x}+\Delta\cdot\boldsymbol{e})-f(\boldsymbol{x})}{\Delta}\boldsymbol{e}$, then $\nabla f(\boldsymbol{x})^\top \boldsymbol{p} > 0$ with probability 1 for a small enough $\Delta$.*

The proof of Theorem 12 is given in the Appendix. Since $\boldsymbol{p}$ is no more than 90° degrees apart from the gradient $\nabla f(\boldsymbol{x})$ (the dot product $\nabla f(\boldsymbol{x})^\top \boldsymbol{p}$ is positive), the next theorem shows that descending according to $\boldsymbol{p}$ is sufficient to reach a local minimum:

**Theorem 13.** *Let $f(\boldsymbol{x}) : \mathbb{R}^N \to \mathbb{R}$ be a differentiable function and $\boldsymbol{p}_{\boldsymbol{x}}$ be a vector such that $\nabla f(\boldsymbol{x})^\top \boldsymbol{p}_{\boldsymbol{x}} > 0$. Suppose $\boldsymbol{x}$ has the following update rule:*

$$\boldsymbol{x}_{m+1} = \boldsymbol{x}_m - \upsilon_m \boldsymbol{p}_{\boldsymbol{x}_m}, \tag{6.16}$$

*then the sequence of $\boldsymbol{x}_m$ converges to a stationary point of $f$ for appropriately chosen step sizes $\upsilon_m$.*

Theorem 13 states that as long as we move in some descent direction, then we are guaranteed to find a local optimum of a function. The step sizes $\upsilon_m$ can be found by many methods, including using fixed step sizes if the function is Lipschitz, using a decreasing sequence, using backtracking and others [122]. The proof of Theorem 13 proceeds almost identically as proving that the gradient descent converges to a stationary point, and can be found for example in [123].

Together, Theorems 12 and 13 tell us that as long as we can compute the function values of $f$, then we can use a descent algorithm to find a local optimum. The next section describes how we can find the function values of the unconstrained problem in (6.13) efficiently using samples.

### *6.4.2 Sample Approximation*

Note that $\mathcal{L}(\boldsymbol{Q})$, the objective in the unconstrained problem in (6.13), is a differentiable function since $\boldsymbol{\epsilon}$ has a continuous density function. Then the update rule discussed in Theorem 13 for $\mathcal{L}(\boldsymbol{Q})$ at $m$th iteration is: $\boldsymbol{Q}_{m+1} = \boldsymbol{Q}_m - \upsilon_m \boldsymbol{p}_{\boldsymbol{Q}_m}$, where $\boldsymbol{p}_{\boldsymbol{Q}_m}$ should be a proxy for $\nabla\mathcal{L}(\boldsymbol{Q})$ in (6.14) that satisfies Theorem 12. In this section, we focus on how to construct $\boldsymbol{p}_{\boldsymbol{Q}_m}$ using samples $\boldsymbol{\epsilon}^{(s)}$.

To start with, the difficult term to compute in (6.14) is $\log(\psi(\boldsymbol{Q}) - \alpha)$, and we focus on this term here. Recall that $\psi(\boldsymbol{Q}) = \Pr\{\underline{\boldsymbol{V}} \leq \boldsymbol{RP} + \boldsymbol{XQ} + \boldsymbol{\epsilon} \leq \overline{\boldsymbol{V}}\}$ and we write the right hand side as $\Pr(\boldsymbol{RP} + \boldsymbol{XQ})$ for brevity in this section. It is easy to compute a sample approximation of $\Pr(\boldsymbol{RP} + \boldsymbol{XQ})$ at a particular $\boldsymbol{Q}$. Denote the sample approximation of function $\psi(\boldsymbol{Q})$ by $\hat{\psi}(\boldsymbol{Q}, \{\boldsymbol{\epsilon}^{(s)}, \forall s \in \mathcal{S}\})$, and let $\boldsymbol{x} = \boldsymbol{RP} + \boldsymbol{XQ}$, then define

$$\begin{aligned}
&\hat{\psi}(\boldsymbol{Q}, \{\boldsymbol{\epsilon}^{(s)}, \forall s \in \mathcal{S}\}) \\
\triangleq &\frac{\sum_{s=1}^{S} \mathbb{1}\{\underline{\boldsymbol{V}} \leq \boldsymbol{RP} + \boldsymbol{XQ} + \boldsymbol{\epsilon}^{(s)} \leq \overline{\boldsymbol{V}}\}}{S} \\
= &\frac{\sum_{s=1}^{S} \mathbb{1}\{\underline{\boldsymbol{V}} \leq \boldsymbol{x} + \boldsymbol{\epsilon}^{(s)} \leq \overline{\boldsymbol{V}}\}}{S} \\
\triangleq &\widehat{\Pr}(\boldsymbol{x}, \{\boldsymbol{\epsilon}^{(s)}, \forall s \in \mathcal{S}\}),
\end{aligned} \tag{6.17}$$

where $S$ is the size of the set $\mathcal{S}$ and $\widehat{\Pr}(\boldsymbol{x}, \{\boldsymbol{\epsilon}^{(s)}, \forall s \in \mathcal{S}\})$ is the sample approximation of $\Pr(\boldsymbol{x})$. The quantity in (6.17) can be evaluated quickly since it only involves $SN$ comparisons using samples $\boldsymbol{\epsilon}^{(s)}$ and a particular value of $\boldsymbol{Q}$. As the sample size grows, $\widehat{\Pr}(\boldsymbol{x}, \{\boldsymbol{\epsilon}^{(s)}, \forall s \in \mathcal{S}\})$ becomes better at approximating $\Pr(\boldsymbol{x})$ [124].

Now we can find an approximation of a descent direction for $\log(\psi(\boldsymbol{Q}) - \alpha)$. First, using the chain rule, the gradient of $\log(\psi(\boldsymbol{Q}) - \alpha)$ is given by

$$\nabla \log(\psi(\boldsymbol{Q}) - \alpha) = \boldsymbol{X}^\top \frac{\nabla \Pr(\boldsymbol{x})}{\psi(\boldsymbol{Q}) - \alpha}, \tag{6.18}$$

where $\boldsymbol{x} = \boldsymbol{RP} + \boldsymbol{XQ}$.

Then we introduce the following corollary of Theorem 12:

**Corollary 1.** *Assume that $f(x) : \mathbb{R} \to \mathbb{R}$ and $\psi(\boldsymbol{y}) : \mathbb{R}^N \to \mathbb{R}$. If $f(\cdot)$ and $\psi(\cdot)$ are both differentiable, then $\nabla_{\boldsymbol{y}} f(\psi(\boldsymbol{y}))^\top \boldsymbol{p} \geq 0$ with probability 1, where $\boldsymbol{p} = \frac{\partial f(x)}{\partial x} \frac{\psi(\boldsymbol{y}+\Delta\cdot\boldsymbol{e}) - \psi(\boldsymbol{y})}{\Delta} \boldsymbol{e}|_{x=\psi(\boldsymbol{y})}$, for a sufficiently small positive scalar $\Delta$ and $\boldsymbol{e}$ is a random unit vector in $\mathbb{R}^N$.*

Combining the chain rule described in (6.18) with Corollary 1 and sample approximation as defined in (6.17), we can find a (random) descent direction of $\log(\psi(\boldsymbol{Q}) - \alpha)$ as:

$$\begin{aligned} &\boldsymbol{X}^\top \boldsymbol{e} \frac{\widehat{\Pr}(\boldsymbol{x} + \Delta \cdot \boldsymbol{e}, \{\boldsymbol{\epsilon}^{(s)}, \forall s \in \mathcal{S}\}) - \widehat{\Pr}(\boldsymbol{x}, \{\boldsymbol{\epsilon}^{(s)}, \forall s \in \mathcal{S}\})}{\Delta} \\ &\cdot \frac{1}{\hat{\psi}(\boldsymbol{Q}, \{\boldsymbol{\epsilon}^{(s)}, \forall s \in \mathcal{S}\}) - \alpha} \\ \triangleq &\frac{\widehat{\nabla} \psi(\boldsymbol{Q}, \{\boldsymbol{\epsilon}^{(s)}, \forall s \in \mathcal{S}\})}{\hat{\psi}(\boldsymbol{Q}, \{\boldsymbol{\epsilon}^{(s)}, \forall s \in \mathcal{S}\}) - \alpha}, \end{aligned} \tag{6.19}$$

where $\boldsymbol{e}$ is a random unit vector in $\mathbb{R}^n$, $\Delta$ is a small positive number and $\boldsymbol{x} = \boldsymbol{RP} + \boldsymbol{XQ}$.

This approximation $\widehat{\nabla} \psi(\boldsymbol{Q}, \{\boldsymbol{\epsilon}^{(s)}, \forall s \in \mathcal{S}\})$ is referred to as *stochastic quasi-gradient* (SQG) [125] of $\psi(\boldsymbol{Q})$. It was initially brought up to solve stochastic programs where the objective function is hard to evaluate. In our problem, we adopt the similar idea and use SQG to approximate the gradient which is hard to compute.

With the introduction of SQG on $\psi(\boldsymbol{Q})$ and the descent direction of $\log(\psi(\boldsymbol{Q}) - \alpha)$ in

(6.19), a (random) descent direction of $\mathcal{L}(\boldsymbol{Q})$ based on samples $\boldsymbol{\epsilon}^{(s)}$ is given by:

$$\widehat{\nabla}\mathcal{L}(\boldsymbol{Q}, \{\boldsymbol{\epsilon}^{(s)}, \forall s \in \mathcal{S}\}) \triangleq \boldsymbol{Q} - \frac{1}{t}\frac{\widehat{\nabla}\psi(\boldsymbol{Q}, \{\boldsymbol{\epsilon}^{(s)}, \forall s \in \mathcal{S}\})}{\hat{\psi}(\boldsymbol{Q}, \{\boldsymbol{\epsilon}^{(s)}, \forall s \in \mathcal{S}\}) - \alpha} + \frac{1}{t}(\overline{\boldsymbol{Q}} - \boldsymbol{Q})^{-1} - \frac{1}{t}(\boldsymbol{Q} - \underline{\boldsymbol{Q}})^{-1},$$

which is a valid $\boldsymbol{p_Q}$ for the update rule.

### *6.4.3 Main Algorithm*

Now we plug in $\widehat{\nabla}\mathcal{L}(\boldsymbol{Q}, \{\boldsymbol{\epsilon}^{(s)}, \forall s \in \mathcal{S}\})$ into the standard log barrier method and arrive at the proposed descent algorithm, shown in Algorithm 5. In Algorithm 5, we have an outer iteration that increases the value of $t$, which forces the optimization problem in (6.13) to be closer to the true optimization problem in (6.8). In the inner iteration when $t$ is fixed, we run the loop till convergence.

**Algorithm 5** Modified log barrier method.

**Input**: $t_0 > 0$, $\upsilon_0 > 0$, $\varepsilon_1, \varepsilon_2, \varepsilon_3 > 0$, $\tau > 1$, $\phi < 1$, a feasible $\boldsymbol{Q}_0$, $m = k = 1$.
**while** $\frac{1}{t_k} \geq \varepsilon_1$ and $\upsilon_k \geq \varepsilon_2$ **do**
    $t_k = \tau t_{k-1}$, $\upsilon_k = \phi \upsilon_{k-1}$.
    **while** $\|\boldsymbol{Q}_m - \boldsymbol{Q}_{m-1}\|_2^2 \geq \varepsilon_3$ **do**
        Compute gradient w.r.t. random sample $\{\epsilon^{(s)}\}$ at $t = t_k$, denote it by $\widehat{\nabla}\mathcal{L}(\boldsymbol{Q}_{m-1}, \{\boldsymbol{\epsilon}^{(s)}, \forall s \in \mathcal{S}\})$.
        Do backtracking until obtaining feasible $\boldsymbol{Q}_m = \boldsymbol{Q}_{m-1} - \upsilon' \widehat{\nabla}\mathcal{L}(\boldsymbol{Q}_{m-1}, \{\boldsymbol{\epsilon}^{(s)}, \forall s \in \mathcal{S}\})$, where $\upsilon'$ is determined by backtracking. Let $\upsilon_k = \upsilon'$.
        $m = m + 1$.
    $k = k + 1$.
**Output** $\boldsymbol{Q}_m$.

In addition, since $\widehat{\nabla}\mathcal{L}(\boldsymbol{Q}_{m-1}, \{\boldsymbol{\epsilon}^{(s)}, \forall s \in \mathcal{S}\})$ is random and the chances that it is exactly orthogonal to the true gradient is zero, Algorithm 5 is guaranteed to converge, as given

in Theorem 13. In the simulations, we show that Algorithm 5 is more efficient than the conventional MIP on both synthetic and real datasets.

In the following section, we show that for a certain family of distributions for $\boldsymbol{\epsilon}$, Algorithm 5 converges to the global optimum (in the sense of sample approximation) because the chance constraint $\psi(\boldsymbol{Q}) \geq \alpha$ becomes a convex constraint.

### *6.5 Convexity of the optimization problem*

In this section, we show that the chance constraint $\psi(\boldsymbol{Q}) \geq \alpha$ is convex for a broad family of probabilistic distributions. Since all other constraints in (6.8) are also convex, the optimization problem is convex and Algorithm 5 converges to the global optimum:

**Theorem 14.** *If the uncertainty $\boldsymbol{\epsilon}$ has a continuous log-concave probabilistic distribution, the optimization problem in* (6.8) *is convex. Then Algorithm 5 converges the global optimum with probability 1.*

Theorem 14 states that even if the feasible region defined by the chance constraint is not obvious at first sight, the problem is computationally tractable with Algorithm 5 which finds the global optimum. We now formally define log-concavity.

**Definition 4.** *A non-negative function $f : \mathbb{R}^N \to \mathbb{R}_+$ is logarithmically concave (or log-concave for short) if its domain is a convex set, and if it satisfies the inequality:*

$$\begin{aligned} f(\theta x + (1-\theta)y) &\geq f(x)^{\theta} f(y)^{1-\theta} f(\theta x + (1-\theta)y) \\ &\geq f(x)^{\theta} f(y)^{1-\theta}, \end{aligned} \tag{6.20}$$

*for all $x, y \in dom(f)$ and $0 < \theta < 1$. In short, if $\log(f(x))$ is concave, then $f(x)$ is log-concave.*

Log-concave distributions includes many of the commonly encountered distribution in practice, including the joint Gaussian, gamma, uniform, logistic, Laplace and others [126]. For example, the forecast errors of solar and wind are usually assumed to follow one of

these distributions. Note that Theorem 14 states that as long as the samples come from a log-concave distribution, the optimization problem is convex. In practice, we would still use Algorithm 5 rather than explicitly fitting a distribution to solve the chance constrained problem.

To prove Theorem 14, we introduce two lemmas that discuss log-concavity of certain functions. Lemma 6 states that the accumulated mass of a log-concave probabilistic function over a convex set is log-concave. Lemma 7 states that applying linear transformation to the variable in a log-concave function yields another log-concave function, given that the linear transformation has full row rank.

**Lemma 6.** *Denote* $F(\boldsymbol{z}) = \int_{\boldsymbol{z}-\boldsymbol{u}}^{\boldsymbol{z}} f(\epsilon_1, \ldots, \epsilon_N)\, d\epsilon_1 \ldots d\epsilon_N$ *where* $u > 0$ *is a given vector. If the distribution* $f(\epsilon_1, \ldots, \epsilon_N)$ *is log-concave in* $\boldsymbol{\epsilon}$*, then* $F(\boldsymbol{z})$ *is log-concave in* $\boldsymbol{z}$*.*

**Lemma 7.** *Assume that* $F(\boldsymbol{z})$ *is a log-concave function,* $\boldsymbol{z} \in \mathbb{R}^N$ *and that* $\boldsymbol{z} = A\boldsymbol{y} + \boldsymbol{b}$ *with* $\boldsymbol{y} \in \mathbb{R}^M$*,* $A \in \mathbb{R}^{N \times M}$*,* $\boldsymbol{b} \in \mathbb{R}^N$*. If* $A$ *has rank* $N$*, then* $g(\boldsymbol{y}) = F(A\boldsymbol{y} + \boldsymbol{b})$ *is also a log-concave function.*

With Lemma 6 and Lemma 7, Theorem 14 follows. The proofs are given in Appendix B.

### *6.6 Simulation*

In this section, we validate Algorithm 5 with a toy problem and the IEEE standard 123 bus distribution system. The solver for MIP is GUROBI [127]. We use Matlab on MacBook Pro with 2.7 GHz Intel Core i5 to conduct all the simulations. First, we introduce the benchmark state-of-the-art method we compare Algorithm 5 against.

### *6.6.1 Sample approximation benchmark*

A natural way to approximate the chance constraint is to use indicator variables to replace the probability constraint with samples [116]:

$$\min_{\boldsymbol{Q}} \ \|\boldsymbol{Q}\|_2 \tag{6.21a}$$

$$s.t. \ \sum_{s\in\mathcal{S}} \mathbb{1}\{\underline{\boldsymbol{V}} \le \boldsymbol{RP} + \boldsymbol{XQ} + \boldsymbol{\epsilon}^{(s)} \le \overline{\boldsymbol{V}}\} \ge \alpha S, \tag{6.21b}$$

$$\underline{\boldsymbol{Q}} \le \boldsymbol{Q} \le \overline{\boldsymbol{Q}}, \tag{6.21c}$$

where $\mathbb{1}\{\cdot\}$ is the indicator function.

In (6.21), we use the empirical estimation $\sum_{s\in\mathcal{S}} \mathbb{1}\{\underline{\boldsymbol{V}} \le \boldsymbol{RP} + \boldsymbol{XQ} + \boldsymbol{\epsilon}^{(s)} \le \overline{\boldsymbol{V}}\}/S$ to replace the true probability $\Pr\{\underline{\boldsymbol{V}} \le \boldsymbol{RP} + \boldsymbol{XQ} + \boldsymbol{\epsilon} \le \overline{\boldsymbol{V}}\}$. However, the indicator function $\mathbb{1}\{\cdot\}$ is discontinuous and non differentiable. To solve the problem in (6.21), introduction of binary variables for each scenario $s$ is necessary. Each binary variable indicates whether the voltage bound is violated or not given the particular sample $s$. We can then reformulate the problem as a mixed integer programming (MIP) problem. In this chapter, for comparison we actually implement an improved version of (6.21) where the number of binary constraints is reduced by $\alpha$. Details are shown in Section B.14.

### *6.6.2 Toy example with multivariate Gaussian random variable*

In this section we illustrate more results on a toy example of a three bus line network. We make the following assumptions on system configuration, where all quantities are expressed in p.u.: $\boldsymbol{P} = \begin{bmatrix} -0.0623 \\ -0.2291 \end{bmatrix}$, $\boldsymbol{R} = \begin{bmatrix} 0.0351 & 0.0351 \\ 0.0351 & 0.1053 \end{bmatrix}$, $\boldsymbol{X} = \begin{bmatrix} 0.1333 & 0.1333 \\ 0.1333 & 0.4000 \end{bmatrix}$, $\boldsymbol{\epsilon}$ follows multivariate Gaussian distribution with $\mu = \begin{bmatrix} 0 \\ 0 \end{bmatrix}, \Sigma = \begin{bmatrix} 0.002 & 0.0014 \\ 0.0014 & 0.006 \end{bmatrix}$, $\overline{\boldsymbol{V}} = \begin{bmatrix} 0.05 \\ 0.05 \end{bmatrix}$, $\underline{\boldsymbol{V}} = \begin{bmatrix} -0.05 \\ -0.05 \end{bmatrix}$, and $\alpha = 0.9$.

In Section 6.3, we have visited the differences between the proposed framework and the per-bus formulation. In this section, we give more results on the proposed descent algorithm in Algorithm 5 and MIP. We show in Table 6.2 that Algorithm 5 is much faster than MIP given samples. We assume that the system operator has knowledge of 2000 samples that depict $\boldsymbol{\epsilon}$.

Since only a finite number of samples are available to the system operator, to be conservative, the heuristics is to increase the value of $\alpha$ by some small value. For example, if the target value of $\alpha$ is 0.9, then we use $\alpha = 0.91$ to solve the optimization problem using samples. This conservative choice of $\alpha$ aims to control the true risk level within desired range. As can be seen from Table 6.2, the empirical risk level is slightly lower than the true risk level due to limited number of observations on the underlying probabilistic distribution. In addition, we find that Algorithm 5 is more efficient in computational time as compared to MIP with an equally good solution with respect to optimization objective, i.e., $\|\boldsymbol{Q}\|_2$ shown in Table 6.2.

Table 6.2: Comparison between Algorithm 5 and MIP given samples.

| | **Algo. 5** | **MIP** |
|---|---|---|
| Empirical risk level | 9% | 9% |
| True risk level | 9.14% | 9.16% |
| $\|\boldsymbol{Q}\|_2$ (p.u.) | 0.0199 | 0.0197 |
| Time (seconds) | 19 | 42 |

In Fig. 6.2, we further validate our proposed descent algorithm by plotting the change in objective function at each iteration. As can be clearly seen, the value of the objective function is effectively decreasing with an approximation of the true gradient.

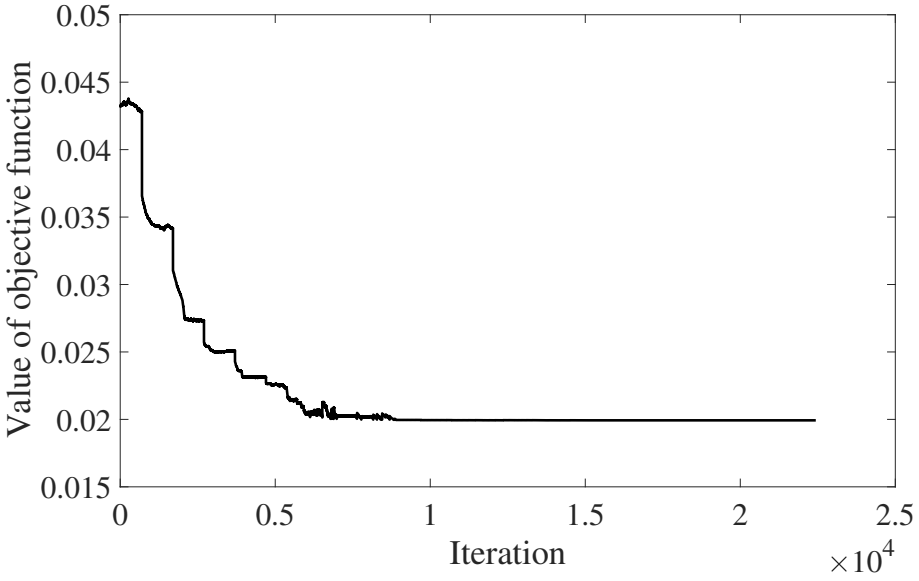


Figure 6.2: Decrease in objective function in (6.13) using Algorithm 5.

### *6.6.3 IEEE 123 bus system with renewable integration*

In this section, we validate the statements by IEEE standard test feeder. Here we use IEEE 123 bus feeder [128] as an example. The test feeder is shown in Fig. 6.3. We assume bus 149 is the reference bus.

The randomness of the system comes from the fluctuation of the renewable generation. We use solar generation data from NREL [106]. Its characteristic is shown in Fig. 6.4. Besides solar energy fluctuations, the system is configured such that the switches between buses 13 and 152, 18 and 135, 54 and 94, 97 and 197 are closed. In addition, we take real power injection as a random vector. We assume that the next scheduling period is 2 p.m. The renewable generation is collected between 2 p.m. - 3 p.m. with 5 minute interval over a past whole year. We set the empirical risk level as 9% (to be conservative), which means that $\alpha = 0.91$ on the samples. The deviation on voltage is set to be no more than 5% of the nominal voltage and the bounds on $\boldsymbol{Q}$ is set to be 0.01 p.u.

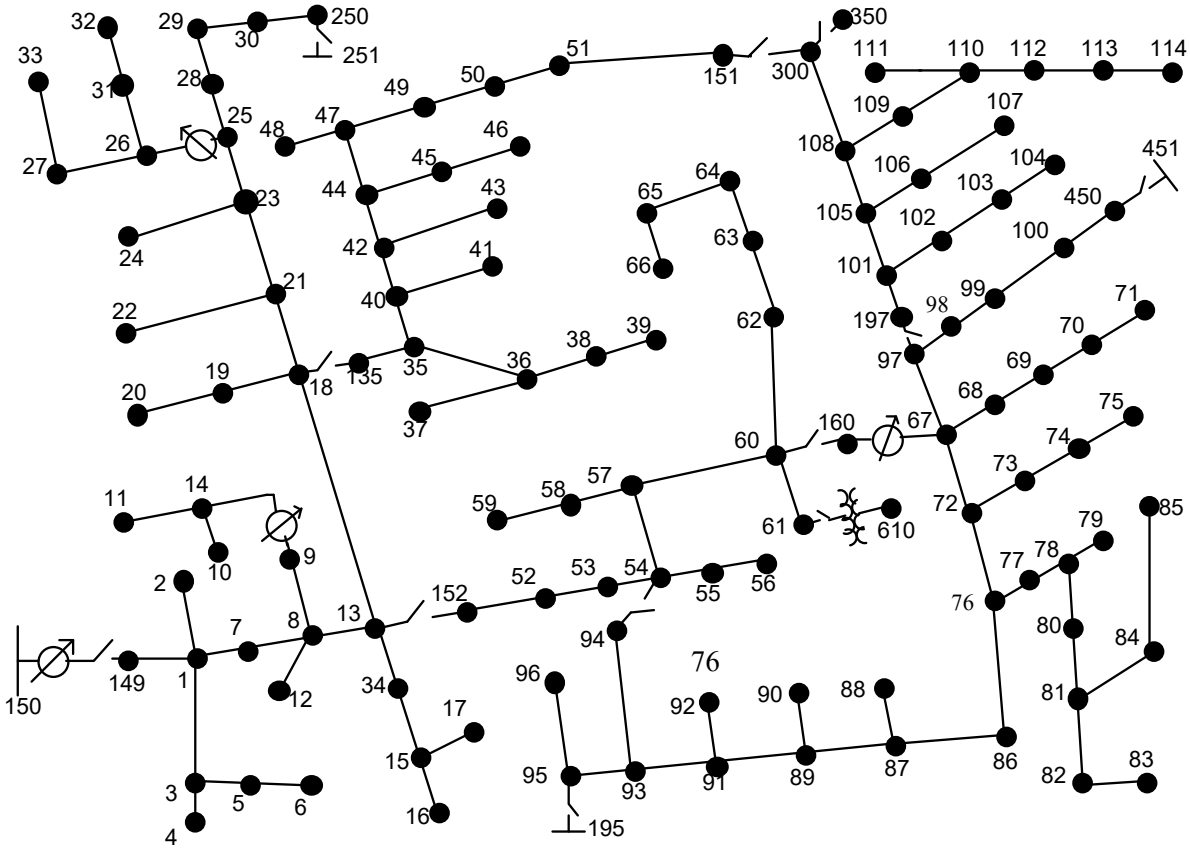


Figure 6.3: Schematic diagram of IEEE 123 bus test feeder.

The results on the 123 bus system are shown in Table 6.3. From Table 6.3, we see that MIP takes a significantly longer time to solve as compared to Algorithm 5, which cannot be adopted in real time dispatch decisions. Both methods are able to achieve the desired risk level, i.e., 9%. The optimal $\boldsymbol{Q}$ returned by Algorithm 5 only differs in less than 5% in norm as compared to the solution returned by MIP.

In addition, from the solution of MIP, we find that the significant amount of reactive power support occurs at buses that are further down the feeder, i.e., bus 70, 71 and bus

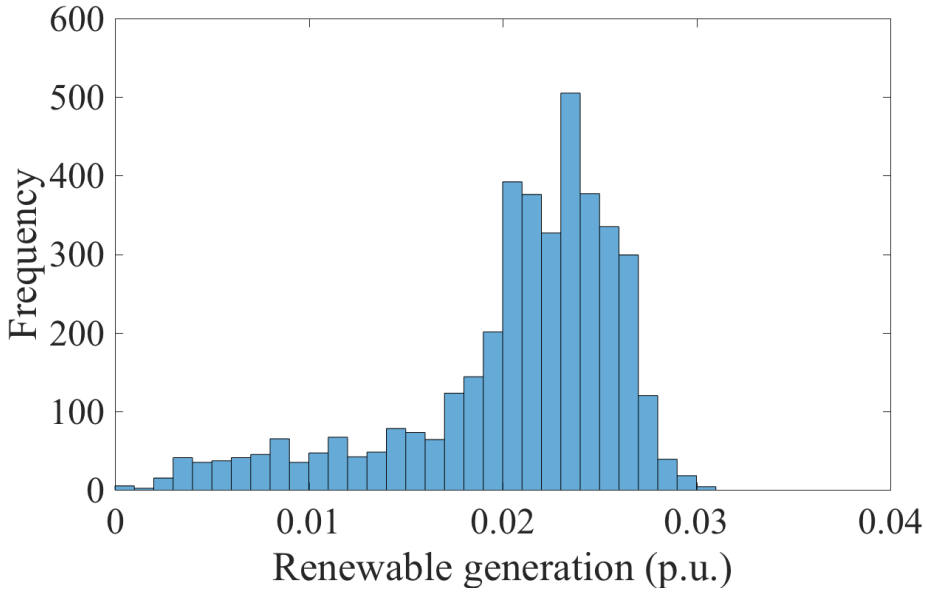


Figure 6.4: Histogram of PV generation between 2 p.m. and 3 p.m..

104. These buses are more vulnerable towards uncertainty in the system thus more reactive power support is needed to avoid large voltage deviation. We find that Algorithm 5 locates those buses in a much faster computational time. Both algorithms are able to find 40 such buses, with Algorithm 5 missing only one bus as compared to the solution by MIP. The most reactive power support occurs at bus 104, with $Q_{104} = -0.0016$ p.u. as in MIP and $Q_{104} = -0.0011$ p.u. as in Algorithm 5. These reactive power support serve to mitigate the impact (over-voltage) by real power injection of random renewables.

## *6.7 Summary*

In this chapter we adopt a stochastic framework to formulate voltage control problems with uncertainty. Compared to existing literature, we use a single chance constraint to capture the uncertainty in the distribution system. We show that this formulation is more realistic and less conservative than placing constraints on every bus in the distribution network. We also propose a tractable algorithm to solve the optimization problem without explicitly knowing

Table 6.3: Comparison between MIP and Algorithm 5 for IEEE 123 bus with renewable generation.

| | **MIP** | **Algo. 5** |
|---|---|---|
| Running time (seconds) | 710 | 302 |
| Empirical risk level | 9.00% | 8.97% |
| $\|\boldsymbol{Q}\|_2$ (p.u.) | 0.0083 | 0.0087 |
| Most sensitive bus | 104 | 104 |
| Number of buses with non-trivial reactive power support | 41 | 40 |

the underlying probabilistic distribution. For a wide range of probabilistic distributions, the proposed algorithm converges to global optimum because the problem is convex. Simulation results validate our statements by standard IEEE test feeders.

# Chapter 7

# CONCLUSIONS AND FUTURE WORKS

## *7.1 Conclusions*

The electrical system is undergoing a transformation in both operation and design. A particular area that is changing drastically is the balance between supply and demand. In the new era of power system operation, operators are starting to explore demand flexibility to balance generation. This type of operation is commonly known as demand response (DR). Flexibilities in such operations stem from load change and planning of appropriate distributed energy resources (DERs), mostly renewable energy resources like solar and wind. Together, they serve to mitigate the system stress and provide more sustainable operation and more monetary returns to the system operator. It is thus crucial for the system operator to accurately estimate the impact of DR programs, either from the effect of a DR signal to stimulate uncertain end consumer's behavior, or from the proper sizing of uncertain DERs in the system.

While DR brings these many benefits to the system operator, the system operator also needs to guarantee a secured operation of the system given uncertainties. For example, the voltage at each bus of the power system needs to be secured within tolerance at all times. The intermittency and randomness of DERs causs problems in voltage fluctuation and which, if not dealt with properly, lead to blackouts in the power system. The system operator thus needs to make robust operation schedules in the presence of such uncertainty.

To answer these questions, we first propose to estimate the effect of DR signal to end consumers by a linear model. We analyze some variants of a general linear model and compare their estimation accuracy in different scenarios. Then we propose an optimal DR signal assignment strategy to best estimate its effect. We show that in a high dimensional setting,

the proposed strategy can achieve order optimal rates in variance reduction, whereas random assignments does not reduce variance even as the number of users grows. In addition, we bring the estimation procedure into a more realistic setting where DR signals are continuous such as price signals, and that the system operator is facing a group of uncertain consumers whose cost functions are unknown. The operator thus makes sequential pricing decisions to learn the cost functions of these consumers as well as minimizing DR cost at the same time. We design an online learning algorithm referred to as iterated linear regression to assist this pricing strategy. Compared with the offline optimal solution, our online algorithm achieves a sublinear regret in the length of time period, i.e., $\Theta(\log T)$.

We then take into consideration the role of DERs in the operation of the power system. We specifically consider distributed PVs as DERs in a microgrid connected to the power sytem. We propose a decentralized market design to obtain optimal sizing of each DER provider in this market. We model this market as a two stage capacity-price game and show that such a game has a Nash equilibrium that coincides with the solution from a social welfare optimization problem. In addition, we show that all Nash equilibria are efficient, in the sense that the collected payment to the energy producers approaches their investment costs.

Last, we propose to use reactive power compensation to alleviate voltage fluctuations resulted from the uncertainty brought by DERs. More specifically, we use a single chance constraint to capture the uncertainty in the distribution system. We show that this formulation is more realistic and less conservative than placing constraints on every bus in the distribution network. We also propose a tractable algorithm to solve the optimization problem without explicitly knowing the underlying probabilistic distribution. For a wide range of probabilistic distributions, the proposed algorithm converges to global optimum because the problem is convex.

### *7.2 Suggestions for the future work*

To better incorporate DERs into the operation of an urban power system, there are several interesting research topics that remain open.

First, uncertainty in a DR program come from both end consumer's demand profile and DERs' generation. If energy consumption can be balanced locally from DERs, it alleviates the burden from the power network and makes the system more sustainable. How to balance these resources is non-trivial and the way to define the best balance between demand and random resources differs significantly from where they are considered deterministic. For example, considering generation and consumption as random variables, one crude way to solve for the best matching between generation and consumption is to minimize the expected squared difference. However, the expected squared difference does not take into consideration more complicated statistical properties, for example temporal correlation. This objective thus provides little insights to match consumption with DER generation in real-time operation, where decisions should be made more frequently. A better and more versatile objective to statistically match energy generation and consumption is one future work and can potentially shed light on a more sustainable operation of power system.

Second, the dispatch decision of DERs in real time is coupled as a multi-period optimization problem. This problem is usually captured under the scheme of stochastic control and can be solved by dynamic programming. Alternatively, the system operator can make use of the flexibility in end consumers to promote energy efficient dispatch decision. For example, less wind is going to be discarded as a result of a better response from consumers. Financial approaches such as forward contracts and options have proven to be an effective mean to promote energy efficiency. Designing proper financial incentives is one hot topic especially when it comes to multi-stage decision for DERs in real time.

In addition, to facilitate these decisions, it is necessary to develop more robust and accurate forecasting tools to predict DER generation. Deep neural networks (DNN) has shown great progress and success in many applications including computer vision, natural

language processing, and speech recognition. Naturally, we can improve the system with DNN in proper applications. For example, DER generation across a power network usually has strong temporal and spatial correlation and is therefore a good data input for either recurrent neural network or convolution neural network. The merge of generative adversarial network (GAN) and its variants also shed light on how we can generate diversified DER generation and pick up the most representative scenarios. In all, the power of new emerging DNN models to solve engineering problems in power system operation is yet to be discovered.

# BIBLIOGRAPHY

[1] P. Siano, "Demand response and smart grids  a survey," *Renewable and Sustainable Energy Reviews*, vol. 30, pp. 461–478, 2014.

[2] P. Palensky and D. Dietrich, "Demand side management: Demand response, intelligent energy systems, and smart loads," *IEEE transactions on industrial informatics*, vol. 7, no. 3, pp. 381–388, 2011.

[3] C. L. Su and D. Kirschen, "Quantifying the effect of demand response on electricity markets," *Power Systems, IEEE Transactions on*, vol. 24, no. 3, pp. 1199–1207, 2009.

[4] D. Wang, X. Guan, J. Wu, P. Li, P. Zan, and H. Xu, "Integrated energy exchange scheduling for multimicrogrid system with electric vehicles," *Smart Grid, IEEE Transactions on, preprint*, 2015.

[5] N. Li, L. Chen, and S. H. Low, "Optimal demand response based on utility maximization in power networks," in *Power and Energy Society General Meeting, 2011 IEEE*, pp. 1–8, IEEE, 2011.

[6] C. Chen, J. Wang, and S. Kishore, "A distributed direct load control approach for large-scale residential demand response," *IEEE Transactions on Power Systems*, vol. 29, no. 5, pp. 2219–2228, 2014.

[7] G. Timilsina, L. Kurdgelashvili, and P. Narbel, "Solar energy: Markets, economics and policies," *Renewable and Sustainable Energy Reviews*, vol. 16, no. 1, pp. 449–465, 2012.

[8] N. Li, G. Qu, and M. Dahleh, "Real-time decentralized voltage control in distribution networks," in *Communication, Control, and Computing (Allerton), 2014 52nd Annual Allerton Conference on*, pp. 582–588, IEEE, 2014.

[9] B. Zhang, A. Dominguez-Garcia, and D. Tse, "A local control approach to voltage regulation in distribution networks," in *North American Power Symposium (NAPS)*, pp. 1–6, IEEE, 2013.

[10] H. Kanchev, D. Lu, F. Colas, V. Lazarov, and B. Francois, "Energy management and operational planning of a microgrid with a pv-based active generator for smart grid applications," *IEEE transactions on industrial electronics*, no. 10, pp. 4583–4592, 2011.

[11] B. Zhang, A. Y. S. Lam, A. D. Domnguez-Garca, and D. Tse, "An optimal and distributed method for voltage regulation in power distribution systems," *IEEE Transactions on Power Systems*, vol. 30, no. 4, pp. 1714–1726, 2015.

[12] M. Farivar, R. Neal, C. Clarke, and S. Low, "Optimal inverter var control in distribution systems with high pv penetration," in *Power and Energy Society General Meeting*, pp. 1–7, IEEE, 2012.

[13] G. Valverde and T. Van Cutsem, "Model predictive control of voltages in active distribution networks," *IEEE Transactions on Smart Grid*, no. 4, pp. 2152–2161, 2013.

[14] H. Zhu and H. Liu, "Fast local voltage control under limited reactive power: Optimality and stability analysis," *IEEE Transactions on Power Systems*, no. 5, pp. 3794–3803, 2012.

[15] P. Sulc, S. Backhaus, and M. Chertkov, "Optimal distributed control of reactive power via the alternating direction method of multipliers," *IEEE Transactions on Energy Conversion*, no. 4, pp. 968–977, 2014.

[16] L. Qian, Y. A. Zhang, J. Huang, and Y. Wu, "Demand response management via real-time electricity price control in smart grids," *Selected Areas in Communications, IEEE Journal on*, vol. 31, no. 7, pp. 1268–1280, 2013.

[17] W. Saad, Z. Han, H. V. Poor, and T. Basar, "Game-theoretic methods for the smart grid: An overview of microgrid systems, demand-side management, and smart grid communications," *IEEE Signal Processing Magazine*, vol. 29, no. 5, pp. 86–105, 2012.

[18] J. C. Holyhead, S. D. Ramchurn, and A. Rogers, "Consumer targeting in residential demand response programmes," in *Proceedings of the 2015 ACM Sixth International Conference on Future Energy Systems*, pp. 7–16, ACM, 2015.

[19] V. M. Balijepalli, V. Pradhan, S. Khaparde, and R. Shereef, "Review of demand response under smart grid paradigm," in *Innovative Smart Grid Technologies-India (ISGT India), 2011 IEEE PES*, pp. 236–243, IEEE, 2011.

[20] G. W. Imbens, "Nonparametric estimation of average treatment effects under exogeneity: A review," *Review of Economics and statistics*, vol. 86, no. 1, pp. 4–29, 2004.

[21] D. A. Freedman, *Statistical models: theory and practice*. Cambridge University Press, 2009.

[22] P. Li, B. Zhang, Y. Weng, and R. Rajagopal, "A sparse linear model and significance test for individual consumption prediction," *IEEE Transactions on Power Systems*, vol. PP, no. 99, pp. 1–1, 2017.

[23] D. Crawley, C. Pedersen, L. Lawrie, and F. Winkelmann, "Energyplus: energy simulation program," *ASHRAE journal*, vol. 42, no. 4, p. 49, 2000.

[24] L. Tian, A. Alizadeh, A. Gentles, and R. Tibshirani, "A simple method for detecting interactions between a treatment and a large number of covariates," *arXiv preprint*, 2012. arXiv:1212.2995.

[25] G. A. F. Seber and A. J. Lee, *Linear regression analysis*. John Wiley and Sons, 2012.

[26] E. A. Stuart, "Matching methods for causal inference: A review and a look forward," *Statistical science: a review journal of the Institute of Mathematical Statistics*, vol. 25, no. 1, pp. 1–29, 2010.

[27] P. Li and B. Zhang, "Linear estimation of treatment effects in demand response: An experimental design approach," *arXiv:1706.09835v2*, 2017.

[28] Pecan Street, "Pecan street online database." `http://www.pecanstreet.org`, 2017.

[29] D. Park, M. El-Sharkawi, R. Marks, L. Atlas, and M. Damborg, "Electric load forecasting using an artificial neural network," *Power Systems, IEEE Transactions on*, vol. 6, no. 2, pp. 442–449, 1991.

[30] G. A. F. Seber and A. J. Lee, *Linear regression analysis*. John Wiley and Sons, 2012.

[31] N. Bhat, V. Farias, and C. Moallemi, "Optimal ab testing," 2015.

[32] S. Fisher, R. Fisher, S. Genetiker, R. Fisher, S. Genetician, G. Britain, R. Fisher, and S. Gnticien, *The design of experiments*. Oliver and Boyd, 1935.

[33] U. Feige, D. Peleg, and G. Kortsarz, "The dense k-subgraph problem," *Algorithmica*, no. 3, pp. 410–421, 2001.

[34] U. Feige and M. Langberg, "Approximation algorithms for maximization problems arising in graph partitioning," *Journal of Algorithms*, no. 2, pp. 174–211, 2001.

[35] Q. Han, Y. Ye, and J. Zhang, "An improved rounding method and semidefinite programming relaxation for graph partition," *Mathematical Programming*, no. 3, pp. 509–535, 2002.

[36] Y. Ye and J. Zhang, "Approximation of dense-n/2-subgraph and the complement of min-bisection," *Journal of Global Optimization*, no. 1, pp. 55–73, 2003.

[37] D. Zhou, M. Balandat, and C. Tomlin, "A bayesian perspective on residential demand response using smart meter data," *ArXiv*, vol. 1608.03862, 2016.

[38] K. H. Brodersen, F. Gallusser, J. Koehler, N. Remy, and S. L. Scott, "Inferring causal impact using bayesian structural time-series models," *Annals of Applied Statistics*, vol. 9, pp. 247–274, 2015.

[39] P. Li and B. Zhang, "An optimal treatment assignment strategy to evaluate demand response effect," *ArXiv e-prints*, 2016. arXiv:1610.00362.

[40] G. Oehlert, "A note on the delta method," *The American Statistician*, no. 1, pp. 27–29, 1992.

[41] G. Kortsarz and D. Peleg, "On choosing a dense subgraph," in *Foundations of Computer Science, 34th Annual Symposium on*, pp. 692–701, IEEE, 1993.

[42] Y. Asahiro, K. Iwama, H. Tamaki, and T. Tokuyama, "Greedily finding a dense subgraph," *Journal of Algorithms*, no. 2, pp. 203–221, 2000.

[43] U. Feige and M. Seltser, "On the densest k-subgraph problem," tech. rep., Weizmann Institute of Science. Department of Applied Mathematics and Computer Science.

[44] A. Srivastav and K. Wolf, "Finding dense subgraphs with semidefinite programming," in *International Workshop on Approximation Algorithms for Combinatorial Optimization*, Springer Berlin Heidelberg, 1998.

[45] A. Bhaskara, M. Charikar, E. Chlamtac, U. Feige, and A. Vijayaraghavan, "Detecting high log-densities: an o (n ) approximation for densest k-subgraph," in *In Proceedings of the forty-second ACM symposium on Theory of computing*, ACM, 2010.

[46] C. Riquelme, R. Johari, and B. Zhang, "Online active linear regression via thresholding," *ArXiv*, vol. 1602.02845, 2016.

[47] ENERNOC, "Create new revenue with demand response." `https://www.enernoc.com/products/businesses/capabilities/demand-response`, 2017.

[48] Ohmconnect, "Demand response programs." `https://www.ohmconnect.com/wiki/learn-more`, 2017.

[49] T. L. Lai and H. Robbins, "Asymptotically efficient adaptive allocation rules," *Advances in applied mathematics*, vol. 6, no. 1, pp. 4–22, 1985.

[50] M. H. Albadi and E. El-Saadany, "A summary of demand response in electricity markets," *Electric power systems research*, vol. 78, no. 11, pp. 1989–1996, 2008.

[51] Department of Energy, "Benefits of demand response in electricity markets and recommendations for achieving them," *Report of the United States Congress*, 2006.

[52] J. S. Vardakas, N. Zorba, and C. V. Verikoukis, "A survey on demand response programs in smart grids: Pricing methods and optimization algorithms," *IEEE Communications Surveys & Tutorials*, vol. 17, no. 1, pp. 152–178, 2015.

[53] K. M. Tsui and S.-C. Chan, "Demand response optimization for smart home scheduling under real-time pricing," *IEEE Transactions on Smart Grid*, vol. 3, no. 4, pp. 1812–1821, 2012.

[54] L. Jiang and S. Low, "Multi-period optimal energy procurement and demand response in smart grid with uncertain supply," in *Decision and Control and European Control Conference (CDC-ECC), 2011 50th IEEE Conference on*, pp. 4348–4353, IEEE, 2011.

[55] P. Samadi, H. Mohsenian-Rad, V. W. Wong, and R. Schober, "Tackling the load uncertainty challenges for energy consumption scheduling in smart grid," *IEEE Transactions on Smart Grid*, vol. 4, no. 2, pp. 1007–1016, 2013.

[56] D. Zhang, S. Li, M. Sun, and Z. ONeill, "An optimal and learning-based demand response and home energy management system," *IEEE Transactions on Smart Grid*, vol. 7, no. 4, pp. 1790–1801, 2016.

[57] D. O'Neill, M. Levorato, A. Goldsmith, and U. Mitra, "Residential demand response using reinforcement learning," in *Smart Grid Communications (SmartGridComm), 2010 First IEEE International Conference on*, pp. 409–414, IEEE, 2010.

[58] Z. Xu, T. Deng, Z. Hu, Y. Song, and J. Wang, "Data-driven pricing strategy for demand-side resource aggregators," *IEEE Transactions on Smart Grid*, 2016.

[59] S. Baltaoglu, L. Tong, and Q. Zhao, "Online learning and pricing for demand response in smart distribution networks," in *Statistical Signal Processing Workshop (SSP), 2016 IEEE*, pp. 1–5, IEEE, 2016.

[60] K. Khezeli and E. Bitar, "Risk-sensitive learning and pricing for demand response," *arXiv preprint arXiv:1611.07098*, 2016.

[61] A. Albert and R. Rajagopal, "Thermal profiling of residential energy use," *IEEE Transactions on Power Systems*, vol. 30, pp. 602–611, Mar. 2015.

[62] L. Yang, D. Callaway, and C. Tomlin, "Dynamic contracts with partial observations: application to indirect load control," in *American Control Conference (ACC)*, pp. 1224–1230, IEEE, 2014.

[63] L. Yang, D. Callaway, and C. Tomlin, "Indirect load control for electricity market risk management via risk-limiting dynamic contracts," in *American Control Conference (ACC)*, pp. 3025–3031, IEEE, 2015.

[64] S. Shalev-Shwartz, "Online learning and online convex optimization," *Foundations and Trends in Machine Learning*, vol. 4, no. 2, pp. 107–194, 2012.

[65] S. Bubeck and N. Cesa-Bianchi, "Regret analysis of stochastic and nonstochastic multi-armed bandit problems," *Foundations and Trends in Machine Learning*, vol. 5, no. 1, pp. 1–122, 2012.

[66] G. P. Chow, *Analysis and Control of Dynamic Economic Systems*. New York: Wiley, 1976.

[67] S. Boyd and L. Vandenberghe, *Convex optimization*. Cambridge university press, 2004.

[68] C. Henderson, "Best linear unbiased estimation and prediction under a selection model," *Biometrics*, pp. 423–447, 1975.

[69] P. Li, H. Wang, and B. Zhang, "A distributed online pricing strategy for demand response programs," *IEEE Transactions on Smart Grid*, 2017.

[70] T. Cormen, *Introduction to algorithms*. MIT press, 2009.

[71] N. Keskin and A. Zeevi, "Dynamic pricing with an unknown demand model: Asymptotically optimal semi-myopic policies," *Operations Research*, vol. 62, no. 5, pp. 1142–1167, 2014.

[72] N. Draper, H. Smith, and E. Pownell, *Applied regression analysis*, vol. 3. New York: Wiley, 1966.

[73] C.-J. Winter, R. L. Sizmann, and L. L. Vant-Hull, *Solar power plants: fundamentals, technology, systems, economics*. Springer Science & Business Media, 2012.

[74] H. Heinrichs, "Sharing Economy: A Potential New Pathway to Sustainability," vol. 22, no. 4, pp. 228–231, 2013.

[75] D. Kalathil, C. Wu, K. Poolla, and P. Varaiya, "The Sharing Economy for the Electricity Storage," vol. PP, no. 99, pp. 1–1, 2017.

[76] T. Couture and Y. Gagnon, "An analysis of feed-in tariff remuneration models: Implications for renewable energy investment," *Energy policy*, vol. 28, no. 9, pp. 955–965, 2010.

[77] R. Wustenhagen and E. Menichetti, "Strategic choices for renewable energy investment: Conceptual framework and opportunities for further research," *Energy policy*, vol. 31, no. 40, pp. 1–0, 2012.

[78] S. Fleten, K. Maribu, and I. Wangensteen, "Optimal investment strategies in decentralized renewable power generation under uncertainty," *Energy*, vol. 32, no. 5, pp. 803–815, 2007.

[79] P. Menanteau, D. Finon, and M. Lamy, "Prices versus quantities: choosing policies for promoting the development of renewable energy," *Energy policy*, vol. 31, no. 8, pp. 799–812, 2003.

[80] L. Hirth, "The market value of variable renewables: The effect of solar wind power variability on their relative price," *Energy economics*, vol. 31, no. 38, pp. 218–236, 2013.

[81] A. Negash and D. Kirschen, "Combined optimal retail rate restructuring and value of solar tariff," pp. 1–5, IEEE, IEEE.

[82] W. D. Grossmann, I. Grossmann, and K. W. Steininger, "Distributed solar electricity generation across large geographic areas, part i: A method to optimize site selection, generation and storage," *Renewable and Sustainable Energy Reviews*, vol. 25, pp. 831–843, 2013.

[83] P. Aragonés-Beltrán, F. Chaparro-González, J. Pastor-Ferrando, and F. Rodríguez-Pozo, "An anp-based approach for the selection of photovoltaic solar power plant investment projects," *Renewable and Sustainable Energy Reviews*, vol. 14, no. 1, pp. 249–264, 2010.

[84] P. Cramton, "Electricity market design," *Oxford Review of Economic Policy*, vol. 33, no. 4, pp. 589–612, 2017.

[85] R. Sioshansi, S. Oren, and R. ONeill, "The cost of anarchy in self-commitment based electricity markets," *Competitive Electricity Markets: Design, Implementation and Performance*, pp. 245–266, 2008.

[86] D. Kirschen and G. Strbac, *Fundamentals of Power System Economics: Kirschen/Power System Economics*. John Wiley & Sons, Ltd, 2013.

[87] S. Borenstein and S. P. Holland, "On the efficiency of competitive electricity markets with time-invariant retail prices," tech. rep., National Bureau of Economic Research, 2003.

[88] C. Claude, C. Anna, N. Fabra, J. c. Rochet, and E. B. De Villemeur, "Capacity competition in electricity markets," 2006.

[89] D. Acemoglu, K. Bimpikis, and A. Ozdaglar, "Price and capacity competition," *Games and Economic Behavior*, vol. 66, no. 1, pp. 1–26, 2009.

[90] F. Wu, F. Zheng, and F. Wen, "Transmission investment and expansion planning in a restructured electricity market," *Energy*, vol. 31, no. 6, pp. 954 – 966, 2006. Electricity Market Reform and Deregulation.

[91] J. Taylor and J. Mathieu, "Strategic bidding in electricity markets with only renewables," in *American Control Conference (ACC)*, pp. 5885–5890, IEEE, 2016.

[92] J. Taylor, J. Mathieu, D. Callaway, and K. Poolla, "Price and capacity competition in balancing markets with energy storage," vol. 8, no. 1, pp. 169–197, 2017.

[93] S. S. Reynolds, "Capacity investment, preemption and commitment in an infinite horizon model," *International Economic Review*, pp. 69–88, 1987.

[94] H. T. Smit and L. Trigeorgis, *Strategic investment: Real options and games*. Princeton University Press, 2012.

[95] M. Goyal and S. Netessine, "Strategic technology choice and capacity investment under demand uncertainty," *Management Science*, vol. 53, no. 2, pp. 192–207, 2007.

[96] M.-Á. de Frutos and N. Fabra, "Endogenous capacities and price competition: The role of demand uncertainty," *International Journal of Industrial Organization*, vol. 29, no. 4, pp. 399–411, 2011.

[97] O. Langniss and R. Wiser, "The renewables portfolio standard in texas: an early assessment," *Energy policy*, vol. 31, no. 6, pp. 527–535, 2003.

[98] B. Zhang, R. Johari, and R. Rajagopal, "Competition and efficiency of coalitions in cournot games with uncertainty," 2015. arXiv:1503.02479.

[99] R. Johari, G. Y. Weintraub, and B. Van Roy, "Investment and market structure in industries with congestion," *Operations Research*, vol. 58, no. 5, pp. 1303–1317, 2010.

[100] A. Ozdaglar and I. Menache, *Network Games: Theory, Models, and Dynamics*. Morgan & Claypool Publishers, 2011.

[101] F. Katiraei and M. R. Iravani, "Power management strategies for a microgrid with multiple distributed generation units," *IEEE transactions on power systems*, vol. 21, no. 4, pp. 1821–1831, 2006.

[102] P. Li., S. Sekar, and B. Zhang., "A capacity-price game for uncertain renewables resources," in *ninth ACM International Conference on Future Energy Systems (ACM e-Energy)*, ACM, 2018.

[103] M. Taylor, K. Daniel, A. Ilas, and E. Y. So, "Renewable power generation costs in 2014," *International Renewable Energy Agency*, 2015.

[104] G. L. Barbose, N. R. Darghouth, D. Millstein, K. LaCommare, N. DiSanti, and R. Widiss, "Tracking the sun 10: The installed price of residential and non-residential photovoltaic systems in the united states," 2017.

[105] R. Margolis, D. Feldman, and D. Boff, "Q4 2016/q1 2017 solar industry update," tech. rep., NREL (National Renewable Energy Laboratory (NREL), Golden, CO (United States)), 2017.

[106] National Renewable Energy Laboratory, "Solar power data for integration studies." `https://www.nrel.gov/grid/solar-power-data.html`, 2018.

[107] D. Wang, X. Guan, J. Wu, P. Li, P. Zan, and H. Xu, "Integrated energy exchange scheduling for multimicrogrid system with electric vehicles," *IEEE Transactions on Smart Grid*, no. 4, pp. 1762–1774, 2013.

[108] K. Turitsyn, P. Sulc, S. Backhaus, and M. Chertkov, "Options for control of reactive power by distributed photovoltaic generators," in *Proceedings of the IEEE*, vol. 99, pp. 1063–1073, IEEE, 2011.

[109] B. A. Robbins, C. N. Hadjicostis, and A. D. Domnguez-Garca, "A two-stage distributed architecture for voltage control in power distribution systems," *IEEE Transactions on Power Systems*, vol. 28, pp. 1470–1482, May 2013.

[110] H. Zhang and P. Li, "Chance constrained programming for optimal power flow under uncertainty," *IEEE Transactions on Power Systems*, no. 4, pp. 2417–2424, 2011.

[111] H. Wu, M. Shahidehpour, Z. Li, and W. Tian, "Chance-constrained day-ahead scheduling in stochastic power system operation," *IEEE Transactions on Power Systems*, no. 4, pp. 1583–1591, 2014.

[112] G. Martinez, Y. Zhang, and G. Giannakis, "An efficient primal-dual approach to chance-constrained economic dispatch," in *IEEE North American Power Symposium*, pp. 1–6, 2014.

[113] Y. Wang, Y. Liu, and D. Kirschen, "Scenario reduction with submodular optimization," *IEEE Transactions on Power Systems*, no. 3, pp. 2479–2480, 2017.

[114] M. Lubin, Y. Dvorkin, and S. Backhaus, "A robust approach to chance constrained optimal power flow with renewable generation," *IEEE Transactions on Power Systems*, no. 5, pp. 3840–3849, 2016.

[115] M. Baran and F. Wu, "Optimal capacitor placement on radial distribution systems," *IEEE Transactions on Power Delivery*, no. 1, pp. 725–734, 1989.

[116] J. Luedtke and S. Ahmed, "A sample approximation approach for optimization with probabilistic constraints," *SIAM Journal on Optimization*, no. 2, pp. 674–699, 2008.

[117] M. Farivar and S. Low, "Branch flow model: Relaxations and convexification," in *Decision and Control (CDC), 2012 IEEE 51st Annual Conference on*, pp. 3672–3679, IEEE, 2012.

[118] L. Gan, N. Li, U. Topcu, and S. Low, "Branch flow model for radial networks: convex relaxation," in *Decision and Control (CDC), 2012 IEEE 51st Annual Conference on*, IEEE, 2012.

[119] P. Li. and B. Zhang., "Distribution system voltage control under uncertainties," in *Asilomar Conference on Signals, Systems, and Computers*, IEEE, 2017.

[120] V. Kekatos, G. Wang, A. Conejo, and G. Giannakis, "Stochastic reactive power management in microgrids with renewables," *IEEE Transactions on Power Systems*, no. 6, pp. 3386–3395, 2015.

[121] A. Saumard and J. Wellner, "Log-concavity and strong log-concavity: a review," *Statistics surveys*, vol. 8, p. 45, 2014.

[122] L. Bottou, "Large-scale machine learning with stochastic gradient descent," in *Proceedings of COMPSTAT'2010*, pp. 177–186, Springer, 2010.

[123] Y. Ermoliev and A. Gaivoronski, "Stochastic quasigradient methods," *SIAG/OPT Views-and-News*, pp. 7–10, 1994.

[124] P. Hsu and H. Robbins, "Complete convergence and the law of large numbers," in *Proceedings of the national academy of sciences*, no. 2, pp. 1762–1774, 1947.

[125] Y. Ermoliev, "Stochastic quasigradient methods. numerical techniques for stochastic optimization," *Springer Series in Computational Mathematics*, no. 10, pp. 141–185, 1988.

[126] M. An, "Log-concave probability distributions: Theory and statistical testing," 1996.

[127] GUROBI, 2017.

[128] W. Kersting, "Radial distribution test feeders," *IEEE Transactions on Power Systems*, no. 3, pp. 975–985, 1991.

[129] H. Seltman, "Approximations for mean and variance of a ratio." unpublished note, 2012.

[130] E. random variables, "Exchangeable random variables — Wikipedia, the free encyclopedia," 2018. [Online; accessed 15-January-2018].

[131] Y. Fang, K. Loparo, and X. Feng, "Inequalities for the trace of matrix product," *IEEE Transactions on Automatic Control*, no. 12, pp. 2489–2490, 1994.

[132] A. Prkopa, "Stochastic programming," *Springer Science and Business Media*, 2013.

[133] J. Luedtke, S. Ahmed, and G. Nemhauser, "An integer programming approach for linear programs with probabilistic constraints," *Mathematical programming*, vol. 122, no. 2, pp. 247–272, 2010.

# Appendix A

# NOMENCLATURE

## *A.1 Chapter 2 and Chapter 3*

| | |
|---|---|
| $N$ | Total number of samples. |
| $i$ | Index of samples, $i = 1, 2, \ldots, N$. |
| $S$ | Index set, {1, 2, . . . , N}. |
| $y_i(\mathbf{Y})$ | Energy consumption (vector form). |
| $x_i$ | Binary DR signal (treatment signal). |
| $\mathbf{z}_i(\mathbf{Z})$ | Covariates of sample $i$ (matrix form). |
| $d$ | Dimension of the covariate. |
| $g(\mathbf{z}_i)$ or $g_i$ | Treatment effect of DR signal. |
| $\bar{g} = \frac{1}{N}\sum_i g_i$, or $\beta$ | Average treatment effect (ATE): the average change in consumption because of demand response signals. |
| $f(\mathbf{z}_i)$ or $f_i$ | Baseline consumption (without DR) of sample $i$. |
| $p$ | Treatment probability ($\frac{1}{N}\sum_i T_i$). |
| $\boldsymbol{\beta}^\dagger$ | Weights of a linear regression. |
| $\beta$ | Weight of interest in the linear regression. |

| | |
|---|---|
| $\tilde{\boldsymbol{z}}_i$ | Regressor of a linear regression. |
| $\epsilon_i$ | Noise in sample $i$. |
| $\mathbf{v}_i = (T_i - p)\mathbf{x}_i$ | Modified covariate for sample $i$. |
| $\mu = \frac{\sum_i x_i}{N}$ | Empirical mean of covariates. |
| $\boldsymbol{Z}$ | Regressor matrix composed of covariates. |

## *A.2 Chapter 4*

| | |
|---|---|
| $i$ | Index of users, $i = 1, 2, \ldots, N$. |
| $t$ | Index of time periods, $\{1, 2, \ldots, T\}$. |
| $\lambda_t$ | Price (DR signal) at time $t$. |
| $\theta$ | Unit price of a standardized size of demand reduction. |
| $y_i^t$ | User $i$'s response at time t. |
| $\beta_i, \alpha_i$ | Parameters in user's utility function. |
| $Y$ | Capacity decision for DR program. |
| $R$ | Regret of an online algorithm. |
| $R_t$ | Instataneous regret at time $t$ of an online algorithm. |
| $d_t$ | DR target at time $t$. |
| $D_t$ | Users' aggregated response at time $t$. |

### *A.3 Chapter 5*

| | |
|---|---|
| $U_i$ | Random variable representing the output of producer $i$, scaled between 0 and 1. The moments of $Z_i$ are denoted as $\mathbb{E}\, Z_i = \mu_i$, $\mathbb{E}(Z_i - \mathbb{E}\, Z_i)^2 = \sigma_i^2$ and $\mathbb{E}\,\lvert Z_i - \mathbb{E}\, Z_i\rvert^3 = \rho_i$. |
| $C_i$ | Capacity of producer $i$. |
| $D$ | Total electricity demand in the market |
| $N$ | Number of producers in the market. |
| $\gamma_i$ | Investment cost for unit capacity for producer $i$. |
| $\xi$ | Efficiency of the game equilibrium. |
| $\boldsymbol{x}_{-i}$ | The quantities chosen by all other producers except $i$, that is $\boldsymbol{x}_{-i} = [x_1, \ldots, x_{i-1}, x_{i+1}, \ldots, x_N]$. |
| $(x)^+ \coloneqq \max(x, 0)$ | Max truncation at zero |
| $(x)^- \coloneqq \min(x, 0)$ | Min truncation at zero |

### *A.4 Chapter 6*

| | |
|---|---|
| $N$ | Number of buses in the distribution system. |
| $P_{ik}, Q_{ik}$ | Real/Reactive power on segment $(i, k)$. |
| $V_i, P_i, Q_i$ | Voltage, real power and reactive power at bus $i$. |
| $\boldsymbol{V}, \boldsymbol{P}, \boldsymbol{Q}$ | Voltage, real and reactive power at all buses written in vector form. |
| $\boldsymbol{R}, \boldsymbol{X}$ | Matrices composed of resistence and reactance of the system. |

| | |
|---|---|
| $\boldsymbol{\epsilon}$ | Noise at all buses written in vector form. |
| $\alpha, \eta$ | Desired probability of the system. |
| $\overline{V}_i, \underline{V}_i$ | Bounds on voltage at bus $i$. |
| $L(\boldsymbol{Q})$ | Lagrangian function of $\boldsymbol{Q}$. |
| $\upsilon_m$ | Stepsize of gradient descent at step $m$. |
| $\psi(\boldsymbol{Q})$ | Probability of voltage stays within bounds, given $\boldsymbol{Q}$. |
| $\mathcal{S}$ | Index set of samples for $\boldsymbol{\epsilon}$. |
| $\hat{\psi}(\boldsymbol{Q}, \{\epsilon^{(s)}, \forall s \in \mathcal{S}\})$ | Approximation of $\psi(\boldsymbol{Q})$ based on samples. |
| $\hat{\nabla}\psi(\boldsymbol{Q}, \{\epsilon^{(s)}, \forall s \in \mathcal{S}\})$ | Approximation of $\nabla\psi(\boldsymbol{Q})$ based on samples. |
| $\hat{\nabla}L(\boldsymbol{Q}, \{\epsilon^{(s)}, \forall s \in \mathcal{S}\})$ | Approximation of $\nabla L(\boldsymbol{Q})$ based on samples. |

# Appendix B

# SOME PROOFS AND DISCUSSIONS

## *B.1 Proof of Lemma 5*

Before proving Lemma 5, let us first introduce Lemma 8 that bounds the values of the diagonals of $P_{z^\perp}$.

**Lemma 8.** *The diagonals of $P_{z^\perp}$ is non negative.*

*Proof of Lemma 8.* Recall that $\boldsymbol{P_{z^\perp}} = \boldsymbol{I} - \boldsymbol{Z}(\boldsymbol{Z}^{\mathrm{T}}\boldsymbol{Z})^{-1}\boldsymbol{Z}^{\mathrm{T}}$, and $\boldsymbol{Z}(\boldsymbol{Z}^{\mathrm{T}}\boldsymbol{Z})^{-1}\boldsymbol{Z}^{\mathrm{T}}$ is a projection matrix, then we have the following:

$$(\boldsymbol{Z}(\boldsymbol{Z}^{\mathrm{T}}\boldsymbol{Z})^{-1}\boldsymbol{Z}^{\mathrm{T}})^2 = \boldsymbol{Z}(\boldsymbol{Z}^{\mathrm{T}}\boldsymbol{Z})^{-1}\boldsymbol{Z}^{\mathrm{T}}. \tag{B.1}$$

Denote the diagonals of the $\boldsymbol{Z}(\boldsymbol{Z}^{\mathrm{T}}\boldsymbol{Z})^{-1}\boldsymbol{Z}^{\mathrm{T}}$ by $v_{ii}$, then we have $v_{ii} = \sum_j v_{ij}^2 = v_{ii}^2 + \sum_{j\neq i} v_{ij}^2$, which implies that $0 \leq v_{ii} \leq 1$. This suggests that the diagonals of $P_{z^\perp}$, denoted by $w_{ii}$, is non-negative. □

*Proof of Lemma 5.* If $|S| \leq k$, then we arbitrarily add vertices to $\tilde{S}$ until it contains exactly $k$ vertices. Since the weight on each edge is non negative and we keep adding more edges into the subgraph induced by $\tilde{S}$, $\xi$ is at least 1 in this case.

Now suppose that $|S| > k$, in this case we need to eliminate vertices from $\tilde{S}$ until it only contains $k$ vertices. Assume that we want to eliminate vertex $i$ from $\tilde{S}$, then the total weights induced by $\tilde{S} \setminus \{i\}$ are:

$$w(\tilde{S}) - (\sum_{j\in\tilde{S}, i\neq j} w_{ij} + w_{ii}). \tag{B.2}$$

If each vertex is removed once, then:

$$\begin{aligned}\sum_{i\in\tilde{S}} w(\tilde{S}\setminus\{i\}) &= \sum_{i\in\tilde{S}} w(\tilde{S}) - (\sum_{j\in\tilde{S},i\neq j} w_{ij} + w_{ii}) \\ &= (|\tilde{S}|-2)w(\tilde{S}) + \sum_{i\in\tilde{S}} w_{ii}.\end{aligned} \tag{B.3}$$

The last equality is because each non-self edge is counted twice during the removal (once at the count of each vertex), but self-edge is only counted once.

Similarly, suppose that $v$ is the node that is removed during the swapping procedure, then according to the swapping procedure in Algorithm 3:

$$\sum_{j\in\tilde{S}} w_{vj} \leq \sum_{j\in\tilde{S}} w_{ij}, \forall i \neq v \in \tilde{S}. \tag{B.4}$$

Then:

$$\begin{aligned}w(\tilde{S}\setminus\{v\}) &\geq \frac{1}{|\tilde{S}|}\sum_{i\in\tilde{S}} w(\tilde{S}\setminus\{i\}) \\ &= \frac{1}{|\tilde{S}|}((|\tilde{S}|-2)w(\tilde{S}) + \sum_{i\in\tilde{S}} w_{ii}) \\ &= \frac{|\tilde{S}|-2}{|\tilde{S}|}w(\tilde{S}) + \frac{\sum_{i\in\tilde{S}} w_{ii}}{|\tilde{S}|} \\ &\geq \frac{|\tilde{S}|-2}{|\tilde{S}|}w(\tilde{S}).\end{aligned} \tag{B.5}$$

The last inequality follows because $w_{ii}$'s are non-negative, which is proved in Lemma 8.

Finally by induction, we obtain the eventual $\tilde{S}$ containing $k$ vertices satisfying:

$$w(\tilde{S}) \geq \frac{k(k-1)}{|S|(|S|-1)}w(S), \tag{B.6}$$

which concludes the final proof. □

### *B.2 Preliminaries for proving Theorems 4 and 5*

Note that Theorem 5 directly implies Theorem 4 since it directly characterizes the performance of the online learning algorithm. We separate the proof of Theorem 5 into two steps, where we first show it for the case $\alpha_i = 0$ for every $i$, then for the case of general $\alpha_i$'s.

Before proving Theorem 5, we need to introduce a few definitions that help the proof. We use asymptotic bounds to analyze the interactions between quantities in the following analysis, since many random quantities are involved and an exact inference may not be possible. The asymptotic bound notation that we use in this dissertation is $\Theta(\cdot)$ and $O(\cdot)$ as defined in Section 4.4. These bounds quantify the orders of the terms involved in computation and ignore constant factors, which simplify computation.

In addition, we derive some useful operations for these notations.

**Remark 2.** *If for some positive functions* $f_1(n)$, $g_1(n)$, $f_2(n)$,$g_2(n)$, $f_1(n) = \Theta(g_1(n))$ *and* $f_2(n) = \Theta(g_2(n))$ *with same* $n_0$, *then* $\frac{f_1(n)}{f_2(n)} = \Theta(\frac{g_1(n)}{g_2(n)})$. *In addition,* $f_1(n)^2 = \Theta(g_(n)^2)$ *and* $f_1(n)f_2(n) = \Theta(g_1(n)g_2(n))$.

Using the asymptotic bound notation we greatly simplify the comparison between different quantities in each of the equations presented earlier. For example, we can write $\hat{\gamma}_1^t$ as a result from least square estimation in the linear regression model presented in (4.16), where $\alpha_i = 0$: $\hat{\gamma}_1^t = \frac{\sum_{s=0}^{t-1}(\sum_i y_i^s)N\lambda_s}{\sum_{s=0}^{t-1} N^2\lambda_s^2}$. Its variance is expressed as: $\text{Var}(\hat{\gamma}_1^t) = \frac{N}{\sum_{s=0}^{t-1} N^2\lambda_s^2}$.

If we know the order of $\lambda_t$ in terms of $\Theta(\cdot)$, etc., then the order of the estimator and its variance can be obtained, which helps to determine the order of the regret $R$.

**Remark 3.** *We assume that* $d_t$ *is bounded away from zero. What is more, assume that* $\alpha_i$ *and* $\beta_i$ *are also bounded away from zero and take some finite values. Along with* (4.11), (4.13) *and assume that the revenue* $\theta$ *is bounded below from zero, we obtain that* $Y^* = \Theta(N)$, *which leads to the fact that* $\lambda_t = \Theta(\frac{1}{N})$ *with high probability.*

*B.2.1 Proof of Theorem 5 with $\alpha_i = 0$*

*Proof.* With Remark 3, we obtain the least square estimator for $\gamma_1$ at time $t$ as the following:

$$\begin{aligned}
\mathrm{Var}(\hat{\gamma}_1^t) &= \frac{N}{\sum_{s=0}^{t-1} N^2 \lambda_s^2} \\
&= \frac{1}{N} \frac{1}{\sum_{s=0}^{t-1} \lambda_s^2} \\
&\overset{(a)}{=} \frac{1}{N} \frac{1}{\lambda_0^2 + (t-1)\left[\Theta\left(\frac{(Y^*)}{N^2}\right)\right]^2} \\
&\overset{(b)}{=} \frac{1}{N} \frac{1}{\lambda_0^2 + (t-1)\Theta\left(\frac{(Y^*)^2}{N^4}\right)} \\
&\overset{(c)}{=} \Theta\left(\frac{N^3}{t(Y^*)^2}\right) \\
&\overset{(d)}{=} \Theta\left(\frac{N}{t}\right),
\end{aligned} \tag{B.7}$$

where (a) follows from the fact that since $\sum_i \frac{1}{\beta_i} = \Theta(N)$ then from (4.12) we know that $\lambda_s = \Theta(\frac{Y}{N^2})$. Equality (b) follows from Remark 2 and (c) is the direct result from further simplification using $\Theta$ notation. Finally (d) comes from the fact that $Y^* = \Theta(N)$.

Using the same simplification from asymptotic bounds and based on the result in (B.7) , we can rewrite the gap $R_t$ in (4.7) as

$$\begin{aligned}
R_t =& C_1 \left[\mathbb{E}\,\lambda_t^2 - (\mathbb{E}\,\lambda_t)^2 + (\mathbb{E}\,\lambda_t - \lambda_t^*)^2\right] \\
\overset{(a)}{=}& C_1 \left[\mathrm{Var}\left(\frac{Y^* d_t}{N\hat{\gamma}_1^t + N}\right)\right. \\
&\left. + \left(\mathbb{E}\left(\frac{Y^* d_t}{N\hat{\gamma}_1^t + N}\right) - \frac{Y^* d_t}{N(\sum_{i\in\mathcal{N}} \frac{1}{\beta_i}) + N}\right)^2\right] \\
\overset{(b)}{=}& C_1 \left[\frac{(Y^*)^2 d_t^2 N^2\, \mathrm{Var}\,\hat{\gamma}_1^t}{(N\sum_{i\in\mathcal{N}} \frac{1}{\beta_i} + N)^4} + \frac{(Y^*)^2 d_t^2 N^4 (\mathrm{Var}\,\hat{\gamma}_1^t)^2}{(N\sum_{i\in\mathcal{N}} \frac{1}{\beta_i} t + N)^3}\right] \\
\overset{(c)}{=}& C_1 \left[\frac{(Y^*)^2 d_t^2 N^2\, \mathrm{Var}\,\hat{\gamma}_1^t}{\Theta(N^8)} + \frac{(Y^*)^2 d_t^2 N^4 (\mathrm{Var}\,\hat{\gamma}_1^t)^2}{\Theta(N^{12})}\right] \\
\overset{(d)}{=}& C_1 \left[\Theta(\frac{1}{tN^3}) + \Theta(\frac{1}{Y^2 N^2 t^2})\right],
\end{aligned} \tag{B.8}$$

where (a) follows according to the result in (4.12), (b) follows from the second order approximation of the expectation of an inverse random variable [129]. Then using Remark 3 and Remark 2, we arrive at equality (c) and (d).

Given that $Y^* = \Theta(N)$ and $C_1 = (\frac{N}{2}\sum_{i=1}^{N}\frac{1}{\beta_i}) + \frac{N}{2}(\sum_{i=1}^{N}\frac{1}{\beta_i})^2 = \Theta(N^3)$, we have

$$\begin{aligned} R_t =& \Theta(N^3)\left[\Theta(\frac{1}{tN^3}) + \Theta(\frac{1}{Y^2N^2t^2})\right] \\ =& \Theta(\frac{1}{t} + \frac{1}{Nt^2}). \end{aligned} \tag{B.9}$$

Since $\frac{1}{Nt^2} = O(\frac{1}{t})$, $R_t = \Theta(\frac{1}{t})$. This indicates that the gap $R_t$ forms a harmonic series with respect to time, which means that the cumulative regret $R = \sum_t R_t$ is $\Theta(\log T)$. This also implies that $R = O(\log T)$. □

### *B.3 Proof of Theorem 5 with* $\alpha_i \neq 0$

*Proof.* First write the linear regression model in (4.16) in a more compact form as:

$$Y_t^\dagger = \begin{bmatrix}\gamma_1 & \gamma_0\end{bmatrix}\begin{bmatrix}N\lambda_t \\ 1\end{bmatrix} + \sum_{i\in\mathcal{N}}\epsilon_i^t, \tag{B.10}$$

where $Y_t^\dagger \triangleq \sum_i \hat{y}_i^t$, $\gamma_1 = \sum_i \frac{1}{\beta_i}$, $\gamma_0 = -\sum_i \frac{\alpha_i}{\beta_i}$. The white noise in the model is $\sum_i \epsilon_i^t \sim \mathcal{N}(0,\sigma^2)$ and $\sigma^2 = N$.

The estimator at time $t$ is obtained from least squares in the following form:

$$\begin{bmatrix}\hat{\gamma}_1 \\ \hat{\gamma}_0\end{bmatrix} = (\mathbf{X}^\top\mathbf{X})^{-1}\mathbf{X}^\top\mathbf{Y}^\dagger, \tag{B.11}$$

where $\mathbf{X} = \begin{bmatrix}N\boldsymbol{\lambda}_t & \mathbf{1}\end{bmatrix}$, $\boldsymbol{\lambda}_t = [\lambda_1, \lambda_2, \ldots, \lambda_t]^\top$ is a column vector and $\mathbf{1}$ is an all one column vector, $\mathbf{Y}^\dagger = [Y_1^\dagger, Y_2^\dagger, ..., Y_t^\dagger]^\top$.

We calculate

$$\begin{aligned}
\operatorname{Var}\begin{bmatrix}\hat{\gamma}_1^t\\ \hat{\gamma}_0^t\end{bmatrix} &= \begin{bmatrix}\operatorname{Var}\hat{\gamma}_1^t & \operatorname{Cov}(\hat{\gamma}_1^t,\hat{\gamma}_0^t)\\ \operatorname{Cov}(\hat{\gamma}_0^t,\hat{\gamma}_1^t) & \operatorname{Var}\hat{\gamma}_0^t\end{bmatrix}\\
&= \left(\mathbf{X}^\top\mathbf{X}\right)^{-1}\sigma^2\\
&= \left(\begin{bmatrix}N\boldsymbol{\lambda}_t^\top\\ \mathbf{1}^\top\end{bmatrix}\begin{bmatrix}N\boldsymbol{\lambda}_t & \mathbf{1}\end{bmatrix}\right)^{-1}\sigma^2\\
&= \begin{bmatrix}N\boldsymbol{\lambda}_t^\top N\boldsymbol{\lambda}_t & N\boldsymbol{\lambda}_t^\top\mathbf{1}\\ \mathbf{1}^\top N\boldsymbol{\lambda}_t & \mathbf{1}^\top\mathbf{1}\end{bmatrix}^{-1}\sigma^2\\
&\overset{(a)}{=} \frac{N}{t\sum_s(N\lambda_s)^2-(\sum_s N\lambda_s)^2}\\
&\quad\cdot\begin{bmatrix}t & -\sum_s N\lambda_s\\ -\sum_s N\lambda_s & \sum_s(N\lambda_s)^2\end{bmatrix},
\end{aligned} \tag{B.12}$$

where equality (a) follows from the matrix inversion and that $\sigma^2 = N$.

Since we argue that $\lambda_t$'s are not the same across different $t$ (given that $d_t$'s are not the same across time), we obtain that $t\sum_s(N\lambda_s)^2 - (\sum_s N\lambda_s)^2$ is bounded below from 0, which validates the least squares estimator from linear regression. What is more, since each $\lambda_t = \Theta(\frac{1}{N})$ according to (4.11) and (4.12), we know that $t\sum_s(N\lambda_s)^2 - (\sum_s N\lambda_s)^2 = \Theta(\frac{1}{t^2})$. Plug this result back in (B.12), we obtain that the estimators at any time $t$ have the following asymptotic bounds on their variances and covariance:

$$\operatorname{Var}\hat{\gamma}_1^t, \operatorname{Var}\hat{\gamma}_0^t, \operatorname{Cov}(\hat{\gamma}_1^t,\hat{\gamma}_0^t) = \Theta(\frac{N}{t}). \tag{B.13}$$

Therefore, the bias of $\lambda_t$ is calculated as:

$$\begin{aligned}
\text{bias}\lambda_t =& \mathbb{E}\,\lambda_t - \lambda_t \\
=& \mathbb{E}\left(\frac{Y^* d_t + \hat{\gamma}_0^t}{N\hat{\gamma}_1^t + N}\right) - \frac{Y^* d_t + \gamma_0}{N\gamma_1 + N} \\
\overset{(a)}{=}& -\frac{\text{Cov}(\hat{\gamma}_0, N\hat{\gamma}_1^t)}{\left(\mathbb{E}(N\hat{\gamma}_1^t + N)\right)^2} + \frac{\text{Var}(N\hat{\gamma}_1^t)\,\mathbb{E}(Y^* d_t + \hat{\gamma}_0^t)}{(N\gamma_1 + N)^3} \\
\overset{(b)}{=}& \Theta(\frac{N \cdot \frac{N}{t}}{N^4}) + \Theta(\frac{N^2 \cdot \frac{N}{t} \cdot N}{N^6}) \\
=& \Theta(\frac{1}{N^2 t}),
\end{aligned} \tag{B.14}$$

where equality (a) comes from second order approximation of the expectation of a ratio between two random variables as in [129] and equality (b) follows from Remark 3 and Remark 2.

Using the same analysis as when $\alpha_i = 0$, and based on (B.13) and (B.14), we obtain the gap $R_t$ as:

$$\begin{aligned}
R_t =& \frac{N}{2}\left(\sum_{i=1}^{N}\frac{1}{\beta_i} + (\sum_{i=1}^{N}\frac{1}{\beta_i})^2\right)\left[\mathbb{E}\,\lambda_t^2 - (\mathbb{E}\,\lambda_t)^2 + (\mathbb{E}\,\lambda_t - \lambda_t^*)^2\right] \\
&+ \sum_{i=1}^{N}\frac{\alpha_i}{\beta_i}\left(\sum_{i=1}^{N}\frac{1}{\beta_i} - 1\right)(\mathbb{E}\,\lambda_t - \lambda_t^*) \\
=& \Theta(N^3)\{\Theta(\frac{1}{tN^3}) + \Theta(\frac{1}{(Y^*)^2 N^2 t^2})\} + \Theta(N^2)\Theta(\frac{1}{N^2 t}) \\
=& \Theta(\frac{1}{t}),
\end{aligned} \tag{B.15}$$

which means that the cumulative regret $R = \sum_t R_t$ is again $\Theta(\log T)$. □

### *B.4 Proof for Proposition 3*

We know that the producers adopt a mixed pricing strategy in the equilibrium for the pricing sub-game. Let $l_i, u_i$ denote the lower and upper support of the distribution corresponding to the mixed strategy of producer $i$. From previous results [89, 91] and assumption A2, we know that $l_i = l_j$ and $u_i = u_j = 1$ for all $i, j$. Therefore, let $p$ denote the common lower support (price) for every producer— it is known that no producer has an atom at the lower

support. Using the basic properties of mixed strategy equilibria (e.g., see [89]), we can infer that the total payment received by any producer $i$ equals its payment when this producer bids a deterministic price of $p$ and all of the other producers bid according to their mixed strategies in the pricing sub-game equilibrium. Explicitly writing this out, we get

$$\pi_i(C_1, C_2, \ldots, C_N) = pE[\min(C_i U_i, D)] = pC_i E[\min(U_i, \frac{D}{C_i})] \tag{B.16}$$
$$\pi_N(C_1, C_2, \ldots, C_N) = pE[\min(C_N U_N, D)] = pC_N E[\min(U_i, \frac{D}{C_N})].$$

Indeed, observe that when any one player selects a price of $p$, all of the capacity generated by this player must be sold because no other player can bid below this price and the probability that other players bid exactly at this price can be ignored due to the lack of atoms. Using the second equation above, we can explicitly characterize $p$ in terms of the payment received by the producer with the highest capacity investment, i.e.,

$$p = \frac{\pi_N(C_1, C_2, \ldots, C_N)}{C_N E[\min(U_i, \frac{D}{C_N})]}.$$

Substituting the above into Equation B.16 gives us:

$$\pi_i(C_1, C_2, \ldots, C_N) = \pi_N(C_1, C_2, \ldots, C_N) \frac{C_i E[\min(U_i, \frac{D}{C_i})]}{C_N E[\min(U_N, \frac{D}{C_N})]}.$$

□

### *B.5 Proof for Theorem 6*

Suppose that at the optimum solution that minimizes Equation (5.5), the aggregate capacity investment by the producers is $C^*_{tot}$, and let $C^*_1 = C^*_2 = \ldots = C^*_N = \frac{C^*_{tot}}{N} \geq 0$. Then, in order to prove Theorem (6), it is sufficient to show that for any capacity $C_1, C_2, \ldots, C_N \geq 0$ with $\sum_{i=1}^{N} C_i = C^*_{tot}$, the following equation is satisfied:

$$\mathbb{E}[(D - \sum_{i=1}^{N} U_i C^*_i)^+] \leq \mathbb{E}[(D - \sum_{i=1}^{N} U_i C_i)^+].$$

In fact, using the transformation that for any capacity vector $(C'_1, \ldots, C'_N)$, $\mathbb{E}[(D - \sum_{i=1}^{N} U_i C'_i)^+] = D - E[\min(D, \sum_{i=1}^{N} U_i C'_i)]$, the above equation can be rewritten as:

$$\mathbb{E}[\min(D, \sum_{i=1}^{N} U_i C^*_i)] \geq \mathbb{E}[\min(D, \sum_{i=1}^{N} U_i C_i)]. \tag{B.17}$$

So, to prove Theorem 6, it is indeed sufficient to prove Equation (B.17). To prove this, we introduce Proposition 4 and Proposition 5.

**Proposition 4.** *Let us consider the following definitions:*

- $X_1 \coloneqq U_1 \frac{C_1}{N} + U_2 \frac{C_2}{N} + \ldots + U_N \frac{C_N}{N}$,
- $X_2 \coloneqq U_1 \frac{C_2}{N} + U_2 \frac{C_3}{N} + \ldots + U_N \frac{C_1}{N}$
- $\ldots$
- $X_N \coloneqq U_1 \frac{C_N}{N} + U_2 \frac{C_1}{N} + \ldots + U_N \frac{C_{N-1}}{N}$

*That is:*

$$X_i = \sum_{j=1}^{N} U_j \frac{C_{i+j-1}}{N}, \tag{B.18}$$

*where $i + j - 1$ is computed modulo $N$.*

*Then:*

$$\mathbb{E}[\min(D, \sum_{i=1}^{N} X_i)] \geq \sum_{i=1}^{N} \mathbb{E}[\min(\frac{D}{N}, X_i)]. \tag{B.19}$$

*Proof.* We prove the inequality by proving that inequality holds for each realization of $X_1 = x_1, X_2 = x_2, \ldots, X_N = x_N$. Denote the whole index set by $\mathcal{N}$. In each realization, there are the following four scenarios:

- Each of $x_i$ is smaller than $\frac{D}{N}$. In this case, $\min(D, \sum_{i=1}^{N} x_i) = \sum_{i=1}^{N} x_i$, and $\min(\frac{D}{N}, x_i) = x_i$. So equality holds.
- Each of $x_i$ is bigger than $\frac{D}{N}$. In this case, $\min(D, \sum_{i=1}^{N} x_i) = D$, and $\min(\frac{D}{N}, x_i) = \frac{D}{N}$. So equality again holds.

- $x_j, j \in \mathcal{J} \subseteq \mathcal{N}$ is bigger than $\frac{D}{N}$, the rest are smaller than $\frac{D}{N}$, but $\sum_{i=1}^{N} x_i \leq D$. In this case, $\min(D, \sum_{i=1}^{N} x_i) = \sum_{i=1}^{N} x_i$. The RHS of (B.19) reduces to $\frac{D}{N}|\mathcal{J}| + \sum_{i \in \mathcal{N} \setminus \mathcal{J}} x_i \leq \sum_{i=1}^{N} x_i$. Therefore, the inequality holds.

- $x_j, j \in \mathcal{J} \subseteq \mathcal{N}$ is smaller than $\frac{D}{N}$, the rest are bigger than $\frac{D}{N}$, but $\sum_{i=1}^{N} x_i \geq D$. The RHS of (B.19) reduces to $\frac{D}{N}(N - |\mathcal{J}|) + \sum_{j \in \mathcal{J}} x_j \leq D$. Therefore, the inequality holds.

In all cases, we have that:

$$\mathbb{E}[\min(D, \sum_{i=1}^{N} X_i)] \geq \sum_{i=1}^{N} \mathbb{E}[\min(\frac{D}{N}, X_i)]. \tag{B.20}$$

□

**Proposition 5.** *With the assumptions in Proposition 4, we have:*

$$\mathbb{E}[\min(\frac{D}{N}, X_i)] = \mathbb{E}[\min(\frac{D}{N}, X_1)], \forall i \in \mathcal{N}. \tag{B.21}$$

To prove Proposition 5, we introduce Fact 1. It is based on exchangeability of independent random variables, and that $U_i$'s' are i.i.d. copies. We refer to [130] for interested users and omit the proof here.

**Fact 1.** *If $U_i$'s are i.i.d. random variables, then:*

$$f(u_1, u_2, \ldots, u_N) = f(u_{S_1}, u_{S_2}, \ldots, u_{S_N}), \tag{B.22}$$

*where $S_1, S_2, \ldots, S_N$ is a permutation of $1, 2, \ldots, S_N$, and $f(\cdot)$ is the density function.*

Now we proceed to prove Proposition 5.

*Proof of Proposition 5.* Using Fact 1, we show that $\mathbb{E}[\min(\frac{D}{N}, X_i)]$ is the same for all $i$:

$$\begin{aligned}
\mathbb{E}[\min(D/N, X_i)] &= \mathbb{E}[\min(D/N, \sum_{j=1}^{N} U_j \frac{C_{i+j-1}}{N})] \\
&\overset{(a)}{=} \mathbb{E}[\min(D/N, \sum_{j=1}^{N} U_{i+j-1} \frac{C_{i+j-1}}{N})] \\
&\overset{(b)}{=} \mathbb{E}[\min(D/N, \sum_{k=1}^{N} U_k \frac{C_k}{N})] \\
&= \mathbb{E}[\min(D/N, X_1)],
\end{aligned} \tag{B.23}$$

where $(a)$ is based on the observation that $[i, i+1, \ldots, i+N-1], \mod N, \forall i$ is a permutation of $[1, 2, \ldots, N]$, and $(b)$ is the result of rearranging $C_{i+j-1}$. □

Now, we are ready to prove (B.17). Let $(X_i)_{i=1}^N$ be as defined in the statement of Proposition 4. The LHS of (B.17) can be written as:

$$\begin{aligned}
\mathbb{E}[\min(D, \sum_{i=1}^{N} U_i C_i^*)] &= \mathbb{E}[\min(D, \sum_i U_i C_{tot}^*/N)] \\
&= \mathbb{E}[\min(D, \sum_i U_i \frac{\sum_i C_i}{N})] \\
&= \mathbb{E}[\min(D, \sum_i U_i X_i)] \\
&\overset{(a)}{\geq} \sum_{i=1}^{N} \mathbb{E}[\min(\frac{D}{N}, X_i)] \\
&\overset{(a)}{=} \sum_{i=1}^{N} \mathbb{E}[\min(\frac{D}{N}, X_1)] \\
&= N\,\mathbb{E}[\min(\frac{D}{N}, X_1)] \\
&= \mathbb{E}[\min(D, \sum_{i=1}^{N} U_i C_i)],
\end{aligned} \tag{B.24}$$

where $(a)$ is based on Proposition 5 and $(b)$ is based on Proposition 4. This concludes the proof. □

### *B.6 Proof for Theorem 7*

Suppose that there are $N$ producers in the market, and suppose that the optimal capacity from solving (5.5) is denote by $C_1^*, C_2^*, ..., C_N^*$, we argue that $C_1^*, C_2^*, ..., C_N^*$ is a Nash equilibrium for the capacity game in (5.1).

We prove the equilibrium for player 1, and the same argument holds for any of the rest players. To show this, we rewrite $C_1^*$ as the following:

$$\begin{aligned}
C_1^* &= arg\min_{C_1}\ \gamma C_1 + \gamma \sum_{i=2}^{N} C_i^* + \mathbb{E}\{(D - \sum_{i=2}^{N} U_i C_i^* - U_1 C_1\}^+ \\
&= arg\min_{C_1}\ \gamma C_1 + D - \mathbb{E}\min\{D, \sum_{i=2}^{N} U_i C_i^* + U_1 C_1\} \\
&= arg\min_{C_1}\ \gamma C_1 - \mathbb{E}\min\{D - \sum_{i=2}^{N} U_i C_i^*, U_1 C_1\} \\
&= arg\min_{C_1}\ \gamma C_1 - \mathbb{E}\min\{(D - \sum_{i=2}^{N} U_i C_i^*)^+, U_1 C_1\} \\
&\qquad\qquad - \mathbb{E}\min\{(D - \sum_{i=2}^{N} U_i C_i^*)^-, U_1 C_1\} \\
&= arg\min_{C_1}\ \gamma C_1 - \mathbb{E}\min\{(D - \sum_{i=2}^{N} U_i C_i^*)^+, U_1 C_1\} - \mathbb{E}(D - \sum_{i=2}^{N} U_i C_i^*)^- \\
&= arg\max_{C_1}\ \mathbb{E}\min\{(D - \sum_{i=2}^{N} U_i C_i^*)^+, U_1 C_1\} - \gamma C_1 \\
&= C_1^\diamond,
\end{aligned} \tag{B.25}$$

which characterizes the optimal solution to the game depicted in (5.1). □

### *B.7 Proof for Theorem 9*

Similar to the proof for Theorem 6, we need to show that (B.17) is true when $U_i = \bar{U} + \hat{U}_i$ as given in (5.9). The proof boils down to show that Proposition 4 and Proposition 5 are true under such asssumption on correlation. Note that the proof for Proposition 4 does not

require that $U_i$'s to be i.i.d., therefore naturally carries over. To show Proposition 5, we need Lemma 9. Then these two propositions validate (B.17), which concludes the proof.

**Lemma 9.** *If* $U_i = \bar{U} + \hat{U}_i$ *as* (5.9)*, then:*

$$f(u_1, u_2, \ldots, u_N) = f(u_{S_1}, u_{S_2}, \ldots, u_{S_N}),$$

*where* $S_1, S_2, \ldots, S_N$ *is a permutation of* $1, 2, \ldots, S_N$*, and* $f(\cdot)$ *is the density function.*

*Proof.*

$$\begin{aligned}
f(u_1, u_2, \ldots, u_N) &= f(\bar{u} + \hat{u}_1, \bar{u} + \hat{u}_2, \ldots, \bar{u} + \hat{u}_N) \\
&= \int_{\bar{u}} f(\{\bar{u} + \hat{u}_1, \bar{u} + \hat{u}_2, \ldots, \bar{u} + \hat{u}_N\} | \bar{U} = \bar{u}) f(\bar{U} = \bar{u}) d\bar{u} \\
&\overset{(a)}{=} \int_{\bar{u}} f(\bar{u} + \hat{u}_1, \bar{u} + \hat{u}_2, \ldots, \bar{u} + \hat{u}_N) f(\bar{U} = \bar{u}) d\bar{u} \\
&\overset{(b)}{=} \int_{\bar{u}} f(\bar{u} + \hat{u}_{S_1}, \bar{u} + \hat{u}_{S_2}, \ldots, \bar{u} + \hat{u}_{S_N}) f(\bar{U} = \bar{u}) d\bar{u} \\
&= f(u_{S_1}, u_{S_2}, \ldots, u_{S_N}),
\end{aligned}$$

where $(a)$ is based on the assumption that $\bar{U}$ is independent of $\hat{U}_i$ (assumption A3), and $(b)$ is based on Fact 1. □

## *B.8 Proof for Theorems 8 and Theorem 10*

### *B.8.1 Berry-Esseen Theorem*

The following Lemma is useful to facilitate the proofs of Theorem 8 and Theorem 10. It relates the behavior of the mean of independent random variables to a standard Gaussian distribution in terms of CDF.

**Lemma 10** (Berry-Esseen Theorem)**.** *There exists a positive constant* $\alpha$*, such that if* $X_1$*,* $X_2$*,* $\ldots$*,* $X_N$*, are independent random variables with* $\mathbb{E}(X_i) = 0$*,* $\mathbb{E}(X_i^2) = \sigma^2 > 0$*, and* $\mathbb{E}(|X_i|^3) = \rho_i < \infty$*, and if we define* $S_N = \frac{\sum_i X_i}{\sqrt{\sum_i \sigma_i^2}}$*, then* $F_N$*, the cumulative distribution function of*

*$S_N$ is close to $\Phi$, the CDF of the standard Gaussian distribution. This is mathematically interpreted as:*

$$|F_N(x) - \Phi(x)| \leq \alpha\psi, \tag{B.26}$$

*where* $\psi = (\sum_i \sigma_i^2)^{-\frac{1}{2}} \max_{1\leq i\leq N} \frac{\rho_i}{\sigma_i^2}$.

### *B.8.2 Some useful lemmas*

Before the detailed proof, let us visit some useful propositions and lemmas that assist the proofs for Theorem 8 and Theorem 10. In what follows, we assume without loss of generality that given any solution $(C_1, C_2, \ldots, C_N)$, it must be the case that $C_1 \leq C_2 \leq \ldots \leq C_N$.

**Proposition 6.** *The partial derivative of* $\pi_N(\boldsymbol{C}_{-N}, C_N) = \mathbb{E}(\min(D - \sum_{j=1}^{N-1} C_i U_i)^+, C_N)$ *is:*

$$\frac{\partial \pi_N(\boldsymbol{C}_{-N}, C_N)}{\partial C_N} = \mathbb{E}\left[\mathbb{1}\{(D - \sum_{j=1}^{N-1} C_j U_j)^+ \geq C_N U_N\} U_N\right], \tag{B.27}$$

*and for all* $i \neq N$.

$$\frac{\partial \pi_N(\boldsymbol{C}_{-N}, C_N)}{\partial C_i} = \mathbb{E}\left[\mathbb{1}\{0 \leq (D - \sum_{j=1}^{N-1} C_j U_j) \leq C_N U_N\}(-U_i)\right]. \tag{B.28}$$

Based on Proposition 6, we have the following lemma on the optimality of the symmetric Nash equilibrium of the game.

**Lemma 11.** *If the invested capacity is symmetric, i.e.,* $C_1 = C_2 = \cdots = C_N = C$, *then:*

- $\gamma = \mathbb{E}\left[\mathbb{1}\left\{(D - C\sum_{j\neq i}^{N} U_j)^+ \geq CU_i\right\} U_i\right]$, *where* $\mathbb{1}\{\cdot\}$ *is the indicator function and takes value 1 if the argument is true, otherwise takes value 0.*

- $NC \leq D/\gamma$.

*Proof.* We begin by proving the first part. Suppose that capacities are the same, i.e., $C_1 = C_2 = \cdots = C_N = C$, the profits for all producers in the capacity game is:

$$N\,\mathbb{E}\left[\min\left((D - C\sum_{j\neq i}^{N} U_j)^+, CU_j\right)\right] - \gamma CN. \tag{B.29}$$

The optimality of a player $i$ in the game is captured as the following:

$$\frac{\partial}{\partial C_i}\,\mathbb{E}\left[\min\left((D - C\sum_{j\neq i}^{N} U_j)^+, C_i U_i\right)\right] - \gamma = 0. \tag{B.30}$$

Differentiating in the expectation with respect to each individual $C_i$ and based on Proposition 6, we have:

$$\gamma = \mathbb{E}\left[\mathbb{1}\left\{(D - C\sum_{j\neq i}^{N} U_j)^+ \geq CU_i\right\} U_i\right], \tag{B.31}$$

where $\mathbb{1}\{\cdot\}$ is the indicator function and takes value 1 if the argument is true, otherwise takes value 0.

Then we proceed to prove the second part, i.e., $NC \leq D/\gamma$.

When there is a social planner making centralized decision as described in (5.5), the total payment from the electricity consumers in the system is

$$\min_{C_i, \forall i=1,2,\ldots,N} \mathbb{E}\left[(D - \sum_{i=1}^{N} C_i U_i)^+\right] + \gamma \sum_{i=1}^{N} C_i, \tag{B.32}$$

where each site should have the same optimal invested capacity $C_1 = C_2 = \cdots = C_N = C$ as discussed in Section 5.5. This also coincides with the symmetric Nash equilibrium in the capacity game.

To show that $NC$ is a bounded by a constant, assuming differentiability and based on (B.32), we know

$$\gamma N = \mathbb{E}\left[1(D \geq C\sum_{i=1}^{N} U_i)\sum_{i=1}^{N} U_i\right] \tag{B.33}$$

$$= \mathbb{E}\left[1(\sum_{i=1}^{N} U_i \leq D/C)\sum_{i=1}^{N} U_i\right] \tag{B.34}$$

$$\leq \mathbb{E}\left[1(\sum_{i=1}^{N} U_i \leq D/C)D/C\right] \tag{B.35}$$

$$= D/C\,\Pr(\sum_{i=1}^{N} U_i \leq D/C) \tag{B.36}$$

$$\leq D/C, \tag{B.37}$$

rearranging, we get $NC \leq D/\gamma$. □

Based on Lemma 11, we now present two lemmas on arbitrary Nash equilibria of the game in Lemma 12 and Lemma 13.

**Lemma 12.** *Given any equilibrium solution of the two-level game $(C_1^\diamond, C_2^\diamond, \ldots, C_N^\diamond)$, it must be the case that $C_1^\diamond \leq \frac{D}{\gamma N}$ and $C_N^\diamond \leq \frac{D}{\gamma}$.*

*Proof.* Assume by contradiction that the first part of the above statement is not true and there exists an equilibrium solution $(C_1^\diamond, C_2^\diamond, \ldots, C_N^\diamond)$ such that $\frac{D}{\gamma N} < C_1^\diamond \leq \ldots \leq C_N^\diamond$. Recall the formula for the payment received by producer $N$, i.e.,
$\pi_N(C_1^\diamond, C_2^\diamond, \ldots, C_N^\diamond) = E[(D - \sum_{i \neq N} C_i^\diamond U_i)^+, C_N^\diamond U_N)]$. Since this is an equilibrium solution, the derivative of this payment must equal the investment cost $\gamma$. More specifically, using the expression for the derivative that was previously derived in Equation (B.31), we have that

$$\left(\frac{d}{dC}\pi_N(C_1^\diamond, C_2^\diamond, \ldots, C)\right)_{C=C_N^\diamond} = \gamma$$
$$\implies \mathbb{E}\left[\mathbb{1}\left\{(D - \sum_{i \neq N} C_i^\diamond U_i)^+ \geq C_N^\diamond U_N\right\} U_N\right] = \gamma.$$

Now, since the symmetric equilibrium solution $(C^*, \ldots, C^*)$ also satisfies this condition, we have that:

$$\mathbb{E}\left[\mathbb{1}\left\{(D - \sum_{i \neq N} C^* U_i)^+ \geq C^* U_N\right\} U_N\right] = \gamma.$$

Further, recall that in the symmetric equilibrium $C^* \leq \frac{D}{\gamma N}$ as derived in Equation (B.37). Since $C_1^\diamond > \frac{D}{\gamma N}$, this implies that $C_1^\diamond > C^*$. Finally, let $\mathcal{E}$ denote the set of events[1] $\mathbb{1}\left\{(D - \sum_{i \neq N} C_i^\diamond U_i)^+ \geq C_N^\diamond U_N\right\}$ and let $\mathcal{E}^*$ denote the events satisfying $\mathbb{1}\left\{(D - \sum_{i \neq N} C^* U_i)^+ \geq C^* U_N\right\}$. Since $C^* < C_1^\diamond \leq C_2^\diamond \leq \ldots \leq C_N^\diamond$, it is not hard to deduce that $\mathcal{E} \subset \mathcal{E}^*$. Indeed for any (non-zero) instantiation $(U_1, \ldots, U_N)$, we have that $(D - \sum_{i \neq N} C_i^\diamond U_i)^+ < (D - \sum_{i \neq N} C^* U_i)^+$ and $C_N^\diamond U_N > C^* U_N$. Therefore, we get that:

[1]For our purposes, an event is a tuple of instantiations of the i.i.d random variables $(U_1, U_2, \ldots, U_N)$ satisfying the required condition

$$\mathbb{E}\left[\mathbb{1}\left\{(D-\sum_{i\neq N}C_i^{\diamond}U_i)^+\geq C_N^{\diamond}U_N\right\}U_N\right]<$$
$$\mathbb{E}\left[\mathbb{1}\left\{(D-\sum_{i\neq N}C^{*}U_i)^+\geq C^{*}U_N\right\}U_N\right]=\gamma,$$

which is a contradiction.

Next, we prove that at equilibrium $C_N^{\diamond}\leq\frac{D}{\gamma}$. The proof is somewhat similar and once again, proceeds by contradiction. Suppose that $C_N^{\diamond}>\frac{D}{\gamma}$. Now, we have:

$$\begin{aligned}\gamma&=\mathbb{E}\left[\mathbb{1}\left\{(D-\sum_{i\neq N}C_i^{\diamond}U_i)^+\geq C_N^{\diamond}U_N\right\}U_N\right]\\&\leq\mathbb{E}\left[\mathbb{1}\left\{D\geq C_N^{\diamond}U_N\right\}U_N\right]\\&<\mathbb{E}\left[\mathbb{1}\left\{D\geq\frac{D}{\gamma}U_N\right\}U_N\right]\\&=\mathbb{E}\left[\mathbb{1}\left\{\gamma\geq U_N\right\}U_N\right]\\&\leq\mathbb{E}\left[\mathbb{1}\left\{\gamma\geq U_N\right\}\gamma\right]\\&\leq Pr(U_N\leq\gamma)\gamma.\end{aligned}$$

Of course, this leads to the claim that $Pr(U_N\leq\gamma)>1$, which is an obvious contradiction.

□

**Lemma 13.** *Suppose that $C_i\leq C_j\leq\frac{D}{k}$ for some $k\leq 1$. Then, we have that:*

$$E[\min(U_j,\frac{D}{C_j})]\leq E[\min(U_i\frac{D}{C_i})].$$
$$E[\min(U_j,\frac{D}{C_j})]\geq kE[U_i].$$

*Proof.* The first part is easy to see. For any instantiation of $U_j$, we have that $\min(U_j,D/C_j)\leq\min(U_j,D/C_i)$ since $C_i\leq C_j$. Taking the expectation, and changing the variable from $U_j$ to $U_i$ (these variables have the same marginal distribution due to either i.i.d assumption, or follows (5.9)), we get that:

$$E[\min(U_j, \frac{D}{C_j})] \leq E[\min(U_j, \frac{D}{C_i})] = E[\min(U_i, \frac{D}{C_i})].$$

The second part of the lemma can be proved as follows: once again fix any instantiation of $U_j$, we have that,

$$\min(U_j, \frac{D}{C_j}) \geq \min(U_j, \frac{D}{D/k}) = \min(U_j, k) \geq k \min(U_j, 1) = kU_j.$$

Taking the expectation, we get the required result. □

Last, we present a lemma on the bound for integrating on a standard Gaussian distribution.

**Lemma 14.** *Let $\Phi(\cdot)$ denote the CDF for standard Gaussian distribution, i.e., zero mean and unit variance. Then:*

$$\Phi(x) - \Phi(y) \leq \frac{1}{\sqrt{2\pi}}(x - y), x > y. \tag{B.38}$$

Lemma 14 is a direct observation based on the density function $f(x)$ of standard Gaussian random variable, i.e., $f(x) = \frac{1}{\sqrt{2\pi}} e^{-x^2}$ which has a maximum value of $\frac{1}{\sqrt{2\pi}}$.

### *B.8.3 Proof for Theorem 10 and Theorem 8*

Now we proceed to prove Theorem 10 and Theorem 8. Note that Theorem 8 is a special case of 10 when $\bar{U} = 0$, in the following proof, we assume that $U_i = \bar{U} + \hat{U}_i$ as in (5.9).

To avoid lengthy notation, let us define $G_i = E[\min(U_i, D/C_i^\diamond)]$ for all $1 \leq i \leq N$. Consider the payment received by the producer with the smallest investment, which happens to be $C_1^\diamond$. As per Equation (5.3), this equals:

$$\begin{aligned}\pi_1(C_1^\diamond, \ldots, C_N^\diamond) &= \pi_N(C_1^\diamond, \ldots, C_N^\diamond)\frac{C_1^\diamond G_1}{C_N^\diamond G_N} \\ &= \pi_N(C_1^\diamond, \ldots, C_N^\diamond)\frac{C_1^\diamond E[U_1]}{C_N^\diamond G_N}.\end{aligned}$$

The second equation comes from our assumption that $N > \frac{1}{\gamma}$, and therefore, by Lemma 12, we have that $C_1 \leq D$ and $G_1 = E[\min(U_1, 1)] = E[U_1]$. In what follows,

we will continue to use $G_1 = E[U_1]$ for consistency but remark that $G_1$ is a constant that is independent of $C_1^\diamond$. The total profit made by this producer is $\pi_1(C_1^\diamond, \ldots, C_N^\diamond) - \gamma C_1^\diamond$. Since this is an equilibrium solution, we have that $\left(\frac{d}{dC}\pi_1(C, C_2^\diamond, \ldots, C_N^\diamond)\right)_{C=C_1^\diamond} = \gamma$. Expanding the differentiation term, we get that:

$$\frac{G_1}{C_N^\diamond G_N}\Bigg(\pi_N(C_1^\diamond, \ldots, C_N^\diamond) - C_1^\diamond E[\mathbb{1}\left\{0 \leq D - \sum_{i\neq N} C_i^\diamond U_i \leq C_N^\diamond U_N\right\} U_1\Bigg) = \gamma. \tag{B.39}$$

In the above equation, we used the fact that $\frac{d}{dC}\pi_N(C, \ldots, C_N^\diamond) = E[\mathbb{1}\left\{0 \leq D - CU_1 + \sum_{i=2}^{N-1} C_i^\diamond U_i \leq C_N^\diamond U_N\right\} - U_1]$. Rearranging Equation (B.39), we get an upper bound for the payment made to producer $N$, namely

$$\pi_N(C_1^\diamond, \ldots, C_N^\diamond) = \gamma\frac{C_N^\diamond G_N}{G_1} + C_1^\diamond E[\mathbb{1}\{0 \leq D - \sum_{i\neq N} C_i^\diamond U_i \leq C_N^\diamond U_N\}U_1]. \tag{B.40}$$

Fix some constant $\kappa$. The rest of the proof proceeds in two cases:

(Case I: $\sum_{i=1}^{N-1} \frac{C_i^\diamond}{C_N^\diamond} \leq \kappa N^{\frac{3}{4}}$)

Intuitively, this refers to the case where the investments are rather asymmetric—i.e., the investment by the 'larger producers' is significantly bigger than that by the 'smaller producers'. Note that in Equation (B.40), $U_1 \leq 1$. Therefore, we get:

$$\begin{aligned}
\pi_N(C_1^\diamond, \ldots, C_N^\diamond) &\leq \gamma\frac{C_N^\diamond G_N}{G_1} + C_1^\diamond E[\mathbb{1}\{0 \leq D - \sum_{i\neq N} C_i^\diamond U_i \leq C_N^\diamond U_N\}] \\
&= \gamma\frac{C_N^\diamond G_N}{G_1} + C_1^\diamond Pr\left(0 \leq D - \sum_{i\neq N} C_i^\diamond U_i \leq C_N^\diamond U_N\right) \\
&\leq \gamma\frac{C_N^\diamond G_N}{G_1} + C_1^\diamond.
\end{aligned}$$

Recall from Lemma 12 that in any equilibrium solution, we must have that $C_1^\diamond \leq \frac{D}{\gamma N}$. Substituting this above, we get that

$$\pi_N(C_1^\diamond, \ldots, C_N^\diamond) \leq \gamma\frac{C_N^\diamond G_N}{G_1} + \frac{D}{\gamma N}.$$

Next, observe that for any $i \neq N$, we can apply Proposition 3 to obtain an upper bound on its profit, namely that:

$$\begin{aligned}
\pi_i(C_1^\diamond, \ldots, C_N^\diamond) &\leq \pi_N(C_1^\diamond, \ldots, C_N^\diamond) \frac{C_i^\diamond G_i}{C_N^\diamond G_N} \\
&\leq \left(\gamma \frac{C_N^\diamond G_N}{G_1} + \frac{D}{\gamma N}\right) \frac{C_i^\diamond G_i}{C_N^\diamond G_N} \\
&= \gamma \frac{C_i^\diamond G_i}{G_1} + \frac{D C_i^\diamond G_i}{\gamma N C_N^\diamond G_N} \\
&\leq \gamma C_i^\diamond + \frac{D C_i^\diamond E[U_i]}{\gamma N C_N^\diamond \gamma E[U_N]} \qquad \text{(B.41)} \\
&= \gamma C_i^\diamond + \frac{D C_i^\diamond}{\gamma^2 N C_N^\diamond}. \qquad \text{(B.42)}
\end{aligned}$$

Equations (B.41) and (B.42) were derived using Lemma 13, namely we used the simple properties that $(i)$ $G_i \leq G_1$, $(ii)$ $G_i \leq E[U_i]$, and $(iii)$ $G_N \geq \gamma E[U_N]$, and finally the fact that $E[U_i] = E[U_N]$.

Summing up Equation B.42 over all $i$ including $i = N$, we get that

$$\sum_{i=1}^{N} \pi_i(C_1^\diamond, \ldots, C_N^\diamond) \leq \gamma \sum_{i=1}^{N} C_i^\diamond + \frac{D}{N\gamma^2} \left(\sum_{i=1}^{N} \frac{C_i^\diamond}{C_N^\diamond}\right).$$

Of course, as per our assumption, we have that $\sum_{i=1}^{N-1} \frac{C_i^\diamond}{C_N^\diamond} \leq \kappa N^{\frac{3}{4}}$. Substituting this above, we get that

$$\begin{aligned}
\sum_{i=1}^{N} \pi_i(C_1^\diamond, \ldots, C_N^\diamond) &\leq \gamma \sum_{i=1}^{N} C_i^\diamond + \frac{D}{N\gamma^2} \left(\kappa N^{\frac{3}{4}} + 1)\right). \\
&\leq \gamma \sum_{i=1}^{N} C_i^\diamond + \frac{D}{\gamma^2} \left(\kappa N^{-\frac{1}{4}} + \frac{1}{N}\right).
\end{aligned}$$

This proves the theorem statement for the case where $\sum_{i=1}^{N-1} \frac{C_i^\diamond}{C_N^\diamond} \leq \kappa N^{\frac{3}{4}}$. Note that the $\frac{1}{N}$ term can be incorporated into the constant $\alpha$, without affecting any of the asymptotic bounds.

(Case II: $\sum_{i=1}^{N-1} \frac{C_i^\diamond}{C_N^\diamond} > \kappa N^{\frac{3}{4}}$)

Let us go back to Equation (B.39) and consider the term
$B = E[\mathbb{1}\left\{0 \leq D - \sum_{i \neq N} C_i^\diamond U_i \leq C_N^\diamond U_N\right\} U_1]$. We will now obtain a tighter upper bound

on this quantity conditional upon $\sum_{i=1}^{N-1} \frac{C_i^\diamond}{C_N^\diamond} > \kappa N^{\frac{3}{4}}$. First note that applying the Cauchy-Schwarz inequality, we can get a lower bound on the sum-of-squares, i.e.,

$$\sum_{i=1}^{N-1}(\frac{C_i^\diamond}{C_N^\diamond})^2 \geq \frac{1}{N-1}(\sum_{i=1}^{N-1} C_i^\diamond/C_N^\diamond)^2 \geq \frac{\kappa^2 N^{3/2}}{N-1} \geq 2\kappa^2 N^{\frac{1}{2}}. \tag{B.43}$$

The final simplification comes from the fact that $N \geq 2$ (since we assumed $N > \frac{1}{\gamma} \geq 1$). Next, we have that:

$$\begin{aligned} B &\leq E[\mathbb{1}\left\{0 \leq D - \sum_{i\neq N} C_i^\diamond U_i \leq C_N^\diamond U_N\right\}] \\ &= Pr\left(D - C_N^\diamond U_N \leq \sum_{i\neq N} C_i^\diamond U_i \leq D\right) \\ &= Pr\left(\frac{D}{C_N^\diamond} - U_N \leq \sum_{i\neq N} \frac{C_i^\diamond}{C_N^\diamond} U_i \leq \frac{D}{C_N^\diamond}\right) \\ &\leq Pr\left(\frac{D}{C_N^\diamond} - 1 \leq \sum_{i\neq N} \frac{C_i^\diamond}{C_N^\diamond} U_i \leq \frac{D}{C_N^\diamond}\right). \end{aligned}$$

We will show that $Pr\left(\frac{D}{C_N^\diamond} - 1 \leq \sum_{i\neq N} \frac{C_i^\diamond}{C_N^\diamond} U_i \leq \frac{D}{C_N^\diamond}\right)$ is decreasing with $N$.

Using the fact that $U_i = \hat{U}_i + \bar{U}$, we can write out the probability more explicitly:

$$\begin{aligned} &Pr\left(\frac{D}{C_N^\diamond} - 1 \leq \sum_{i\neq N} \frac{C_i^\diamond}{C_N^\diamond} U_i \leq \frac{D}{C_N^\diamond}\right) \\ &= Pr\left(\frac{D}{C_N^\diamond} - 1 \leq \sum_{i\neq N} \frac{C_i^\diamond}{C_N^\diamond} (\hat{U}_i + \bar{U}) \leq \frac{D}{C_N^\diamond}\right). \end{aligned} \tag{B.44}$$

Let us denote $U_0 = \sum_{i\neq N} \frac{C_i^\diamond}{C_N^\diamond} \bar{U}$ and $U' = \sum_{i\neq N} \frac{C_i^\diamond}{C_N^\diamond} \hat{U}_i$. From the assumption A3 along with (5.9) we know that $\bar{U}$ is independent of $\hat{U}_i$, therefore $U_0$ is independent of $U'$. The probability in (B.44) can be written as an integral over the possible values for $U_0$ with $f_{U_0}(\cdot)$

being the probability density function for the random variable $U_0$. So, we have:

$$\begin{aligned}
&Pr\left(\frac{D}{C_N^\diamond}-1\le\sum_{i\neq N}\frac{C_i^\diamond}{C_N^\diamond}U_i\le\frac{D}{C_N^\diamond}\right)\\
&=Pr\left(\frac{D}{C_N^\diamond}-1\le U_0+U'\le\frac{D}{C_N^\diamond}\right)\\
&\overset{(a)}{=}\int_0^{\frac{D}{C_N^\diamond}}f_{U_0}(u)Pr\left(\frac{D}{C_N^\diamond}-1\le U_0+U'\le\frac{D}{C_N^\diamond}|U_0=u\right)du\\
&\overset{(b)}{=}\int_0^{\frac{D}{C_N^\diamond}}f_{U_0}(u)Pr\{\frac{D}{C_N^\diamond}-1-u\le U'\le\frac{D}{C_N^\diamond}-u\}du,
\end{aligned}\tag{B.45}$$

where $(a)$ uses the property of conditional probability, and $(b)$ is based on the fact that $U_0$ and $U'$ are independent.

We now show that $Pr\left(\frac{D}{C_N^\diamond}-1-u\le U'\le\frac{D}{C_N^\diamond}-u\right)$ is decreasing w.r.t. $N$, for any $u$.

Since $U'=\sum_{i\neq N}\frac{C_i^\diamond}{C_N^\diamond}\hat{U}_i$, where $\hat{U}_i$'s are i.i.d. random variables and $\mathbb{E}\,\hat{U}_i=\hat{\mu}$, $\mathbb{E}(\hat{U}_i-\mathbb{E}\,\hat{U}_i)^2=\hat{\sigma}^2>0$, $\mathbb{E}\,|\hat{U}_i-\mathbb{E}\,\hat{U}_i|^3=\hat{\rho}<\infty$, this variable has a mean $\mu'=\hat{\mu}\sum_{i=1}^{N-1}C_i^\diamond/C_N^\diamond\ge\hat{\mu}\kappa N^{\frac{3}{4}}$. Similarly, the variance of $U'$ can be written as $(\sigma')^2=\hat{\sigma}^2\sum_{i=1}^{N-1}(\frac{C_i^\diamond}{C_N^\diamond})^2$. Now, applying Equation (B.43), we get the following lower bound for variance:

$$(\sigma')^2\ge 2\hat{\sigma}^2\kappa^2N^{\frac{1}{2}}.\tag{B.46}$$

Note that $\frac{C_i^\diamond}{C_N^\diamond}\hat{U}_i$ are independent random variables because $\hat{U}_i$'s are i.i.d.. What is more, we know that $\frac{C_i^\diamond}{C_N^\diamond}\hat{U}_i$ has mean $\bar{\mu}_i=\frac{C_i^\diamond}{C_N^\diamond}\hat{\mu}$, non negative variance $\bar{\sigma}_i^2=(\frac{C_i^\diamond}{C_N^\diamond})^2\hat{\sigma}^2$ and finite centered third moment $\bar{\rho}_i=(\frac{C_i^\diamond}{C_N^\diamond})^3\hat{\rho}$. Denote $S_N=\frac{U'-\sum_i\bar{\mu}_i}{\sqrt{\sum_i\bar{\sigma}_i^2}}$ and let $F_N$ denote the CDF of $S_N$. We rewrite the probability of interest as the following:

$$\begin{aligned}
&Pr\left(\frac{D}{C_N^\diamond}-1-u\le\sum_{i\neq N}\frac{C_i^\diamond}{C_N^\diamond}\hat{U}_i\le\frac{D}{C_N^\diamond}-u\right)\\
=&Pr\left(\frac{D}{C_N^\diamond}-1-u\le U'\le\frac{D}{C_N^\diamond}-u\right)\\
=&Pr\left(\frac{\frac{D}{C_N^\diamond}-1-u-\sum_i\bar{\mu}_i}{\sqrt{\sum_i\bar{\sigma}_i^2}}\le\frac{U'-\sum_i\bar{\mu}_i}{\sqrt{\sum_i\bar{\sigma}_i^2}}\le\frac{\frac{D}{C_N^\diamond}-u\sum_i\bar{\mu}_i}{\sqrt{\sum_i\bar{\sigma}_i^2}}\right)\\
=&F_N\left(\frac{\frac{D}{C_N^\diamond}-u-\sum_i\bar{\mu}_i}{\sqrt{\sum_i\bar{\sigma}_i^2}}\right)-F_N\left(\frac{\frac{D}{C_N^\diamond}-1-u-\sum_i\bar{\mu}_i}{\sqrt{\sum_i\bar{\sigma}_i^2}}\right).
\end{aligned}\tag{B.47}$$

We can now apply the Berry-Esseen Theorem from Lemma 10 to get an upper bound:

$$
\begin{aligned}
&Pr\left(\frac{D}{C_N^\diamond}-1-u\leq\sum_{i\neq N}\frac{C_i^\diamond}{C_N^\diamond}\hat{U}_i\leq\frac{D}{C_N^\diamond}-u\right)\\
=&F_N\left(\frac{\frac{D}{C_N^\diamond}-u-\sum_i\bar{\mu}_i}{\sqrt{\sum_i\bar{\sigma}_i^2}}\right)-F_N\left(\frac{\frac{D}{C_N^\diamond}-1-u-\sum_i\bar{\mu}_i}{\sqrt{\sum_i\bar{\sigma}_i^2}}\right)\\
\overset{(a)}{\leq}&\Phi\left(\frac{\frac{D}{C_N^\diamond}-u-\sum_i\bar{\mu}_i}{\sqrt{\sum_i\bar{\sigma}_i^2}}\right)-\Phi\left(\frac{\frac{D}{C_N^\diamond}-1-u-\sum_i\bar{\mu}_i}{\sqrt{\sum_i\bar{\sigma}_i^2}}\right)\\
&+2\alpha(\sum_i\bar{\sigma}_i^2)^{-\frac{1}{2}}\max_i\frac{\bar{\rho}_i}{\bar{\sigma}_i^2}\\
\overset{(b)}{\leq}&\Phi\left(\frac{\frac{D}{C_N^\diamond}-u-\sum_i\bar{\mu}_i}{\sqrt{\sum_i\bar{\sigma}_i^2}}\right)-\Phi\left(\frac{\frac{D}{C_N^\diamond}-1-u-\sum_i\bar{\mu}_i}{\sqrt{\sum_i\bar{\sigma}_i^2}}\right)\\
&+2\alpha(2\bar{\sigma}^2\kappa^2N^{-\frac{1}{4}})\max_i(\frac{C_i^\diamond}{C_N^\diamond}\frac{\bar{\rho}}{\bar{\sigma}^2})\\
\overset{(c)}{\leq}&\frac{1}{\sqrt{2\pi}}\frac{1}{\sqrt{\sum_i\bar{\sigma}_i^2}}+2\alpha(2\bar{\sigma}^2\kappa^2N^{-\frac{1}{4}})(\frac{\bar{\rho}}{\bar{\sigma}^2})\\
\overset{(d)}{\leq}&\kappa'N^{-\frac{1}{4}},
\end{aligned}
\tag{B.48}
$$

where $\Phi(\cdot)$ is the CDF for standard Gaussian distribution. Inequality $(a)$ applies Berry Esseen Theorem to $F_N(x)$ at $x=\frac{\frac{D}{C_N^\diamond}-u-\sum_i\bar{\mu}_i}{\sqrt{\sum_i\bar{\sigma}_i^2}}$ and $x=\frac{\frac{D}{C_N^\diamond}-1-u-\sum_i\bar{\mu}_i}{\sqrt{\sum_i\bar{\sigma}_i^2}}$. Inequality $(b)$ is based on (B.46). Inequality $(c)$ is based on Lemma 14. Inequality $(c)$ also depends on the fact that $\frac{C_i^\diamond}{C_N^\diamond}<1,\forall i$. Lastly, $(d)$ uses the fact that $\frac{1}{\sum_i\bar{\sigma}_i^2}\leq\frac{1}{\sqrt{2\sigma^2\kappa^2N^{\frac{1}{2}}}}$ from (B.46), and rewrites the constants into $\kappa'$ for brevity.

Plugging the above upper bound back to (B.45), we get that:

$$
\begin{aligned}
&Pr\left(\frac{D}{C_N^\diamond}-1\leq\sum_{i\neq N}\frac{C_i^\diamond}{C_N^\diamond}U_i\leq\frac{D}{C_N^\diamond}\right)\\
\leq&\kappa'N^{-\frac{1}{4}}\int_0^{D/C^\diamond{}_N}f_{U_0}(u)du\\
\leq&\kappa'N^{-\frac{1}{4}}.
\end{aligned}
\tag{B.49}
$$

If $\bar{U}=0$, then $U_i$'s are i.i.d. random variables, then $U_0=0$ and the bound naturally carries over, as stated in the following corollary.

**Corollary 2.** *If $U_i$'s are i.i.d. random variables, then it is a special case of correlated $U_i$'s in Assumption A3 when $\bar{U}$, and the upper bound in* (B.48) *is valid for i.i.d. $U_i$'s, i.e.:*

$$Pr\left(\frac{D}{C_N^\diamond} - 1 \leq \sum_{i \neq N} \frac{C_i^\diamond}{C_N^\diamond} U_i \leq \frac{D}{C_N^\diamond}\right) \leq \kappa' N^{-\frac{1}{4}}. \tag{B.50}$$

Now we can complete the proof. Going back to (B.40), and substituting the above upper bound to get that:

$$\begin{aligned}\pi_N(C_1^\diamond, \ldots, C_N^\diamond) &\leq \gamma \frac{C_N^\diamond G_N}{G_1} + C_1^\diamond \kappa' N^{-\frac{1}{4}} \\ &\leq \gamma \frac{C_N^\diamond G_N}{G_1} + \frac{D}{\gamma N} \kappa' N^{-\frac{1}{4}}. \end{aligned} \tag{B.51}$$

Next, we upper bound the aggregate payment made to the producers using Proposition 3. Recall that $G_i \leq G_1$ for all $i$ and that $G_N \geq \gamma E[U_N]$ as per Lemma 13. We now get that:

$$\begin{aligned}\sum_{i=1}^N \pi_i(C_1^\diamond, \ldots, C_N^\diamond) &\leq \sum_{i=1}^N \pi_N(C_1^\diamond, \ldots, C_N^\diamond) \frac{\bar{C}_i G_i}{C_N^\diamond G_N} \\ &\leq \sum_{i=1}^N \left(\gamma \frac{C_N^\diamond G_N}{G_1} + \frac{D G_i}{\gamma N G_N} \kappa' N^{-\frac{1}{4}}\right) \frac{\bar{C}_i G_i}{C_N^\diamond G_N} \\ &=\leq \gamma \sum_{i=1}^N C_i^\diamond \frac{G_i}{G_1} + \frac{D}{\gamma^2 N} \kappa' N^{-\frac{1}{4}} \sum_{i=1}^N \frac{\bar{C}_i}{C_N^\diamond} \\ &\leq \gamma \sum_{i=1}^N C_i^\diamond + \frac{D}{\gamma^2 N} \kappa' N^{-\frac{1}{4}} \times N \\ &= \gamma \sum_{i=1}^N C_i^\diamond + \frac{D}{\gamma^2} \kappa' N^{-\frac{1}{4}}. \end{aligned}$$

In the penultimate equation, we used the fact that $C_i^\diamond \leq C_N^\diamond$ and so, trivially, $\sum_{i=1}^N \frac{C_i^\diamond}{C_N^\diamond} \leq N$. This completes the proof of the second case, and hence, the theorem. □

### *B.9 Proof for Theorem 11*

To prove that there is only one symmetric Nash equilibrium, we need to show that there is a unique $C$ such that $C_1 = C_2 = \cdots = C_N = C$ which minimizes the total profit in the game:

$$N\,\mathbb{E}\left[\min\left((D - C\sum_{j \neq i}^N U_j)^+, CU_j\right)\right] - \gamma C N. \tag{B.52}$$

The optimality condition on $C$ to minimize this payment is shown in (B.31).

Showing a unique $C$ maximizes (B.52) is equivalent to showing that the right hand side that involves $C$ in (B.31) has only one intersection with $\gamma$, i.e., $\mathbb{E}\left[\mathbb{1}\left\{(D - C\sum_{j\neq i}^{N} U_j)^+ \geq CU_i\right\} U_i\right]$ is monotonic with respect to $C$. This can be seen from the fact that as $C$ increases, $(D - C\sum_{j\neq i}^{N} U_j)^+$ decreases for each realization of $U_j$ and $CU_i$ increases by each realization of $U_i$. Therefore the term inside the expectation is monotonically decreasing as $C$ increases. □

### *B.10 Proof of Theorem 12 and Corollary 1*

For this proof, we use the small $o$ notation, where $f(x) = o(g(x))$ as $x \to 0$ means that $\lim_{x\to 0} \frac{f(x)}{g(x)} = 0$. The proof of Theorem 12 is given by the following set of equations:

$$\begin{aligned}
\nabla f(\boldsymbol{x})^\top \boldsymbol{p} &= \nabla f(\boldsymbol{x})^\top \frac{f(\boldsymbol{x} + \Delta \cdot \boldsymbol{e}) - f(\boldsymbol{x})}{\Delta} \boldsymbol{e} \\
&\overset{(a)}{=} \nabla f(\boldsymbol{x})^\top \frac{\nabla f(\boldsymbol{x})^\top \Delta \cdot \boldsymbol{e} + o(\|\Delta \cdot \boldsymbol{e}\|)}{\Delta} \boldsymbol{e} \\
&= (\nabla f(\boldsymbol{x})^\top \boldsymbol{e})^2 + \frac{o(\|\Delta \cdot \boldsymbol{e}\|)}{\Delta} \nabla f(\boldsymbol{x})^\top \boldsymbol{e} \\
&= (\nabla f(\boldsymbol{x})^\top \boldsymbol{e})^2 + \frac{o(\|\Delta \cdot \boldsymbol{e}\|)}{\|\Delta \cdot \boldsymbol{e}\|} \nabla f(\boldsymbol{x})^\top \boldsymbol{e},
\end{aligned} \tag{B.53}$$

where $(a)$ follows from the first order Taylor expansion of a differentiable function. Note that $\frac{o(\|\Delta \cdot \boldsymbol{e}\|)}{\|\Delta \cdot \boldsymbol{e}\|} \to 0$ as $\|\Delta \cdot \boldsymbol{e}\| = \Delta \to 0$, for every $\boldsymbol{e}$. Then with probability 1 we can take $\Delta$ small enough and ensure that $\nabla f(\boldsymbol{x})^\top \boldsymbol{p} > 0$. The proof of Corollary 1 follows in a similar

fashion using the chain rule:

$$\begin{aligned}
&\nabla_{\boldsymbol{y}} f(g(\boldsymbol{y}))^\top \boldsymbol{p} \\
=&(J_g(\boldsymbol{y})^\top \nabla f(\boldsymbol{x})|_{\boldsymbol{x}=g(\boldsymbol{y})})^\top \boldsymbol{p} \\
=&\nabla f(\boldsymbol{x})^\top J_g(\boldsymbol{y}) J_g(\boldsymbol{y})^\top \frac{f(\boldsymbol{x}+\Delta \boldsymbol{e})-f(\boldsymbol{x})}{\Delta}\boldsymbol{e} \\
=&\mathrm{tr}(J_g(\boldsymbol{y}) J_g(\boldsymbol{y})^\top \frac{f(\boldsymbol{x}+\Delta \boldsymbol{e})-f(\boldsymbol{x})}{\Delta}\boldsymbol{e}\nabla f(\boldsymbol{x})^\top) \\
\overset{(a)}{\geq}&\lambda_{min}(J_g(\boldsymbol{y}) J_g(\boldsymbol{y})^\top)\mathrm{tr}(\frac{f(\boldsymbol{x}+\Delta \boldsymbol{e})-f(\boldsymbol{x})}{\Delta}\boldsymbol{e}\nabla f(\boldsymbol{x})^\top) \\
\overset{(b)}{=}&\lambda_{min}(J_g(\boldsymbol{y}) J_g(\boldsymbol{y})^\top)\mathrm{tr}(\nabla f(\boldsymbol{x})^\top \frac{f(\boldsymbol{x}+\Delta \boldsymbol{e})-f(\boldsymbol{x})}{\Delta}\boldsymbol{e}) \\
\overset{(c)}{\geq}&0,
\end{aligned} \tag{B.54}$$

where $(a)$ is the direct result from [131] to bound trace of a symmetric matrix by its smallest eigenvalue $\lambda_{min}(\cdot)$, $(b)$ comes from the fact that trace is invariant of cyclic permutations, and inequality $(c)$ is again based on Theorem 12 and that $\lambda_{min}(J_g(\boldsymbol{y})J_g(\boldsymbol{y})^\top) \geq 0$. More specifically, if $J_g(\boldsymbol{y})J_g(\boldsymbol{y})^\top \succ 0$, then $\nabla_{\boldsymbol{y}} f(g(\boldsymbol{y}))^\top \boldsymbol{p} > 0$.

### *B.11 Proof of Theorem 14*

Assuming Lemmas 6 and 7 are true, we prove Theorem 14 then we prove the lemmas. We reformulate $\Psi(\boldsymbol{Q})$ into:

$$\Psi(\boldsymbol{Q}) \tag{B.55a}$$

$$= \Pr\{\boldsymbol{0} \leq -\underline{\boldsymbol{V}} + \boldsymbol{R}\boldsymbol{P} + \boldsymbol{X}\boldsymbol{Q} + \boldsymbol{\epsilon} \leq -\underline{\boldsymbol{V}} + \overline{\boldsymbol{V}}\} \tag{B.55b}$$

$$= \Pr\{\boldsymbol{0} \leq \boldsymbol{Y}(\boldsymbol{Q}) + \boldsymbol{\epsilon} \leq \boldsymbol{u}\}, \tag{B.55c}$$

$$= \Pr\{-\boldsymbol{Y}(\boldsymbol{Q}) \leq \boldsymbol{\epsilon} \leq \boldsymbol{u} - \boldsymbol{Y}(\boldsymbol{Q})\}, \tag{B.55d}$$

where $\boldsymbol{Y}(\boldsymbol{Q}) = -\underline{\boldsymbol{V}} + \boldsymbol{R}\boldsymbol{P} + \boldsymbol{X}\boldsymbol{Q}$ and $-\underline{\boldsymbol{V}} + \overline{\boldsymbol{V}} = \boldsymbol{u}$.

Let $\boldsymbol{z} = \boldsymbol{u} - \boldsymbol{Y}(\boldsymbol{Q})$.Then (B.55d) can be compactly written as:

$$\Pr\{\boldsymbol{z} - \boldsymbol{u} \leq \boldsymbol{\epsilon} \leq \boldsymbol{z}\} \triangleq F(\boldsymbol{z}). \tag{B.56}$$

With Lemma 6, we know that $F(\boldsymbol{z})$ is log concave in $\boldsymbol{z}$. Since $\boldsymbol{z} = \boldsymbol{u} - \boldsymbol{Y}(\boldsymbol{Q}) = \boldsymbol{A}\boldsymbol{Q} + \boldsymbol{b}$, where $\boldsymbol{A}$ is full rank and $\boldsymbol{b}$ is a constant, Lemma 7 implies $\Psi(\boldsymbol{Q})$ is a log-concave function.

### *B.12 Proof of Lemma 6*

Before proving Lemma 6, we introduce Lemma 15 that is necessary in the proof.

**Lemma 15.** *A convolution over two log-concave functions is log concave [132].*

Using Lemma 15, we now proceed to prove Lemma 6.

*Proof to Lemma 6.* Let $f(\cdot)$ be the PDF of $\boldsymbol{\epsilon}$ that is defined on $\mathbb{R}^N$. Let $r(\cdot)$ be defined as below:

$$r(\boldsymbol{x}) = \begin{cases} 1, & \text{if } \mathbf{0} \leq \boldsymbol{x} \leq \boldsymbol{u} \\ 0, & \text{otherwise.} \end{cases} \tag{B.57}$$

It is easy to check that $r(\cdot)$ is log concave. Let us use $\star$ to denote convolution operation. The convolution of $f$ and $r$ is:

$$\begin{aligned} (f \star r)(\boldsymbol{z}) &= \int_{[\mathbf{0},\boldsymbol{u}]} f(\boldsymbol{z} - \boldsymbol{y}) r(\boldsymbol{y}) d\boldsymbol{y} \\ &= \int_{[\mathbf{0},\boldsymbol{u}]} f(\boldsymbol{z} - \boldsymbol{y}) d\boldsymbol{y} \\ &= -\int_{[\boldsymbol{z},\boldsymbol{z}-\boldsymbol{u}]} f(\boldsymbol{w}) d\boldsymbol{w} \\ &= \int_{[\boldsymbol{z}-\boldsymbol{u},\boldsymbol{z}]} f(\boldsymbol{w}) d\boldsymbol{w} \\ &= F(\boldsymbol{z}) \end{aligned} \tag{B.58}$$

From Lemma 15 and that $f$ and $r$ are both log concave, we conclude that $F(\boldsymbol{z})$ is log concave in $\boldsymbol{z}$. □

### *B.13 Proof of Lemma 7*

*Proof to Lemma 7.* Since log-concavity of a function $F(\boldsymbol{z})$ is equivalent to $\log(F(\boldsymbol{z}))$ is concave, we have the second order condition on concavity:

$$\nabla^2 \log(F(\boldsymbol{z})) \preccurlyeq 0, \tag{B.59}$$

which after some simplification yielding the following form:

$$F(\boldsymbol{z})\nabla^2 F(\boldsymbol{z}) - \nabla F(\boldsymbol{z})\nabla F(\boldsymbol{z})^\top \preccurlyeq 0. \tag{B.60}$$

Let us denote $F(\boldsymbol{z})\nabla^2 F(\boldsymbol{z}) - \nabla F(\boldsymbol{z})\nabla F(\boldsymbol{z})^\top$ by $H_F(\boldsymbol{z})$.

To show that $g(\boldsymbol{y}) = F(A\boldsymbol{y}+\boldsymbol{b})$ is log-concave, it is equivalent to show that $g(\boldsymbol{y})\nabla^2 g(\boldsymbol{y}) - \nabla g(\boldsymbol{y})\nabla g(\boldsymbol{y})^\top \preccurlyeq 0$.

We first compute $\nabla g(\boldsymbol{y})$ as the following:

$$\nabla g(\boldsymbol{y}) = A^\top \nabla F(\boldsymbol{z})|_{\boldsymbol{z}=A\boldsymbol{y}+b}, \tag{B.61}$$

and $\nabla^2 g(\boldsymbol{y})$ as the following, with the fact that $\nabla^2(A\boldsymbol{y}+b) = 0$:

$$\nabla^2 g(\boldsymbol{y}) = A^\top(\nabla^2 F(\boldsymbol{z})|_{\boldsymbol{z}=A\boldsymbol{y}+b})A. \tag{B.62}$$

So $g(\boldsymbol{y})\nabla^2 g(\boldsymbol{y}) - \nabla g(\boldsymbol{y})\nabla g(\boldsymbol{y})^\top$ is equivalent to $A^\top H_F(A\boldsymbol{y}+b)A$. Let us denote this new quantity as $H_g(\boldsymbol{y}) = A^\top H_F(A\boldsymbol{y}+b)A$.

Since $H_F(\boldsymbol{z}) \preccurlyeq 0, \forall \boldsymbol{z} \in \mathbb{R}^N$, it suggests that $\forall \boldsymbol{w} \in \mathbb{R}^N$ and $A\boldsymbol{y}+b \in \mathbb{R}^N$, we know:

$$\boldsymbol{w}^\top H_F(A\boldsymbol{y}+b)\boldsymbol{w} \leq 0. \tag{B.63}$$

Since $A$ has rank $N$, we know that $\boldsymbol{w} = A\boldsymbol{z'}$ spans the whole subspace $\mathbb{R}^N$, $\forall \boldsymbol{z'} \in \mathbb{R}^M$. Therefore:

$$\boldsymbol{z'}^\top A^\top H_F(A\boldsymbol{y}+b)A^\top \boldsymbol{z'} \leq 0, \tag{B.64}$$

which is equivalent to :

$$\boldsymbol{z'}^\top H_g(\boldsymbol{y})\boldsymbol{z'} \leq 0, \forall \boldsymbol{z'} \in \mathbb{R}^M. \tag{B.65}$$

This suggests that $H_g$ is negative semi definite, and therefore concludes the proof.

□

### *B.14 Reduced formulation of integer programming*

The reduction procedure here is similar to the reformulation in [133]. In our case, we want to reduce the following constraint in the integer programming shown in (6.21):

$$\sum_{s\in\{1,\ldots,S\}} \mathbb{1}\{\underline{\boldsymbol{V}} \leq \boldsymbol{RP} + \boldsymbol{XQ} + \boldsymbol{\epsilon}^{(s)} \leq \overline{\boldsymbol{V}}\} \geq \alpha S, \tag{B.66}$$

where $S$ is the number of scenarios. This constraint is equivalent written as:

$$\begin{aligned}\sum_{s\in\{1,\ldots,S\}} &\mathbb{1}\{\underline{\boldsymbol{V}} - (\boldsymbol{RP} + \boldsymbol{XQ}) \leq \boldsymbol{\epsilon}^{(s)} \leq \overline{\boldsymbol{V}} - (\boldsymbol{RP} + \boldsymbol{XQ})\} \\ &\geq \alpha S,\end{aligned} \tag{B.67}$$

where $S$ is the number of scenarios. Introducing binary variable $\iota_s$, we obtain the following representation of (B.67):

$$\begin{aligned}&\text{if } \underline{\boldsymbol{V}} - (\boldsymbol{RP} + \boldsymbol{XQ}) \leq \boldsymbol{\epsilon}^{(s)} \leq \overline{\boldsymbol{V}} - (\boldsymbol{RP} + \boldsymbol{XQ}), \\ &\text{then } \iota_s = 0, \text{otherwise } \iota_s = 1, s \in \{1, ..., S\}, \\ &\sum_{s\in\{1,\ldots,S\}} \iota_s \leq (1-\alpha)S.\end{aligned} \tag{B.68}$$

Therefore, the number of constraints for original MIP problem in (6.21) is at least $2NS$, where $N$ is the dimension of decision variable $\boldsymbol{Q}$, and $S$ is the dimension of decision variable $\boldsymbol{\iota} = [\iota_1, \cdots, \iota_S]$.

In order to reduce the number of constraints, we let $U$ denote constraints in(B.68). Let $\Theta_i^{'}$ be the constraint for each dimension $i$ in $\boldsymbol{\epsilon}^{(s)}$ such that:

$$\begin{aligned}&\text{if } \underline{\boldsymbol{V}}_i - (\boldsymbol{R}_i^\top \boldsymbol{P} + \boldsymbol{X}_i^\top \boldsymbol{Q}) \leq \boldsymbol{\epsilon}_i^{(s)}, \\ &\text{then } \iota_s = 0, \text{othewise } \iota_s = 1, \\ &s \in \{1, ..., S\}, \\ &\sum_s \iota_s \leq (1-\alpha)S,\end{aligned} \tag{B.69}$$

and $\Theta_i^{''}$ be:

$$\begin{aligned}
&\text{if } \boldsymbol{\epsilon}_i^{(s)} \leq \overline{\boldsymbol{V}}_i - (\boldsymbol{R}_i^\top \boldsymbol{P} + \boldsymbol{X}_i^\top \boldsymbol{Q}),\\
&\text{then } \iota_s = 0, \text{otherwise } \iota_s = 1,\\
&s \in \{1, ..., S\},\\
&\sum_s \iota_s \leq (1-\alpha)S.
\end{aligned} \tag{B.70}$$

Then $\Theta = \Theta_1^{'} \cap \Theta_2^{'} \cap ... \cap \Theta_n^{'} \cap \Theta_1^{''} \cap \Theta_2^{''} \cap ... \cap \Theta_N^{''}$.

We now focus on the reduction of $\Theta_i^{'}$. Let $\boldsymbol{h}_i = [h_i^{(1)}, h_i^{(2)}, ..., h_i^{(S)}]$ be sorted in ascending order of $\boldsymbol{\epsilon}_i = \{\boldsymbol{\epsilon}_i^{(1)}, \boldsymbol{\epsilon}_i^{(2)}, ..., \boldsymbol{\epsilon}_i^{(S)}\}$. Let $\tau = \lfloor (1-\alpha)S \rfloor$, Then $\Theta_i^{'}$ is equivalent to:

$$\begin{aligned}
&\underline{\boldsymbol{V}}_i - (\boldsymbol{R}_i^\top \boldsymbol{P} + \boldsymbol{X}_i^\top \boldsymbol{Q}) + (h_i^{(k)} - h_i^{(\tau+1)})\iota^{(k)} \leq h_i^{(k)},\\
&k \in \{1, 2, ..., \tau\},\\
&\sum_s \iota_s \leq (1-\alpha)S,\\
&\iota_s \in \{0, 1\},
\end{aligned} \tag{B.71}$$

where $\iota^{(k)}$ is a permutation of $\iota_s$ according to $\boldsymbol{h}_i$. More specifically, $\iota^{(k)} = \iota_s$ such that $h_i^{(k)} = \boldsymbol{\epsilon}_i^{(s)}$.

The inequality (B.71) means that if $\iota^{(k)} = 0$, then $\underline{\boldsymbol{V}}_i - (\boldsymbol{R}_i^\top \boldsymbol{P} + \boldsymbol{X}_i^\top \boldsymbol{Q}) \leq h_i^{(k)}$, otherwise $\underline{\boldsymbol{V}}_i - (\boldsymbol{R}_i^\top \boldsymbol{P} + \boldsymbol{X}_i^\top \boldsymbol{Q}) \leq h_i^{(\tau+1)}$ is a trivial inequality.

We can reduce $\Theta_1^{''}$ in the same way:

$$\begin{aligned}
&\overline{\boldsymbol{V}}_i - (\boldsymbol{R}_i^\top \boldsymbol{P} + \boldsymbol{X}_i^\top \boldsymbol{Q}) + (h_i^{(k)} - h_i^{(N-\tau)})\iota_{(k)} \geq h_i^{(k)},\\
&k \in \{S - \tau + 1, ..., S\},\\
&\sum_s \iota_s \leq (1-\alpha)S,\\
&\iota_s \in \{0, 1\}.
\end{aligned} \tag{B.72}$$

This means that if $\iota_s = 0$, then $\overline{\boldsymbol{V}}_i - (\boldsymbol{R}_i^\top \boldsymbol{P} + \boldsymbol{X}_i^\top \boldsymbol{Q}) \geq h_i^{(k)}$, otherwise $\overline{\boldsymbol{V}}_i - (\boldsymbol{R}_i^\top \boldsymbol{P} + \boldsymbol{X}_i^\top \boldsymbol{Q}) \geq h_i^{(N-\tau)}$ is a trivial inequality.

Now we replace constraint (B.66) by (B.71) and (B.72) for each $i \in \{1, \cdots, N\}$, the total number of constraints is reduced from $2NS$ to $2(1-\alpha)NS$, where $\alpha$ is usually near 1.

# Appendix C

# AUTHOR'S BIBLIOGRAPHY


1. **Pan Li**, Shreyas Sekar, and Baosen Zhang, "A capacity-price game for uncertain renewables resources", in *ACM e-energy*, 2018.

2. **Pan Li**, Shreyas Sekar, and Baosen Zhang, "Exploiting uncertainty to create buyer-Optimal outcomes in renewable energy markets", in *MD4SG '18*.

3. **Pan Li**, Baihong Jin, Dai Wang and Baosen Zhang, "Distribution system voltage control under uncertainties using tractable chance constraints", under review of *IEEE Transactions on Power Systems*.

4. **Pan Li**, and Baosen Zhang, "Linear estimation of treatment effects in demand response: an experimental design approach", submitted to *IEEE Transactions on Power Systems*.

5. Yize Chen, **Pan Li**, and Baosen Zhang, "Bayesian Renewables scenario generation via deep generative networks", in *52nd Annual Conference on Information Sciences and Systems*, IEEE, 2018.

6. **Pan Li**, and Baosen Zhang, "Distribution system voltage control under uncertainties", in *Asilomar Conference on Signals, Systems, and Computers*, IEEE, 2017.

7. **Pan Li**, Hao Wang, and Baosen Zhang, "A distributed online pricing strategy for demand response programs", in *IEEE Transactions on Smart Grid*, 2017.

8. **Pan Li**, and Baosen Zhang, "An optimal treatment assignment strategy to evaluate demand response effect", in *54th Allerton Conference on Communication, Control and Computing*, 2016.

9. **Pan Li**, and Baosen Zhang, "Estimating treatment effects in demand response", in *Statistical Signal Processing Workshop*, IEEE, 2016, pp. 1–5.

10. **Pan Li**, Baosen Zhang, Yang Weng, and Ram Rajagopal, "Autoregressive model for individual consumption data-Sparsity recovery and significance test", in *Power and Energy Society General Meeting*, IEEE, 2016, pp. 1–5.

11. **Pan Li**, Baosen Zhang, Yang Weng, and Ram Rajagopal, "A Sparse linear model and significance test for individual consumption prediction", in *IEEE Transactions on Power Systems*, 2016.

# VITA

Pan Li received Master's and Bachelor's degree from School of Electronics and Information Engineering at Xi'an Jiaotong University, Xi'an, Shaanxi, China, in June 2014 and September 2011 respectively. She also holds Diplome d'Ingenieur (Master's degree equivalent) from Ecole Centrale de Lille, Villeneuve d'Ascq, France from June 2014. Currently, Pan is a Ph.D. candidate in Department of Electrical Engineering at University of Washington, Seattle, United States. Previous, Pan was a software engineer intern at Pinterest (2017) and research intern at ArcelorMittal (2011). Her primary research is in applying machine learning algorithms and mathematical tools to understand the operation of networked physical systems, i.e., a power grid.